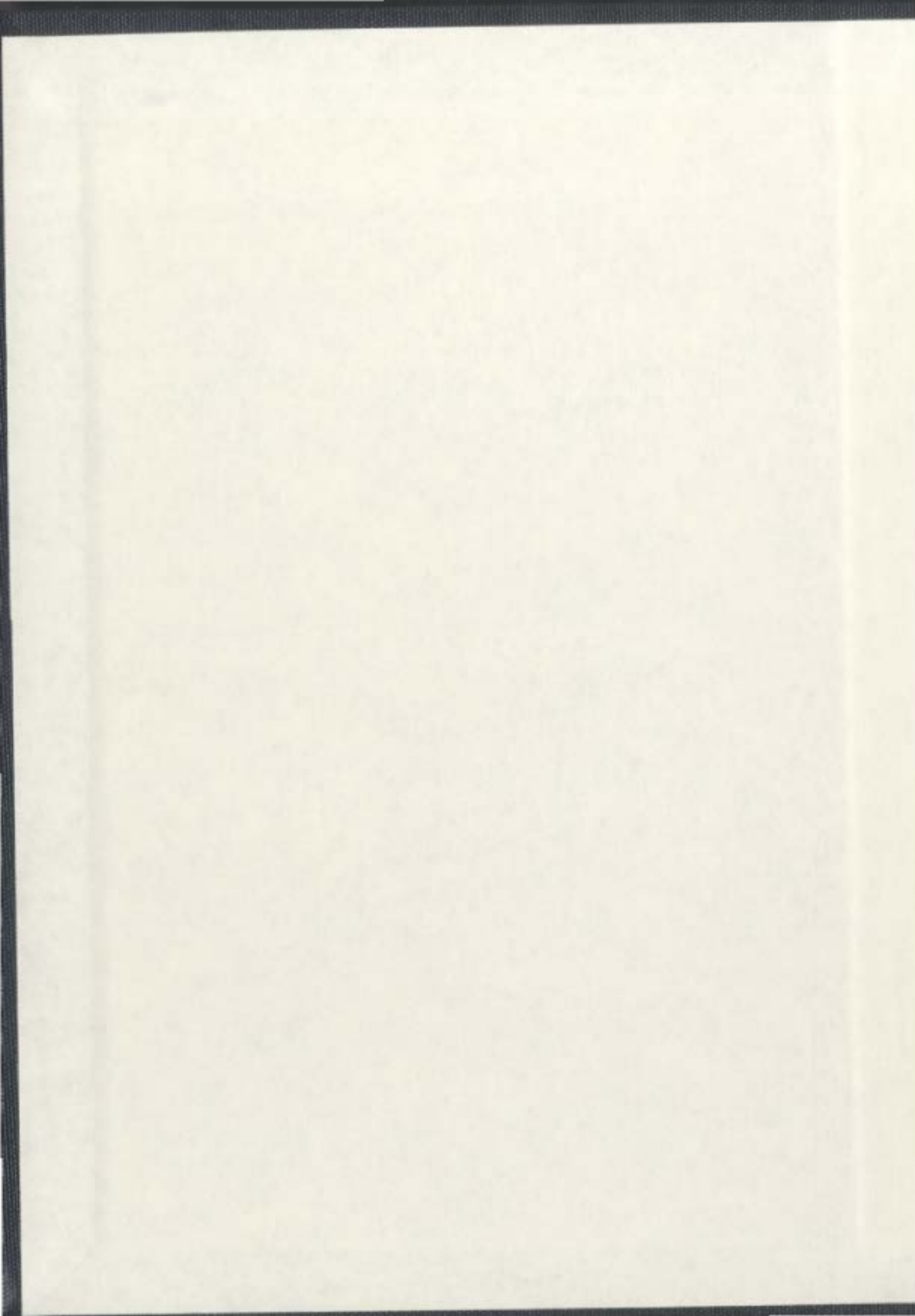
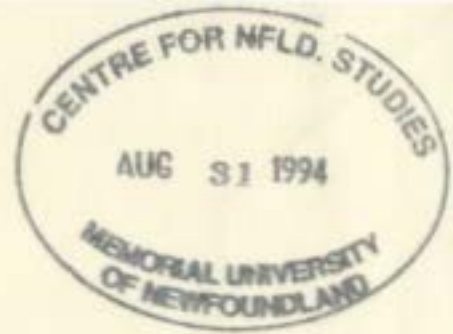


VARIATIONAL PRINCIPLES BASED METHODS
FOR INTEGRITY ASSESSMENTS

HARIKRISHNAN INDERMOHAN





VARIATIONAL PRINCIPLES BASED METHODS

FOR INTEGRITY ASSESSMENTS

by

© Harikrishnan Indermohan

A thesis submitted to the

School of Graduate Studies

in the partial fulfilment of the

requirements for the degree of

Doctor of Philosophy

Faculty of Engineering and Applied Science

Memorial University of Newfoundland

December, 2006

St. John's, Newfoundland



Library and
Archives Canada

Bibliothèque et
Archives Canada

Published Heritage
Branch

Direction du
Patrimoine de l'édition

395 Wellington Street
Ottawa ON K1A 0N4
Canada

395, rue Wellington
Ottawa ON K1A 0N4
Canada

Your file *Votre référence*
ISBN: 978-0-494-31319-0
Our file *Notre référence*
ISBN: 978-0-494-31319-0

NOTICE:

The author has granted a non-exclusive license allowing Library and Archives Canada to reproduce, publish, archive, preserve, conserve, communicate to the public by telecommunication or on the Internet, loan, distribute and sell theses worldwide, for commercial or non-commercial purposes, in microform, paper, electronic and/or any other formats.

The author retains copyright ownership and moral rights in this thesis. Neither the thesis nor substantial extracts from it may be printed or otherwise reproduced without the author's permission.

AVIS:

L'auteur a accordé une licence non exclusive permettant à la Bibliothèque et Archives Canada de reproduire, publier, archiver, sauvegarder, conserver, transmettre au public par télécommunication ou par l'Internet, prêter, distribuer et vendre des thèses partout dans le monde, à des fins commerciales ou autres, sur support microforme, papier, électronique et/ou autres formats.

L'auteur conserve la propriété du droit d'auteur et des droits moraux qui protègent cette thèse. Ni la thèse ni des extraits substantiels de celle-ci ne doivent être imprimés ou autrement reproduits sans son autorisation.

In compliance with the Canadian Privacy Act some supporting forms may have been removed from this thesis.

Conformément à la loi canadienne sur la protection de la vie privée, quelques formulaires secondaires ont été enlevés de cette thèse.

While these forms may be included in the document page count, their removal does not represent any loss of content from the thesis.

Bien que ces formulaires aient inclus dans la pagination, il n'y aura aucun contenu manquant.


Canada

ABSTRACT

The assessment of load carrying capacity under applied loads is an important goal in designing mechanical components and structures. Limit analysis is carried out to determine the load at which uncontained plastic flow occurs in the component under consideration. Lower bound limit loads are vital from the structural integrity standpoint and are germane to fitness-for-service assessments.

The existing lower bound limit load determination methods using elastic modulus adjustment procedures (EMAP) such as the classical and m_α -multiplier methods have a dependence on the maximum equivalent stress. These methods are therefore sensitive to localized plastic action, which occurs in components with thin or slender construction, or those containing notches and cracks. The lower bounds obtained using the present methods have an oscillatory behavior during successive elastic iterations.

The m_β -multiplier method developed in this thesis is obtained by considering a distribution of stress rather than a single maximum equivalent stress. As a result, good limit load estimates can be obtained especially for shape-sensitive structures and components with cracks and notches.

The applicability of the m_β -multiplier method is extended such that the method can determine limit loads of pressure components exhibiting anisotropy. As a result, collapse

load analysis can be performed for perforated heat exchanger tubesheet that is currently modeled as an equivalent solid plate with anisotropic properties.

Simplified procedures for fitness-for-service assessment, suitable for use by plant engineers, is also developed. A variational formulation in plasticity is used to develop these procedures. The concept of “integral mean of yield” is utilized to problems involving locally thinned areas and local hot spots in the context of industrial pressure vessels and piping.

The lower bound limit loads obtained by the m_β -method and the fitness-for-service assessment methods are compared with corresponding results of inelastic finite elastic analyses.

ACKNOWLEDGEMENTS

I would like to express my gratitude to my supervisor Prof. R. Seshadri for his intellectual guidance, full-fledged inspiration and immense expertise that added substantially to my graduate experience. I appreciate his vast knowledge and skill in many areas that provided me the opportunity to work on remarkable industrial related projects. Through numerous enthusiastic and challenging discussions, I also gained significant knowledge and confidence in the area of solid mechanics. I am also grateful for his financial support endowed on me throughout my graduate program.

I would like to thank Dr. S. Adluri for his stimulating and outstanding teaching in computational mechanics courses. His ability to explain advanced concepts in a fundamental level is noteworthy and the concepts gained from his courses helped considerably in my research. I thank Dr. M. Booton for his Engineering Analysis course, which emphasized on variational principles in mechanics and was useful in developing the background of my research. I thank Dr. A. Swamidas for his course on Structural Dynamics, which provided me with a background, knowledge and experience on the dynamic ingredient of the mechanical design process.

I thank Babcock and Wilcox Company, Cambridge for providing me the opportunity to work on heat exchanger tubesheets. A special thanks goes out to Dr. Wolf Reinhardt, without whose (profound) knowledge and experience on tubesheet application, the tubesheet project would not have been successful.

I thank the School of Graduate Studies, for granting the financial support during my stay in Memorial University. I also thank the Associate Dean of Graduate Studies, and acknowledge Ms. M. Crocker, Office of the Associate Dean, for her assistance and guidance in all my concerns throughout my graduate program. I thank Ms. Lisa O'Brien and Heather O'Brien, Canada Research Chairs' Office, for their administrative assistance during my last stages of my graduate program. I thank the members of CCAE for the computing services provided by them during my study.

I must thank Dr. F. Khan, a mentor and friend, whose motivation, encouragement and moral support were always present during the difficult times of my graduate life. I would also like to thank my parents for their profound support and patience throughout my entire life.

TABLE OF CONTENTS

ABSTRACT.....	II
ACKNOWLEDGEMENTS.....	IV
LIST OF FIGURES	XII
LIST OF TABLES.....	XV
NOMENCLATURE	XVI
CHAPTER 1: INTRODUCTION.....	1
1.1 Limit Analysis	1
1.2 Integrity Assessment of Structures.....	3
1.3 Robust Methods in Pressure Vessel Design	5
1.4 Objectives of the thesis.....	7
1.5 Organization of the thesis.....	8
1.6 Original Contributions.....	10
CHAPTER 2: THEORETICAL CONCEPTS AND REDUCED MODULUS METHODS	12
2.1 Introduction	12
2.2 Plasticity Theory and Limit Design.....	13
2.3 Classical Limit Load Theorems.....	16
2.3.1 Analytical Limit Solutions.....	16
2.3.2 Statically Admissible Stress Fields.....	18
2.3.3 Lower Bound Theorem	18
2.3.4 Kinematically Admissible Velocity Fields	19

2.3.5	Upper Bound Theorem	20
2.4	Thick-Walled Cylinder	20
2.4.1	Lower Bound Limit Pressure	21
2.4.2	Upper Bound Limit Pressure	24
2.5	Pressure Vessel Design.....	26
2.6	Inelastic Finite Element Analysis.....	28
2.7	Development of Reduced Modulus Methods for Pressure Component Design..	30
2.7.1	Methods based on Partial Elastic Modulus Modification.....	30
2.7.2	Gloss r-node Method.....	33
2.7.2.1	Concept of r-nodes	33
2.7.2.2	r-nodes and Multiple Plastic Hinges	36
2.7.2.3	Procedure to Determine r-nodes.....	36
2.7.2.4	Applications of the r-node Method	38
2.7.3	Elastic Compensation Method	39
2.7.3.1	Determination of Lower Bound Limit Loads.....	39
2.7.3.2	Determination of Upper Bound Limit Loads	41
2.7.3.3	Features Relating to the Elastic Compensation Method	42
2.7.3.4	Theoretical Justification for the Upper Bounds	44
2.8	Limitations of the Reduced Modulus Methods	45
2.9	Closure.....	46
CHAPTER 3: VARIATIONAL PRINCIPLES IN LIMIT ANALYSIS		47
3.1	Introduction	47

3.2	Mura's Variational Formulation.....	47
3.3	The Extended Lower Bound Theorem	53
3.4	Finite Element Implementation of Mura's Formulation	56
3.5	m-alpha Multiplier Method	59
3.6	Upper Bound Multiplier – m^0	62
3.6.1	Local Plastic Collapse – Notion of Reference Volume (V_R).....	62
3.6.2	Plastic Flow Parameter	64
3.7	Bounds on the Limit Load Multipliers.....	66
3.7.1	Mura's Lower Bound Multiplier - m'	67
3.7.2	Upper Bound Multiplier - m_1^0	68
3.7.3	Upper Bound Multiplier - m_2^0	69
3.7.4	Multiplier – m-alpha	70
3.8	Closure.....	73
CHAPTER 4: LOWER BOUND LIMIT LOAD DETERMINATION – THE M-BETA		
MULTIPLIER METHOD.....		
		74
4.1	Introduction	74
4.2	Theoretical Considerations.....	75
4.2.1	Integral Mean of Yield Criterion	75
4.2.2	Upper and Lower Bound Limit Load Multipliers.....	76
4.3	M-Beta Multiplier Method	79
4.3.1	Derivation of m_β - multiplier.....	79
4.3.2	Significance of G	81

4.4	Numerical Examples	83
4.4.1	Thick-walled Cylinder under Internal Pressure	83
4.4.2	Beam under Pure Bending	90
4.5	Discussions.....	95
CHAPTER 5: THE M-BETA MULTIPLIER METHOD FOR LIMIT LOAD		
DETERMINATION OF COMPONENTS WITH LOCAL PLASTIC COLLAPSE.....		
		97
5.1	Introduction	97
5.2	Concept of Reference Volume	99
5.3	Finite Element Modeling of Cracks	104
5.4	Numerical Examples	107
5.4.1	Elastic Modulus Adjustment Scheme	107
5.4.2	Evaluation of m-beta multiplier	108
5.4.3	Thick Unwelded Flat Head under internal pressure	108
5.4.4	Welded-in flat head under internal pressure	111
5.4.5	Plate with a center crack	114
5.4.6	Compact Tension Specimen	117
5.4.7	Plate with Multiple Cracks.....	120
5.5	Closure.....	123
CHAPTER 6: LIMIT LOAD OF ANISOTROPIC COMPONENTS USING THE M-		
BETA MULTIPLIER METHOD		
		125
6.1	Introduction	125
6.2	Anisotropic Constitutive Relationships.....	127

6.2.1	Hill's Yield Criterion	127
6.2.2	Non-Dimensionalized form of Hill's Yield Criterion.....	128
6.3	M-Beta Method for Anisotropic Materials.....	129
6.3.1	Integral Mean of Yield Criterion	129
6.3.2	Flow Rule.....	130
6.3.3	Upper Bound Multiplier - m^0	130
6.4	Numerical Examples Based on Hill's Criterion	131
6.4.1	Elastic Modulus Adjustment Scheme	131
6.4.2	Initial Elastic Properties.....	132
6.4.3	Orthotropic Cylinder under Internal Pressure.....	134
6.4.4	Transversely Isotropic Bridgman Notch Specimen under Tensile Load	135
6.5	Heat Exchanger Tubesheet.....	137
6.5.1	Fourth-order Yield Criterion.....	138
6.5.2	Geometric Properties	140
6.5.3	Base Material Properties.....	140
6.5.4	Repeated Elastic Analysis – Hill's Criterion	142
6.5.5	Repeated Elastic Analysis – Fourth Order Criterion	144
6.6	Discussions.....	146
 CHAPTER 7: FITNESS-FOR-SERVICE METHODOLOGY BASED ON VARIATIONAL PRINCIPLES IN PLASTICITY		
7.1	Introduction	148
7.2	Theoretical Considerations.....	149

7.3	Integrity Assessment Method – Level 2	150
7.3.1	Reference Volume for a Thin Cylinder	150
7.3.2	Locally Thinned Areas (LTA)	153
7.3.3	Local Hot Spots.....	156
7.4	Numerical Examples	159
7.4.1	Required Shell Thickness Calculations	160
7.4.2	Evaluation of RSF for Locally Thinned Areas (LTA).....	160
7.4.3	Evaluation of RSF for Hot Spots	165
7.4.4	Thermo-elastic Calculations	167
7.5	Discussions	169
CHAPTER 8: CONCLUSIONS AND FUTURE RESEARCH.....		171
8.1	Conclusions	171
8.2	Future Research.....	174
PUBLICATIONS AND PRESENTATIONS DURING THE PH. D PROGRAM.....		176
REFERENCES		177
APPENDIX: ANSYS APDL MACROS		184

LIST OF FIGURES

Figure 2.1	Constitutive Models	17
Figure 2.2	Thick Walled Cylinder under Internal Pressure	21
Figure 2.3	Stress Distribution in a Thick Walled Cylinder	22
Figure 2.4	Follow-up Angle (θ) on the GLOSS Diagram	34
Figure 2.5	R-Nodes in a Beam subjected to Pure Bending	35
Figure 2.6	Indeterminate Beam subjected to Uniformly Distributed Load and the Two-Bar Model	37
Figure 2.7	Convergence of Maximum Elastic Stress in an Iterative Elastic FEA	40
Figure 3.1	An Elastic-Perfectly-Plastic Body	48
Figure 3.2	Variation of m^0 and m' with iteration ζ	58
Figure 3.3	Leapfrogging to the Limit State	61
Figure 3.4	Identification of the Reference Volume, V_R	63
Figure 3.5	Region of Lower and Upper Boundedness of m_α	72
Figure 4.1	m_β - multiplier : Reference Curve ($\beta = \beta_R$)	82
Figure 4.2	Variation of Limit Load Multipliers – Thick Walled Cylinder	88
Figure 4.3	Beam Subjected to Pure Bending	91
Figure 5.1	Total and Reference Volumes	99
Figure 5.2	Overestimation of m_I^0, m''	100
Figure 5.3	Singular Elements in FEA	105

Figure 5.4	Thick Unwelded Flat Head under Internal Pressure	109
Figure 5.5	FE Mesh of Thick Unwelded Flat Head under Internal Pressure	110
Figure 5.6	Variation of Limit Load Multipliers – Thick Unwelded Flat Head	111
Figure 5.7	Welded-in Flat Head under Internal Pressure	112
Figure 5.8	FE Mesh of Welded-in Flat Head under Internal Pressure	112
Figure 5.9	Variation of Limit Load Multipliers – Welded-in Flat Head	113
Figure 5.10	Plate with a Center Crack	114
Figure 5.11	FE Mesh of Plate with a Center Crack	115
Figure 5.12	Variation of Limit Load Multipliers – Plate with a Center Crack	116
Figure 5.13	Compact Tension Specimen	117
Figure 5.14	FE Mesh of Compact Tension Specimen	118
Figure 5.15	Variation of Limit Load Multipliers – Compact Tension Specimen	119
Figure 5.16	Plate with Multiple Cracks	120
Figure 5.17	FE Mesh of Plate with Multiple Cracks	121
Figure 5.18	Variation of Limit Load Multipliers – Plate with Multiple Cracks	122
Figure 6.1	Orthotropic Cylinder under Internal Pressure	135
Figure 6.2	Transversely Isotropic Bridgman Notch Specimen	137
Figure 6.3	Equivalent Solid Model of a Tubesheet	142
Figure 6.4	Tubesheet – Hill’s Criterion	144
Figure 6.5	Tubesheet – Fourth Order Criterion	145
Figure 7.1	A Rectangular LTA in a Cylindrical Vessel	151

Figure 7.2	Reference Dimensions for Localized Effects	153
Figure 7.3	LTA in a Thin Cylinder	154

LIST OF TABLES

Table 5.1	Values of V_R/V_T , m_1^0/m_2^0 and G for Cracked Components	123
Table 6.1	Values of V_R/V_T , m_1^0/m_2^0 and G for Tubesheet	146
Table 7.1	LTA with 1/16" Corroded Thickness	164
Table 7.2	LTA with 1/8" Corroded Thickness	164
Table 7.3	LTA with 1/4" Corroded Thickness	165
Table 7.4	Material Properties of Carbon Steel	168

NOMENCLATURE

Symbols

ε_{ij}	strain tensor
$\dot{\varepsilon}_{ij}$	strain rate tensor
$\dot{\varepsilon}_{ij}^*$	kinematically admissible strain rate tensor
$d\varepsilon_{ij}^P$	plastic strain increment tensor
ε_e	von-Mises equivalent strain
ε_r	radial strain component in a thick walled cylinder
ε_θ	tangential strain component in a thick walled cylinder
ε_z	longitudinal strain component in a thick walled cylinder
σ_x	stress component in x-direction
σ_y	stress component in y-direction
σ_z	stress component in z-direction
σ_e	von-Mises equivalent stress
σ_e^0	statically admissible equivalent stress
$(\sigma_e)_{r-node}$	r-node effective stress
$\bar{\sigma}_n$	combined r-node effective stress
σ_{ij}	stress tensor
σ_{kk}	mean stress tensor
σ_{ij}^0	statically admissible stress tensor
σ^0	statically admissible mean stress tensor
σ_r	radial stress component in a thick walled cylinder
σ_θ	tangential stress component in a thick walled cylinder
σ_z	longitudinal stress component in a thick walled cylinder
σ_y	yield stress in tension
σ_{arb}	arbitrary stress
σ_i	maximum unaveraged nodal equivalent stress
σ_M	maximum equivalent stress
σ_{ref}	reference stress
$\bar{\sigma}$	equivalent stress corresponding to an anisotropic yield criterion
σ_{eU}	equivalent stress in a uncorroded portion in a thin cylinder

σ_{eC}	equivalent stress in a corroded portion in a thin cylinder
σ_{yH}	yield stress in a hot spot region
ν_{ij}	Poisson's ratios in xy, yz, xz planes
$f(s_{ij})$	yield criterion
s_{ij}	deviatoric stress tensor
s_{ij}^0	statically admissible deviatoric stress tensor
s_1	average of in-plane normal stress components
s_2	half-difference of in-plane normal stress components
s_3	in-plane shear stress component
k	yield strength in shear
ν	Poisson's ratio
δ_{ij}	kronecker's delta
$d\lambda$	proportional constant
n_j	normal vector
γ_1	proportional constant
γ_2	proportional constant
μ^0	flow parameter corresponding to a statically admissible state
μ	flow parameter corresponding to a limit state
α_{ij}	non-dimensional anisotropic parameters
D	internal work of dissipation per unit volume
E	Young's Modulus
E_o	Initial elastic modulus (before iteration)
E_s	Secant modulus
E_i	Elastic modulus at i^{th} iteration
G	non-zero parameter
P, Q, R, T	in-plane coefficients corresponding to the fourth-order yield criterion
Y_1, Y_2, Y_3	out-of-plane coefficients corresponding to the fourth-order yield criterion
$S_{y_{xx}}$	tensile yield stress in x-direction
$S_{y_{zz}}$	tensile yield stress in z-direction
S_{y_b}	biaxial in-plane yield stress in tension
S_{y_s}	yield stress in in-plane shear
$S_{y_{os}}$	yield stress in out-of-plane shear
G_{ij}	shear moduli in xy, yz, xz directions
S_T	surface on which tractions are applied
S_V	surface on which velocities are applied

T_i	applied traction
V_k	volume of a finite element
V_T	total volume of a structure
V_R	reference volume
V_D	dead zone volume
V_C	corroded volume or a volume corresponding to cold temperature
V_H	hot spot volume
u	radial displacement component in a thick walled cylinder
v_i^*	kinematically admissible velocity tensor
v_i	velocity tensor
S	Stress Intensity
S_m	Code allowable stress intensity
W	external work done per unit length
N	total number of elements
J	elastic-plastic energy release rate
C^*	creep growth parameter
σ_n	nominal stress
q	elastic modulus adjustment parameter
i	iteration number
\dot{D}	increment of plastic dissipation per unit volume
ζ	iteration variable
C_{ijkl}	fourth-order material tensor
X_C	local parameter in the circumferential direction
X_L	local parameter in the longitudinal direction
$RSF1$	Remaining Strength Factor based on m^0 multiplier
$RSF2$	Remaining Strength Factor based on m_α multiplier
$RSF3$	Remaining Strength Factor based on m_L multiplier

Limit Load Multipliers

m^0	statically admissible multiplier
m^*	kinematically admissible multiplier
m	safety factor
m_u	classical upper bound multiplier
m_L	classical lower bound multiplier
m'	Mura's lower bound multiplier
m_1^0	Upper bound multiplier based on constant flow parameter

- m_2^0 Upper bound multiplier based on distributed flow parameter
 m_α statically admissible multiplier based on partly converged m^0 and m_L
 m_β statically admissible multiplier that considers a distribution of stress in a structure
 m_d^0 Multiplier, m^0 for a damaged component
 $m_{\alpha d}$ Multiplier, m_α for a damaged component
 m_{Ld} Multiplier, m_L for a damaged component

Acronyms

ASME	American Society of Mechanical Engineers
FEA	Finite element analysis
EMAP	Elastic modulus adjustment procedures
GLOSS	Generalized Local Stress and Strain
RSF	Remaining Strength Factor
LTA	Locally Thinned Area

CHAPTER 1: INTRODUCTION

1.1 Limit Analysis

In designing a mechanical structure or a component, a designer must ensure that its design is safe and durable while simultaneously giving importance to its performance and economy. The aspects of mechanical design philosophy predominantly include selection of material of construction, determination of potential modes of failure and the method of stress analysis adopted. The material selection is primarily based on the operating environment and its cost. While the process of identifying the failure modes has the ability to avert the structure from catastrophic failure, they have to be judiciously assessed by an appropriate method of stress analysis.

This thesis concerns applications of generic pressure components, which finds its use in oil and gas, chemical, fertilizers and power generation industries. Pressure vessels entail complex shapes that are sources of stress concentration problems and therefore confine the choice of materials to ones that possess enough ductility. Furthermore, pressure vessels are subject to eight possible modes of failure. However, the exposition in this thesis is restricted to failure mechanism associated with gross plastic deformation. As the failure mechanism is inelastic, ideally, a structure's behavior should be assessed by limit analysis. The primary area of research conducted in this thesis is on limit analysis, which addresses the failure mechanism associated with gross plastic deformation.

For many years, pressure component design was based on elastic analysis. In elastic design, the stress in the structure is not allowed to exceed yield. However, it is evident that the structure will safely carry its intended load even after the stress at a point in the structure exceeds the yield stress. Moreover, local plastic flow occurs at locations of stress raisers and geometric discontinuity and thus the design based on elastic analysis renders an uneconomical design.

In fact, limit analysis is concerned with the determination of load-carrying capacity of structures. The load at which uncontained plastic flow occurs in a structure is termed as the limit load. The advantage of limit analysis is that it takes into account the post-yield strength of structures that can generate an economical design. The knowledge of limit loads is also vital from the structural integrity standpoint.

Limit loads can be estimated using analytical techniques, classical bounding theorems and non-linear analysis, which is primarily based on finite element analysis. Analytical limit solutions are obtained with ease for structures with simple geometry and loading. However, it is mathematically intractable to obtain collapse loads for complex structural configurations. With advanced computer technology, opportunities are available to perform inelastic analysis using non-linear finite element analysis. Nevertheless, non-linear analysis has its own limitations, as the analysis is involved and requires careful interpretation of results and designer's expertise.

Therefore, there is an incentive to develop alternate limit analysis techniques that are simple, approximate and efficient. The technique termed elastic modulus adjustment procedures (EMAP) is based on linear elastic analyses and have been adopted in this thesis to estimate lower bound limit loads.

1.2 Integrity Assessment of Structures

Structural and Mechanical Integrity assessment is one of the principal tasks that has been implemented by the aerospace, fossils, mining, petrochemical, nuclear power generation and the oil and gas industries. It plays a major role in preserving safety and economy of the plant, equipment and system operation. The integrity assessment is a multidisciplinary effort and with regard to the oil and gas industries, it involves interactions of diverse fields such as process chemistry, process engineering, thermofluids, mechanics, materials, applied physics and computational technology. The assessment activities are carried out in three phases – design, construction and post construction. The post construction activity is further subdivided into operations, inspection, maintenance and restoration activities.

Integrity evaluations encompass a thorough knowledge of the working loads, material behavior and operating environment of the plant's aggregate life. During the continued service of the plant, the equipments are exposed to several ageing issues such as crack formation and growth, corrosion and erosion, fatigue, elevated temperature effects, blister formation, neutron irradiation, creep deformation etc. Therefore, the structural integrity

assessment is often based on systematic and proactive identification of failure modes in the structure and characterization of the deterioration processes.

A pragmatic approach to devising the failure modes is by grouping them into (1) immediate failure – failures that occur without warning on a single application of loads and (2) delayed or progressive failure – failures that occur due to repeated application of loads, or time-dependent effects. The repeated application of loads is usually attributed to startup-shutdown occurrences or severe thermal transients. Stringent design limits are placed on the first category since the failures occur without warning and intervention is not possible. Less stringent design limits are placed on the second category since incipient damage can be detected, and planned intervention is possible through timely inspections and repairs.

In addition to identifying the potential failure modes, periodic inspection is carried out in the ageing equipment and deterioration checks are made. By characterizing the observed defects, fitness-for-service methodology can be developed thereby devising the acceptance criteria and evaluation procedures that establish the suitability of the structure's continued service.

Structural integrity assessment in an operating plant is practiced at three levels:

- Level 1 – This level of assessment is excessively conservative and based upon inspection data.

- Level 2 – Such an assessment possesses simplified conservative screening criteria adopted in conjunction with a minimum quantity of inspection data. As well, this level of assessment is intended for use by facilities or plant engineers, although some owner-operator organizations consider it more suitable for a central engineering evaluation.
- Level 3 – This type of assessment requires sophisticated analysis or advanced computational procedures executed by experts.

By periodically assessing the integrity of structures, their remaining life can be estimated and the operating parameters of the plant are controlled effectively.

1.3 Robust Methods in Pressure Vessel Design

Pressure vessels are usually designed according to the guidelines furnished in the Boiler and Pressure Vessels Code (ASME, 2001). Over the years, the Code has undergone significant changes and the latter part of Code rules are based on stress categorization approach. The approach is a direct consequence of using elastic analysis and guards against the inelastic failure mechanisms of gross plastic collapse under static loading and ratcheting under cyclic loading.

The stress categorization approach in conjunction with the interpretation of finite element analysis (FEA) results has been found to be difficult (Hechmer and Hollinger, 1991). The fundamental barriers in stress categorization made researchers to move away from design

based on elastic analysis to that based on inelastic analysis that directly addresses the inelastic failure modes.

Inelastic FEA is an elaborate technique in which the load is applied in increments and the equilibrium for each load increment is established by satisfying certain convergence criteria. The disadvantage of inelastic analysis is that it requires greater computing resources to perform iterative analysis, storage of intermediate results, proper definition of material models, selection of appropriate elements, careful control of load increments and designer's knowledge in performing the analysis.

The indicated disadvantages of inelastic analysis have directed the researchers to determine limit loads using simplified, robust and efficient design methods based on elastic analysis. Robust methods are less demanding and require minimum computational resources. It has been demonstrated that carrying out a linear elastic FEA with elastic modulus modification can simulate the plastic stress distribution in a structure (Seshadri, 1991a). Several robust methods have been developed during the past two decades to estimate lower bound limit loads. These methods include GLOSS R-node (Seshadri and Fernando, 1992), Elastic Compensation method (Mackenzie and Boyle, 1993a) and the m_α -method (Seshadri and Mangalaramanan, 1997).

Lower bound limit load estimates are relevant for pressure component design and are acceptable quantities for ascertaining primary stress limits. Essentially, the robust methods attempt to find the most efficient distribution of primary stresses for a given set

of loads. This is obtained by subsequently modifying the uniform elastic modulus of a structure at various locations.

These methods have their own limitations. It has been argued that r-node method is difficult to apply for three dimensional structures. In elastic compensation method, there is no criterion that assures the maximum stress in the structure will converge after several iterations. The problem of convergence is prevalent for shape-sensitive structures with notches and cracks. For such structures, the maximum stress in an iterative elastic analysis technique “moves around” leading to poor lower bounds. The lower bounds of the m_α -multiplier have been questioned after few iterations and there is no guarantee that the method estimates lower bound limit loads at initial iterations for structures subject to local plastic collapse.

1.4 Objectives of the thesis

The objectives of this thesis are:

1. To develop a lower bound limit load determination method called m_β - multiplier method that accounts for the entire stress distribution in a structure rather than a maximum elastic stress in a structure.
2. Apply the m_β - method to typical pressure component configurations and cracked components and verify the results with those of conventional analysis techniques.

3. To extend the m_β -method to anisotropic components that obey Hill's yield criterion and to investigate its application to heat exchanger tubesheets that obey fourth-order yield criterion.
4. To develop Level 2 integrity assessment methods, that evaluate the "Remaining Strength Factor (RSF)" of pressure vessels and piping containing locally thinned areas (LTA) and hot spots. These simplified procedures perform "fitness-for-service" assessments and are suitable for use by plant engineers.

1.5 Organization of the thesis

This thesis is organized into 8 chapters. In Chapter 1, various facets associated with limit analysis and the role of reduced modulus methods in evaluating primary stresses in pressurized components are discussed. The significance of limit analysis in integrity assessment of mechanical structures is also illustrated. The objectives and the original contributions to research are further enumerated.

In Chapter 2, theoretical aspects pertaining to plasticity theory and limit design are discussed. Conventional techniques of limit analysis such as analytical techniques, lower and upper bound theorems and inelastic finite element analysis are described. An overview of simplified methods called the reduced modulus methods that estimate limit loads using linear elastic analysis are furnished.

Chapter 3 provides a detailed derivation of Mura's variational formulation, which is an alternate approach to classical limit analysis. Several limit load multipliers such as m^0 , m' and m_α are derived from Mura's variational approach and their upper and lower boundedness are explored in detail.

The classical lower bound multiplier m_L and m_α - multiplier are based on a maximum elastic stress in a structure. A multiplier, m_β that relies on an entire stress distribution in a structure is derived in Chapter 4. Simple examples are worked out to demonstrate the evaluation of upper and lower bound limit load multipliers and the results are compared with the exact limit multiplier.

In Chapter 5, the m_β -multiplier method is applied to structures that are subjected to local plastic action. The concept of reference volume is useful for such applications in which the stress distributions obtained from EMAP do not converge to near limit type distribution is exemplified. The m_β -method developed in this chapter is applied to typical pressure vessel and cracked component configurations and is compared with the results of inelastic finite element analyses.

The applicability of the m_β -method to anisotropic components is investigated in Chapter 6. The application of m_β -method to heat exchanger tubesheets that obey fourth-order yield criterion is also explored. Further details relevant to fourth-order yield criterion

such as compressibility and 60 degree rotational symmetry of tubesheets are also illustrated.

In Chapter 7, Level 2 “fitness-for-service” methodology pertinent to plant engineers is developed. Simplified methods that evaluate “Remaining Strength Factor (RSF)” of pressure vessels and piping containing locally thinned areas and hot spots are also presented. The methods are validated using the results of inelastic finite element analyses.

Chapter 8 summarizes the overall evaluation of the m_β -method. The thesis concludes by providing recommendations on areas of future research.

1.6 Original Contributions

The contributions of the thesis are listed as follows:

- A lower bound limit load determination method called m_β - method that accounts for the entire stress distribution in a structure is developed. The method is derived from Mura’s inequality and is used in conjunction with EMAP and a sequence of linear elastic finite element analyses.
- The concept of reference volume is developed for structures in which the stress distributions obtained from EMAP do not converge to a near limit-type distribution.
- A systematic method is established to evaluate the deviation of stress distributions obtained from EMAP to limit-type distribution.

- The application of m_β -method is investigated for typical pressure component configurations and cracked components. The lower bound limit loads obtained using the m_β -method are shown to be better than the classical lower bound limit loads.
- The m_β -method is extended to determine the limit loads of anisotropic components that obey Hill's criterion.
- Collapse load of tubesheets, which are modeled as equivalent solid plate and obey fourth-order yield criterion is estimated using the m_β -method. The fourth-order yield criterion incorporates compressibility and 60 degree rotational symmetry of tubesheets.
- Simplified Level 2 Fitness-for-Service assessment methods suitable for plant engineers are developed. These methods evaluate "Remaining Strength Factor" of a thin cylinder containing locally thinned areas and hot spots.

CHAPTER 2: THEORETICAL CONCEPTS AND REDUCED MODULUS METHODS

2.1 Introduction

The theoretical concepts pertaining to limit analysis and different methods of estimating limit loads are discussed in this chapter. It is unwieldy to obtain limit load solutions using analytical techniques. Therefore, a pragmatic approach is to evaluate limit loads by using limit load theorems. Lower bound limit loads are useful from a perspective of safe design approach whereas upper bound limit loads are useful in estimating power requirements for metal cutting and forming processes.

Some of the reduced modulus methods related to the present research are also discussed briefly in this chapter. The reduced modulus methods are robust methods that emerged as an alternative to inelastic analysis. These methods are simplified, and provide acceptable results at minimum time and cost, and useful during the initial stages of the design process. The modulus adjustment techniques were initially developed to assess the inelastic effects in mechanical components and structures and were later used to estimate limit loads on the basis of linear elastic analysis.

2.2 Plasticity Theory and Limit Design

The theory of elasticity deals with solid bodies, which return to their original shape upon removal of external forces. On the other hand, plasticity theory deals with solid bodies, in which the deformation does not disappear completely when the external forces are removed. The behavior of bodies that the theory of plasticity deals with is characterized as elastic-plastic.

The objective of performing stress analysis is to find the distribution of stress and strain that satisfies the equilibrium conditions, compatibility conditions and the constitutive relationships. For a given structure subjected to prescribed loads and displacements, the conditions of equilibrium and compatibility do not change whether the state of stress or strain is elastic or plastic. The main and distinct ingredients of elasticity and plasticity theories are listed further.

The fundamental aspects of linear elasticity theory are:

- (1) The stresses and strains are related by the appropriate form of Hooke's law. For an isotropic material the elastic strains are related to the stresses according to the following relationship:

$$\varepsilon_{ij} = \frac{1+\nu}{E} \sigma_{ij} - \frac{\nu}{E} \sigma_{kk} \delta_{ij} \quad (2.1)$$

- (2) In an external loading process, a complete reversibility of deformation is reached.

- (3) The final strains depend on the end stresses, and not upon the stress history or the strain path.

The underlying principles, mathematical interpretations and physical significances of elastic-plastic constitutive relationships relevant to the theory of plasticity and its basic applications can be found in a number of references (Calladine, 1969, Mendelson, 1968, Hill, 1971, Johnson and Mellor, 1983, Chen and Han, 1988). The key features of plasticity theory are:

- (1) Permanent deformations are induced as the stress at a certain location exceeds the yield strength of the material. The onset of plastic flow is characterized by the appropriate use of yield criteria. For instance, the von-Mises yield criterion is given by,

$$f(s_{ij}) = \frac{1}{2} s_{ij} s_{ij} - k^2 \quad (2.2)$$

- (2) The final strains depend on the history of loading. Therefore, to find the final strain, incremental strains must be summed over the entire strain path.
- (3) The stress-strain relationship in the plastic range is given by Prandtl – Reuss equation, and is characterized as flow rule. It considers that the plastic strain increment is, at

to collapse. The load at collapse is termed as the limit load and the design based on limit load is called the limit design.

In the design based on elastic analysis, the elastic stress at any point in the structure is not allowed to exceed the allowable stress of the material. The allowable stress is usually the yield strength of the material divided by a factor of safety.

It is apparent that the ductile materials can withstand strains much larger than those corresponding to the elastic limits. As the plastic flow occurs beyond the yield limit, redistribution of stresses occurs and therefore, reserve strength inherent in the material can be made use of. The argument is that the structure will carry the intended loads safely even after certain parts of structure experiences the onset of plastic flow. Therefore, the design based on elastic analysis can be highly uneconomical when compared to the limit design.

In limit analysis, an idealized elastic-perfectly-plastic material model is assumed whereas a strain-hardening material model as shown in Figure 2.1 represents a more accurate plastic behavior. The strain-hardening model replicates a real life structural response. However, an elastic-perfectly-plastic model would be more appropriate for design as the model is simple and implicitly incorporates a failure mechanism.

2.3 Classical Limit Load Theorems

2.3.1 Analytical Limit Solutions

In analytical elastic-plastic analysis, stress and strain distributions at any point in the structure are determined for loads from initial yield until collapse. Such limit load solutions for practical applications like beams (Popov, 1990), frames (Horne, 1979), plates (Save and Massonet, 1972), and simple pressure vessel configurations like thick cylinders (Chakrabarty, 1987), dished ends (Gill, 1970) etc. are currently available.

Complete elastic-plastic solutions are generally more involved and cumbersome. The complexities arise from the irreversibility of plastic flow, its dependence on loading history, and the necessity of carrying out an analysis in an incremental manner. Furthermore, most of the engineering structures are complex and it may be difficult or impossible to obtain closed form solutions except for relatively simple structures. Certain approximating assumptions are made to obtain such analytical solutions, that in the end, prove unrealistic.

Lower and Upper bound theorems are recourse to obtain approximate limit solutions. The “bounding” theorems establish lower and upper bounds to the collapse load. The intent of limit analysis is to determine the load-carrying capacity of structures. Therefore, using these theorems the intermediate elastic-plastic stages are circumvented and collapse state of the structure is investigated directly.

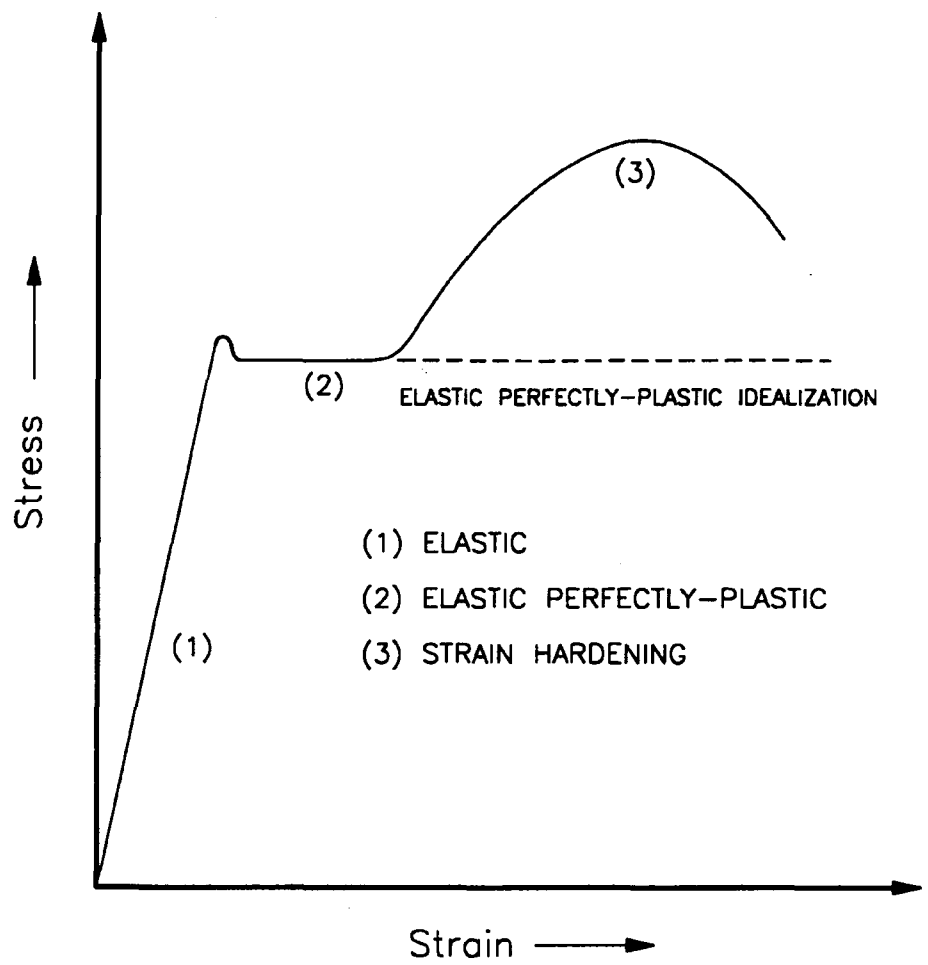


Figure 2.1 Constitutive Models

2.3.2 Statically Admissible Stress Fields

A stress field σ_{ij}^0 is said to be statically admissible if it satisfies,

$$\sigma_{ij}^0{}_{,j} = 0 \quad \text{in } V_T, \quad (2.4)$$

$$\sigma_{ij}^0 n_j = m^0 T_i \quad \text{in } S_T, \quad (2.5)$$

$$f(s_{ij}^0) = \frac{1}{2} s_{ij}^0 s_{ij}^0 - k^2 \leq 0 \quad \text{in } V_T, \quad (2.6)$$

where

$$s_{ij}^0 = \sigma_{ij}^0 - \delta_{ij} \sigma^0, \quad (2.7)$$

$$\sigma^0 = \frac{1}{3} \sigma_{kk}. \quad (2.8)$$

The proportional constant m^0 defined in equation (2.5) is termed as the statically admissible multiplier.

2.3.3 Lower Bound Theorem

If any stress distribution throughout the structure can be found which is everywhere in equilibrium internally and balances certain external loads and at the same time does not violate the yield condition, those loads will be carried safely by the structure (Calladine, 1969). This is the lower bound theorem and it provides a lower bound on limit load.

The theorem merely states that the structure carries the applied load by rearranging the internal stresses to its best advantage, if at all possible. The lower bound approach is an

“equilibrium approach” as only statically admissible stress distributions are considered and without placing any restrictions on the mode of deformation. The best statically admissible stress distribution considered gives the maximum lower bound, which is the best estimate of the limit load.

2.3.4 Kinematically Admissible Velocity Fields

A velocity field v_i^* is said to be kinematically admissible if it satisfies,

$$\delta_{ij} v_{i,j}^* = 0 \quad \text{on } S_V, \quad (2.9)$$

$$v_i^* = 0 \quad \text{on } S_V, \quad (2.10)$$

$$\int_{S_r} T_i v_i^* dS > 0. \quad (2.11)$$

The kinematically admissible multiplier m^* is defined as,

$$m^* = \frac{k \int_V (2 \dot{\varepsilon}_{ij}^* \dot{\varepsilon}_{ij}^*)^{1/2} dV}{\int_{S_r} T_i v_i^* dS}. \quad (2.12)$$

The strain rate fields $\dot{\varepsilon}_{ij}^*$ are derived from the velocity fields v_i^* as,

$$\varepsilon_{ij}^* = \frac{1}{2}(v_{i,j}^* + v_{j,i}^*). \quad (2.13)$$

2.3.5 Upper Bound Theorem

If an estimate of the plastic collapse load of a body is made by equating internal rate of dissipation of energy to the rate at which external force do work in any postulated mechanism of deformation of the body, the estimate will be either high, or correct (Calladine, 1969). This is the upper bound theorem and provides an upper bound on limit load.

The upper bound theorem basically specifies that if a path of failure exists, the structure will take that path. The upper bound approach is a “geometric” approach as only the mode of deformation or the kinematically admissible velocity fields are studied without satisfying the equilibrium equations. Of all the possible kinematically admissible velocity fields the one, which gives the least upper bound, is the limit load. Furthermore, it is vital to state that residual or thermal stresses or deflections have no influence on the limit load.

2.4 Thick-Walled Cylinder

A thick walled cylinder with inner radius a and outer radius b subjected to uniform internal pressure p , as shown in Figure 2.2, is considered to demonstrate the application of lower and upper bound theorems to estimate the collapse load.

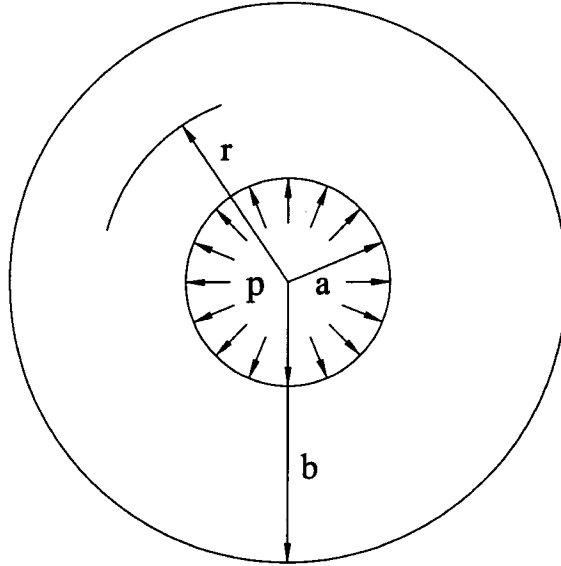


Figure 2.2 Thick Walled Cylinder under Internal Pressure

2.4.1 Lower Bound Limit Pressure

According to lower bound theorem, any statically admissible stress distribution, which satisfies the equilibrium condition and does not violate the yield criterion, estimates a lower bound limit load. In case of a thick cylinder, the equilibrium condition is:

$$\frac{d\sigma_r}{dr} = \frac{\sigma_\theta - \sigma_r}{r}. \quad (2.14)$$

The stress boundary conditions are

$$\sigma_r = -p \quad \text{at } r = a, \quad (2.15a)$$

$$\sigma_r = 0 \quad \text{at } r = b, \quad (2.15b)$$

and, in the longitudinal direction,

$$p\pi a^2 = \int_a^b 2\pi\sigma_z r dr. \quad (2.15c)$$

According to the lower bound theorem, any statically admissible stress distribution can be considered to estimate a lower bound limit load. As illustrated in Figure 2.3, the actual elastic stress distribution that satisfies equilibrium and the boundary conditions, is given by,

$$\sigma_r = \frac{pa^2}{b^2 - a^2} \left(1 - \frac{b^2}{r^2} \right), \quad (2.16a)$$

$$\sigma_\theta = \frac{pa^2}{b^2 - a^2} \left(1 + \frac{b^2}{r^2} \right). \quad (2.16b)$$

The yield criterion is assumed to be governed by the Tresca's yield criterion, which is expressed as

$$|\sigma_\theta - \sigma_r| = \sigma_y. \quad (2.17)$$

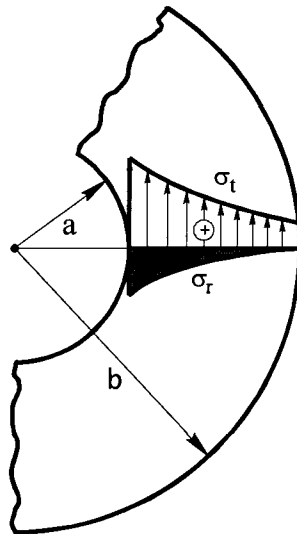


Figure 2.3 Stress Distribution in a Thick Walled Cylinder

A lower bound limit pressure p_L can be determined by substituting the stress distributions in equations (2.16) in the yield criterion in equation (2.17) as,

$$p_L = \frac{\sigma_y (b^2 - a^2)}{a^2}. \quad (2.18)$$

Instead of the stress distribution in equations (2.16), we consider an arbitrary distribution for σ_r as,

$$\sigma_r = A \ln r + B. \quad (2.19)$$

The constants A and B are evaluated by substituting σ_r in the boundary conditions in equations (2.15) and therefore,

$$\sigma_r = \frac{P}{\ln\left(\frac{b}{a}\right)} (\ln r - b). \quad (2.20)$$

Substituting equation (2.20) for σ_r in the equilibrium equation (2.14), we obtain σ_θ distribution as,

$$\sigma_\theta = \frac{P}{\ln\left(\frac{b}{a}\right)} (1 + \ln r - b). \quad (2.21)$$

If σ_r and σ_θ obey the Tresca yield criterion (2.17), we obtain the lower bound limit pressure p_L ,

$$p_L = \sigma_y \ln\left(\frac{b}{a}\right). \quad (2.22)$$

2.4.2 Upper Bound Limit Pressure

An upper bound limit pressure can be determined for the thick walled cylinder under internal pressure by assuming kinematically admissible velocity fields. For instance, the radial displacement u can be assumed as,

$$u = \frac{C}{r}. \quad (2.23)$$

At the inner surface $r = a$, $u = u_a$.

Therefore,

$$u = a \frac{u_a}{r}. \quad (2.24)$$

The strains can be expressed in terms of radial displacements as,

$$\varepsilon_r = \frac{du}{dr}, \quad (2.25)$$

$$\varepsilon_\theta = \frac{u}{r}. \quad (2.26)$$

As well, axial strain $\varepsilon_z = 0$ for the case of long cylinder due to the assumption of plain strain.

Substituting equation (2.24) in equations (2.25) and (2.26), the ε_r and ε_θ are expressed as,

$$\varepsilon_r = -a \frac{u_a}{r^2}, \quad (2.27)$$

$$\varepsilon_\theta = a \frac{u_a}{r^2}. \quad (2.28)$$

It is verified that ε_r and ε_θ , in equations (2.27) and (2.28) respectively, satisfies the incompressibility condition,

$$\varepsilon_r + \varepsilon_\theta + \varepsilon_z = 0. \quad (2.29)$$

The internal work of dissipation per unit volume, D , is expressed as

$$\begin{aligned} D &= \varepsilon_r \sigma_r + \varepsilon_\theta \sigma_\theta \\ &= \frac{u_a a}{r^2} (\sigma_\theta - \sigma_r). \end{aligned} \quad (2.30)$$

Since the stress distributions σ_r and σ_θ lie on the yield surface, and application of Tresca yield criterion gives,

$$D = \frac{u_a a}{r^2} \sigma_y. \quad (2.31)$$

The external work done by the internal pressure per unit length is given by,

$$W = 2\pi a p u_a. \quad (2.32)$$

Equating the internal energy of dissipation in equation (2.31) and the external work done in equation (2.32) we obtain an upper bound limit pressure as

$$p_L = \sigma_y \ln \left(\frac{b}{a} \right). \quad (2.33)$$

This is the same as the lower bound limit pressure in equation (2.22), therefore the limit pressure obtained in equation (2.33) is exact. Furthermore, the lower bound limit pressure obtained by considering the stress distribution in equation (2.16a) and equation (2.16b) is less than that given in equation (2.21) and (2.22) for $b > a$ thereby validating the lower bound theorem.

2.5 Pressure Vessel Design

Pressure vessels are usually designed according to the criteria given in the ASME Boiler & Pressure Vessel Code (ASME, 2001). The first edition of the code was issued several decades ago and has periodically incorporated significant changes since then. The earlier editions of code design rules pursued “design by rule” approach, which is based on relatively simple mechanics. Such design rules were re-examined (Cloud, 1972) such that they can accommodate more stringent safety requirements suitable for nuclear radiation hazards and to reduce over-conservatism in previous code rules.

Essentially, the changes in the code guidelines are intended to guard against three specific failure modes - gross plastic deformation, incremental plastic collapse and fatigue (ASME, 1972). These failure modes are precluded by failure criteria based on limit, shakedown and fatigue theories. The fundamental idea behind the changes in design rules is to indirectly address the inelastic failure mechanisms by simply performing elastic analysis.

The latter part of the code design philosophy is based on “design by analysis” approach. According to the approach, the designer is required to perform a detailed elastic stress analysis and categorize the calculated stress into primary, secondary and peak constituents and apply the specified allowable stress limits. Primary stress is an equilibrium stress field associated with gross plastic deformation under static loading. Secondary stress arises from compatibility requirements and is associated with ratchetting

under cyclic loading. Peak stress is highly localized and is associated with fatigue failure under cyclic load.

The design by analysis procedure was principally based on thin shell discontinuity theory. The stress distribution obtained from shell discontinuity analysis is in the form of membrane and bending stress and therefore, the code stress categories and stress limits are also in the same format. It is therefore difficult to equate the calculated stresses and code categories unless the design is based on shell analysis.

Currently, most of the design by analysis is performed using FEA. It is obvious that pressure vessel geometries are preferred to be modeled using shell type finite elements so that the post-processed results are obtained in the form of membrane and bending stresses used in the code. However, presence of pressure vessel assembly details such as reinforcements, fillets etc impose difficulty in using shell elements and require solid elements to be used. Now the problem with solid element type models is categorizing the calculated stress, which is not in the membrane plus bending format used in the codes. Especially with three-dimensional solid models, stress categorization becomes cumbersome (Hechmer and Hollinger, 1986).

One way of overcoming this problem is by using stress linearization technique (Kroenke, 1973). Stress linearization is a technique in which a stress classification line is chosen where the shell type deformations (plane sections remain plane) are expected. Along this line the calculated stresses through the thickness of the elements are linearized in order to

classify membrane and bending components. However, this procedure was found to be difficult in interpretation and the general validity of stress linearization has been questioned (Hechmer and Hollinger, 1991). This has led many workers to propose an approach away from design based on elastic analysis to a more fundamental approach in which the inelastic failure modes are assessed by performing inelastic analysis.

2.6 Inelastic Finite Element Analysis

The finite element method is a numerical technique, which can be applied for a wide range of engineering structures and continua. Generally, engineering structures are complex in geometry and loading. Such problems are mathematically intricate to be solved by classical analytical methods. FEA is a discrete analysis technique in which a large structure is divided into a number of simpler regions for which approximate solutions are ready-made. The procedure results in a large number of simultaneous algebraic equations, which are effectively solved using a computer.

With the recent advancements in computer technology, non-linear finite element methods make inelastic analysis a viable approach for many engineers. If non-linear analysis can be performed, application of code rules is considerably simpler than the elastic stress categorization approach. Inelastic analysis is often performed using commercially available software packages (ANSYS, 2000, ABAQUS, 2002).

Structures with linear elastic response are comparatively easier to solve than those experiencing inelastic deformation. In linear elastic analysis, the load-displacement relationship is linear. The problem is solved in a single-stage solution procedure. In inelastic analysis, the load-displacement relationship is non-linear and therefore, the total load is applied in increments. The problem is solved in an iterative manner, and is based on a piecewise linear or incremental solution method. For each load increment, the stiffness matrix is updated to take account of changes in material properties of the elastic-plastic region. Moreover, each load step must satisfy certain convergence criteria, thereby balancing the calculated internal forces and moments and the applied load.

Inelastic FEA is elaborate and provides considerable information about the constitutive behavior between the yield stress and collapse state of the structure. The analysis is complex and requires greater computing resources in order to perform several iterations to find the equilibrium displacements of load increments and store the intermediate results. With the abundant availability of computing memory in gigabytes, the restrictions on computing resources to perform non-linear FEA have significantly diminished.

However, the non-linear FEA poses certain drawbacks. The definition of material models and the control of load increments to define the material properties have to be done precisely. Knowledge of available non-linear techniques is mandatory to achieve convergence. Convergence failure often occurs for the load steps when the plasticity spread is significant and near collapse states thereby underestimating the limit loads.

Selection of appropriate element and its mesh density greatly affects the inelastic analysis results. The designer's experience and expertise also plays a major role in deciding the solution control process.

It is clear from the discussions made so far that the inelastic FEA is involved than the elastic analysis. Therefore, the selection of non-linear analysis has become subjective and there is a significant need to develop a relatively simple analysis procedure, which pressure vessel designers may use to utilize the inelastic design rules without having to become involved in complex inelastic analysis.

2.7 Development of Reduced Modulus Methods for Pressure Component Design

Reduced modulus methods are robust approximate methods, which are simple, reliable and based on linear elastic analysis. Robustness in this context implies the ability to provide acceptable results on the basis of less than reliable input, together with conceptual insight and economy of computational effort (Seshadri and Marriott, 1992). An established robust method the called reduced modulus method, primarily developed for stress categorization has been proven to be useful.

2.7.1 Methods based on Partial Elastic Modulus Modification

The development of reduced modulus methods is an attempt to aid the designer by identifying the distinction between primary and secondary stresses according to Code

rules. The method was initially developed by Jones and Dhalla (1981, 1986) to classify clamp-induced pipe stress in Liquid Metal Fast Breeder Reactor plants. They proposed that if the local stress developed by pipe/clamp interaction is redistributed, then the stress may be considered secondary. An inelastic analysis may be required to show how this redistribution proceeds, since it occurs only after yield. In the past, non-linear analysis was simply impracticable and so, an approach called the elastic secant modulus procedure was proposed.

The procedure is based on the concept that the local inelasticity can be simulated by reducing the elastic modulus of highly loaded elements. The proportion of stress at a location in a structure is adjudged primary or secondary if the ‘trend in relaxation’ (Dhalla, 1984) follows a load-controlled or deformation-controlled line. The characteristic of load-controlled stresses is that they are in equilibrium with the applied forces and moments and are statically determinate, whereas, the deformation controlled stresses occur in statically indeterminate locations.

Subsequently, Marriott (1988) showed instances of pressure vessel configurations where a designer could be misled in determining the stress classification as primary or secondary by inspection alone. He further proposed a reduced modulus procedure that utilized a series of iterative elastic analysis. According to the procedure, a linear elastic analysis is first performed and the elements with stress intensity S that exceeds the code

allowable stress, S_m are identified. The elastic modulus E_o of those elements are then modified according to the equation

$$E_m = \left(\frac{S_m}{S} \right) E_o. \quad (2.34)$$

It is evident that the change in the stress intensity after the second iteration indicates whether the stress component at any particular location is dominantly primary or secondary. Using the procedure for stress classification, Marriott illustrated that by obtaining equilibrium stress states for each iteration, lower bound limit loads can be evaluated. In his approach, a lower bound solution exists if the maximum stress after a number of iterations is less than the yield stress. The approach satisfies the lower bound theorem, which states that if a stress state is in equilibrium with the applied load and nowhere exceeds the yield stress then the applied load is a lower bound limit load.

A simple and systematic reduced modulus method called Generalized Local Stress and Strain (GLOSS) Analysis was proposed by Seshadri (1991a). The GLOSS method is based on two linear elastic FEA in which the first analysis is done with homogeneous material properties with mechanical and thermal loads applied to the structure. A second linear elastic FEA is performed by artificially reducing the elastic moduli of the elements that exceed the yield stress according to the equation

$$E_s = \left[\frac{\sigma_y}{\sigma_e} \right] E_o. \quad (2.35)$$

The ‘relaxation modulus’ is then evaluated in a GLOSS diagram, which is a plot of normalized equivalent stress and strain based on two linear elastic FEA. A simplified procedure to simulate the inelastic analysis of pressure components, that was demonstrated by Seshadri and Kizhatil (1990, 1991) proved effective for stress classification (Seshadri, 1990a). Other applications of GLOSS include multiaxial relaxation and creep damage (Seshadri, 1990b, 1991b), and, elevated temperature component design (Vaidyanathan et al. 1989).

In the ASME stress classification framework, primary stresses are load-controlled stresses. This is indicated as a 90-degree follow-up angle on the GLOSS plot (Figure 2.4). Load controlled stresses are statically determinate and are insensitive to inelastic constitutive relationships.

2.7.2 Gloss r-node Method

2.7.2.1 Concept of r-nodes

A simple method for determining the plastic collapse loads of mechanical components called GLOSS r-node method was proposed using the concept of r-nodes (Seshadri and Fernando, 1992). The method relies on identifying the “redistribution nodes” (r-nodes) in a structure. The r-nodes are described as skeletal points and can be thought of as nodes of redistribution of stresses.

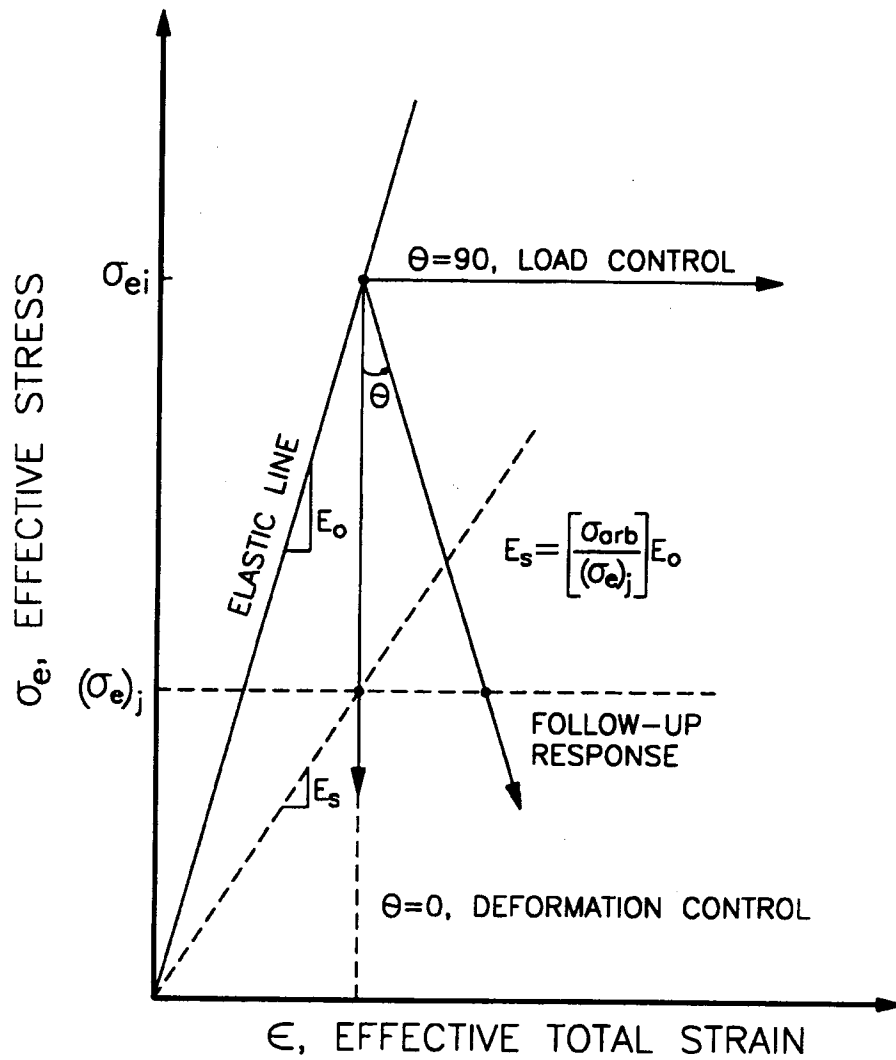


Figure 2.4. Follow-up Angle (θ) on the GLOSS Diagram

The concept of redistribution of stresses is akin to simulating the inelastic behavior of mechanical components. When the stresses in a given structure reach yield, redistribution occurs throughout the structure except at the load-controlled locations that are identically r-node locations (Figure 2.5). Therefore, the stress at r-node is called as the reference stress, which does not change throughout the inelastic redistribution process. Since the

2.7.2.2 r-nodes and Multiple Plastic Hinges

If a structure is statically determinate and inelastically deformed, only one plastic hinge forms prior to collapse of the structure. If a structure is statically indeterminate, a series of plastic hinges form and collapse occurs until the structure transforms itself into statically determinate, thereby developing a collapse mechanism. For statically indeterminate structures, the combined r-node effective stress is expressed as

$$\bar{\sigma}_n = \frac{\sum_{j=1}^N \sigma_{nj}}{N} \quad (2.39)$$

and the collapse load is given by

$$P_L = \left[\frac{\sigma_y}{\bar{\sigma}_n} \right] P \quad (2.40)$$

The formation of two plastic hinges in an indeterminate beam subjected to uniformly distributed load and its equivalent two-bar model is shown in Figure 2.6.

2.7.2.3 Procedure to Determine r-nodes

The procedure to identify r-nodes is straightforward. A linear elastic analysis is first performed and a pseudo-elastic stress distribution is obtained. A second linear elastic analysis is then performed by modifying the original elastic modulus E_o , according to the equation

$$E_s = \left[\frac{\sigma_{arb}}{(\sigma_e)_j} \right] E_o \quad (2.41)$$

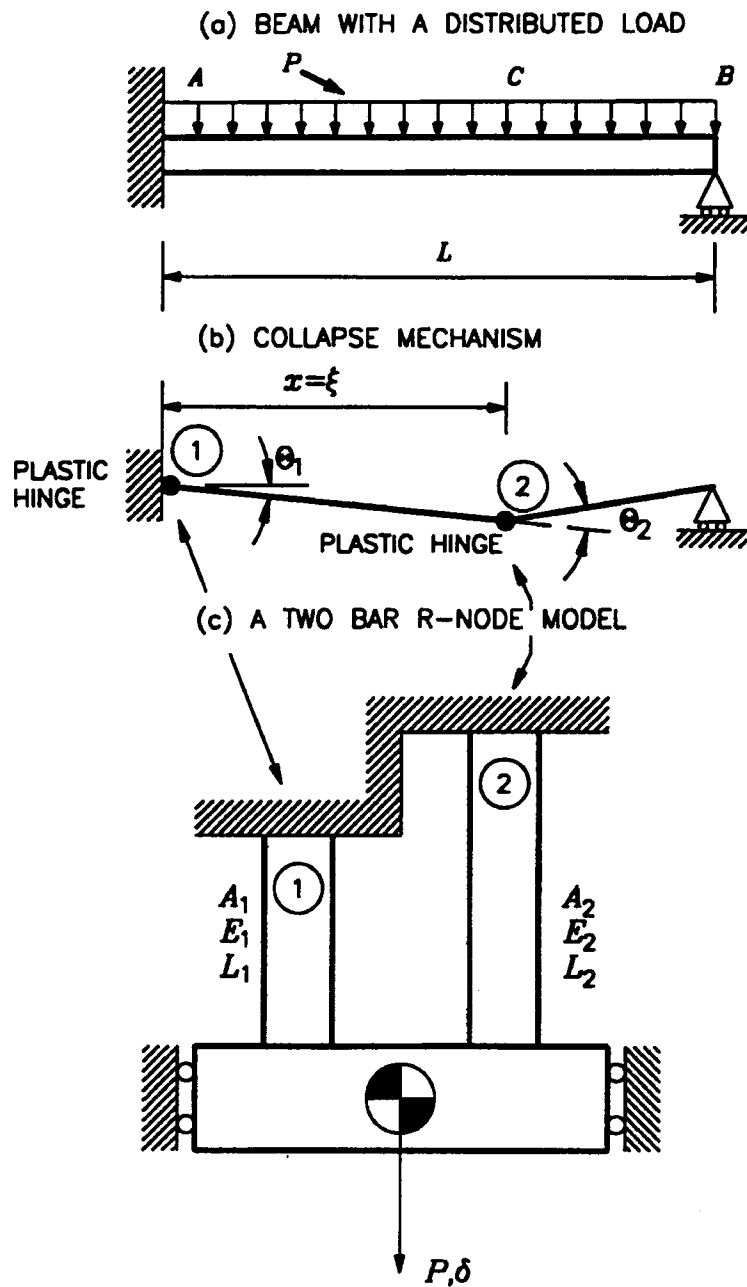


Figure 2.6. Indeterminate Beam subjected to Uniformly Distributed Load and the Two-Bar Model

where $(\sigma_e)_j$ is the equivalent stress at any given location j in the structure. The r-node locations are identified as the locations where the stresses remain unchanged for the two elastic analyses and the equivalent stresses at r-nodes reach yield at collapse load.

In r-node analysis, distinct r-node peaks may form that could represent well-defined plastic hinge locations or hinge contours. A reasonably good estimate of limit loads was obtained by carefully identifying the r-node peaks. Several aspects pertaining to proper identification of r-nodes from simple structures such as beams, frames, plates and complex structures like typical pressure vessel configurations were discussed by Seshadri (1997). The r-node stress peaks can be considered as a multi-bar model and the physical understanding of the redistribution and collapse process was depicted as conceptual model of r-node theory (Mangalaramanan, 1997a)

2.7.2.4 Applications of the r-node Method

Structures of applications in space are designed to possess minimum and optimal weight. The concept of r-nodes was utilized in designing the component with minimum weight (Mangalaramanan and Seshadri, 1997) so that the structure can perform its intended function with an optimal shape. The geometry of the structure was modified in such a way that uniform r-node stresses throughout the structure were achieved and it further collapses as a result of gross plastic deformation.

The fundamental concepts of r-nodes, reference stress, limit load and ASME stress classification framework were unified by Seshadri and Marriott (1992). The r-node stress was treated as reference stress and the limit load was arrived from the reference stress equation

$$\sigma_{ref} = \left(\frac{P_L}{P} \right) \sigma_y \quad (2.42)$$

It is essential to note that the equations (2.38) and (2.42) are identical and σ_{r-node} is used as σ_{ref} in the above equation. Using the r-node method, Seshadri and Kizhatil (1995) showed that the determination of limit loads for cracked components is useful in the determination of elastic-plastic energy release rate, J and creep growth parameter, C^* .

2.7.3 Elastic Compensation Method

2.7.3.1 Determination of Lower Bound Limit Loads

A simplified reduced modulus method called elastic compensation method to estimate limit loads for pressure vessel design was proposed by Mackenzie and Boyle (1993a). In this method, several equilibrium stress fields were generated in an iterative elastic FEA and the lower bound theorem was invoked to obtain conservative limit loads.

The statically admissible stress fields obtained in an iterative manner were achieved by adjusting the elastic modulus of each element and such elastic modulus adjustments simulate inelasticity. It was observed that the method arrived at stress distributions similar to limit type stress distribution. A typical convergence of maximum elastic stress in iterative elastic FEA is as shown in Figure 2.7. Since only linear elastic analysis was

performed, any linear solution can be simply scaled to obtain the limit load of the component.

The procedure to obtain lower bound limit load in elastic compensation method is outlined here. Initially, a conventional linear elastic FEA is performed for an arbitrary load. A second linear elastic FEA is then performed by adjusting the elastic modulus of each element according to the equation

$$E_{i+1} = \left(\frac{\sigma_n}{\sigma_i} \right) E_i \quad (2.43)$$

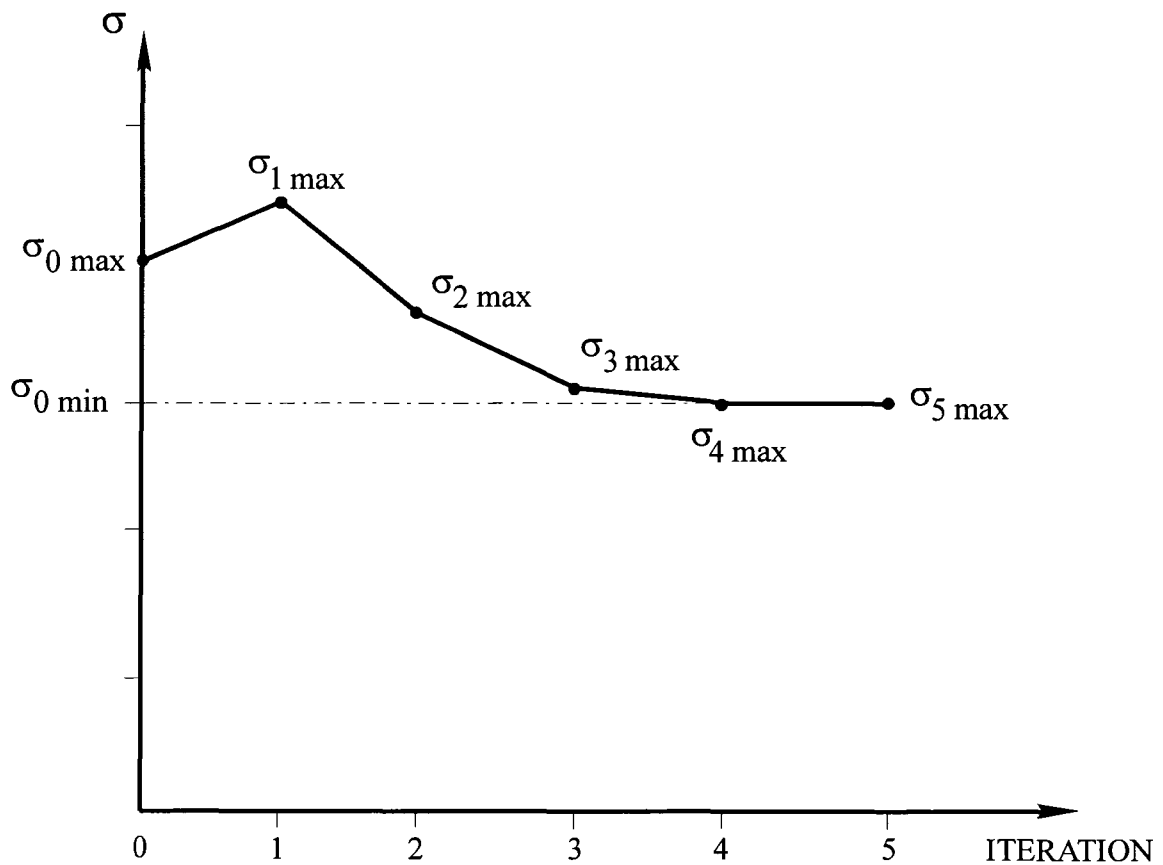


Figure 2.7 Convergence of Maximum Elastic Stress in an Iterative Elastic FEA

where σ_i is the maximum unaveraged nodal equivalent stress for an element in a finite element discretization. The significance of modifying the elastic modulus is to redistribute the stress in the component. The iterative procedure is carried out until the maximum stress reaches the lowest possible value thereby effectively minimizing the maximum stress in the component.

The lower bound limit load is identified by invoking the lower bound theorem, which states that, for a given load if the statically admissible stress exists in which the stress nowhere exceeds the yield stress of the material, then the load is a lower bound limit load. The limit load is determined from the equation

$$P_L = P_d \frac{\sigma_y}{\sigma_{\min}} \quad (2.44)$$

where P_d is applied load and σ_{\min} is the lowest possible maximum stress obtained after several iterations. It was emphasized that the method can be automated in any finite element software. The user simply solves the initial elastic model and then invokes the macro to obtain the limit load.

2.7.3.2 Determination of Upper Bound Limit Loads

As well as deriving lower bounds, upper bound limit loads were estimated (Mackenzie et al., 1993b) using the elastic compensation method. Essentially, in order to invoke the upper bound theorem, compatible sets of displacement and strain increments need to be defined. In elastic compensation method, the iterative procedure results in a solution similar to an anisotropic inhomogeneous state. The compatible displacements and

kinematically admissible strain fields consequent to each iteration were used to define the geometrically possible mode of deformation in a structure.

Using the principle of virtual work, the upper bound theorem may be expressed as

$$\sum P \dot{u} \leq \int_V \dot{D} dV \quad (2.45)$$

where P is the applied load. In the elastic compensation method, for an applied load P_n , the strain energy U_n and energy dissipation D_n can be calculated for each iteration i .

Therefore, the upper bound limit load is obtained as

$$P_{Li}^u = \frac{D_{ni}}{U_{ni}} P_n. \quad (2.46)$$

The best upper bound limit load is

$$P_L^u = \min(P_{Li}^u). \quad (2.47)$$

The elastic compensation method was demonstrated to estimate lower bound limit loads for nozzle–sphere interactions under internal pressure and radial loading (Nadarajah et al., 1993), torispherical heads under internal pressure (Shi et al., 1993) and axisymmetric thin shells under internal pressure (Boyle et al., 1997).

2.7.3.3 Features Relating to the Elastic Compensation Method

The key factors affecting the limit loads estimated by the iterative finite element procedure illustrated in elastic compensation method were studied in depth (Mackenzie et al., 1994). The parameters considered were mesh density and element order as they lead a major role in restricting the computing resources. It was found that the mesh density and

the element order could significantly affect the accuracy of the method. Best results are obtained when higher order elements with a fine mesh density are used. However, designers often restrict themselves with fairly course meshes especially when modeling 3D elements due to limitations in computational grounds. The use of averaged (nodal) stresses to estimate approximate limit loads was proposed when dealing with course meshes. Such an analysis might violate the lower bound theorem, as the nodal stresses are not equilibrium stress fields. However, the justification is appealing when 3-D pressure vessel configurations are modeled.

The method was used to analyze a branch pipe tee connection (Planq and Berton, 1998) subject to internal pressure with end axial load effect or out-of-plane moment. Mohamed et al. (1999) also applied the method to determine limit and shakedown loads. The technique was first applied to thick spherical and cylinder shells subjected to combined pressure and thermal gradient. Besides applying to thin spherical shells with cylindrical nozzle under internal pressure, suggestions were made for more analysis and verification for thermal loading cases.

Apart from limit loads, shakedown loads were also estimated for pressure vessel components (Mackenzie and Boyle, 1993c) and for axisymmetric nozzles (Mackenzie et al., 1995).

The progress of the elastic compensation method was reviewed by Mackenzie et al. (2000). It was noted that the analytical solutions of beam problems achieved accurate results than the finite element solution due to the use of discontinuous stiffness

modification in the finite element model. This resulted in an apparent over-conservatism in the lower bound solution. Therefore, it was suggested that modification of stiffness in a continuous varying form, that is, element level stiffness modification, may produce reasonably accurate results.

Moreover, the performance of elastic compensation method was studied for nozzle-cylinder intersections. The limit and shakedown interaction diagrams of nozzle-cylinder intersections subject to combined internal pressure and in-plane nozzle moment loading were obtained, and were found to be useful for sizing nozzles in cylindrical vessels. Practical issues in a complex pressure vessel configuration such as cylinder's representative length, which participates in the overall behavior and effect of fillet radius, were considered in the analysis.

2.7.3.4 Theoretical Justification for the Upper Bounds

The theoretical facets of elastic compensation method were established by Ponter and Carter (1997). They found that the collapse load of a von Mises yield criterion can be simulated by incompressible linear elastic stress distribution with a spatial variation of a shear modulus. It was further proved that the upper bound trajectory decreases monotonically in an iterative elastic analysis and converges to the collapse solution. However in most of the practical problems, the upper bound solution decreases monotonically to the least upper bound. It was also emphasized that the proof for the lower bound is lacking or possibly does not exist. Ponter et al. (2000) showed that the incompressibility in an iterative elastic analysis could be replicated by choosing

Poisson's ratio close to 0.5. Such a choice produces stress distribution, which converges to the yield surface.

2.8 Limitations of the Reduced Modulus Methods

The reduced modulus methods elaborated in this chapter are simplified methods to evaluate limit loads, which are related to primary stress. ASME Task Group (Pastor and Hechmer, 1997) was set up to discuss the methods for calculating the primary stress, the ASME limits on primary stress and use of Code stress classification table in pressure vessel design. The use of state-of-the-art analysis techniques to design pressure vessels was illustrated and the guidance of satisfying Code primary stress limits to the analysis results was provided. The report acknowledged the use of both GLOSS r-node method and elastic compensation method in pressure vessel design to satisfy primary stress limits.

However, these methods have their own drawbacks. It may be straightforward to identify r-nodes for simple structures whereas it has been argued that the identification of r-nodes is complex for general three-dimensional components. Seshadri (1997) has provided guidelines for identifying r-nodes nevertheless designers have to depend on practical experience to guess the r-node locations.

The lower bound limit loads estimated using the elastic compensation method, rely on the maximum equivalent stress in a structure. The maximum stress does not converge even after several iterations and there is no criterion that guarantees its convergence. The

criteria for convergence have been established for upper bound limit loads. However, their applicability to safe design may be confronted as they converge to the least possible upper bound and not the exact limit load. Furthermore, there is hardly any guidance to judge the difference between the least upper bound and the exact limit load.

2.9 Closure

The concepts inherent in the reduced modulus methods such as reference stress and load controlled stress are related to the lower bound theorem. The advantage of reduced modulus methods is that they are simple, based on linear elastic analysis and are applicable to complex components. However application of inelastic analysis to complex components especially three-dimensional structures may be laborious and time-consuming. Lower bound limit load estimates are obtained from a sequence of linear elastic analyses and the techniques have replaced the utilization of non-linear finite element analysis.

Mura and co-workers (1965) introduced the extended lower bound theorem using variational principles and have replaced the application of lower bound theorem to determine lower bound limit loads. Further explanations and investigations on the Mura's variational formulation and other successful methods that are based on Mura's formulation are presented in the following chapter.

CHAPTER 3: VARIATIONAL PRINCIPLES IN LIMIT ANALYSIS

3.1 Introduction

In this chapter, a detailed discussion on Mura's variational formulation (Mura et al. 1965), which is an alternate approach to the classical limit theorems, is presented. By making use of statically admissible stress distributions and kinematically admissible strain distributions and invoking the integral mean of yield, pseudo elastic distributions of stress that exceed yield were utilized for determining upper and lower bound limit loads.

It was realized that lower bound limit load determined using Mura's extended lower bound theorem, are no better than classical lower bound limit load. In an attempt of improvement, Seshadri and Mangalaramanan (1997) proposed m_α -method, which is used in conjunction with EMAP. Further explanations and discussions on the methods developed from Mura's variational formulation are presented in this chapter.

3.2 Mura's Variational Formulation

Consider a structure made of elastic-perfectly-plastic material that is in equilibrium under surface traction T_i applied on surface S_T , and on surface S_V , constraint $v_i = 0$ is applied as shown in Figure 3.1. It is assumed that the surface traction is applied in proportional loading, that is, external tractions is assumed to be ηT_i , where η is a

monotonically increasing parameter. For small values of η , the structure will be in a purely elastic state. As η is gradually increased, plastic flow starts to occur at a point and spreads to several parts in the structure. When the load of mT_i is applied where $\eta = m$, the structure will be in a state of impending plastic collapse. The set of loads mT_i is the collapse load of a structure and m is the safety factor.

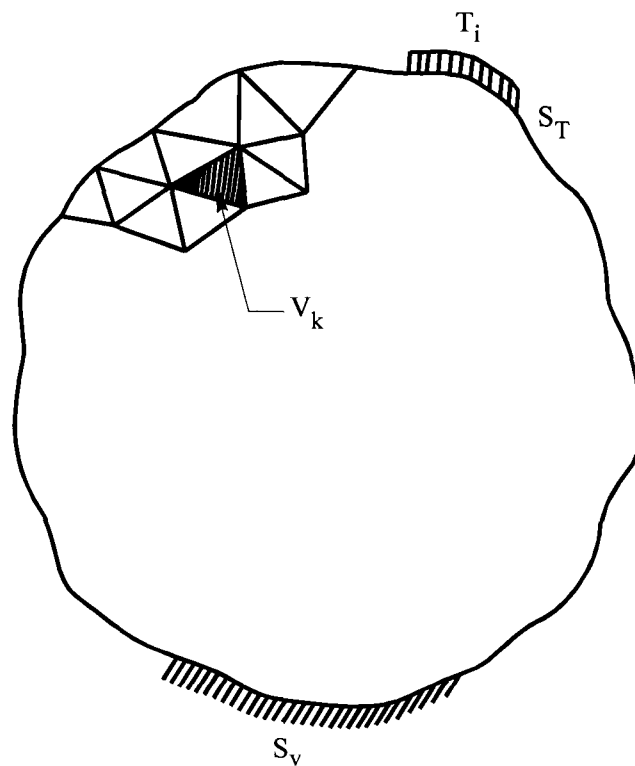


Figure 3.1. An Elastic-Perfectly-Plastic Body

At the state of impending plastic collapse, the following conditions are satisfied.

$$\sigma_{ij,j} = 0 \quad \text{in } V_T, \quad (3.1)$$

$$\sigma_{ij} n_j = m T_i \quad \text{on } S_T, \quad (3.2)$$

$$s_{ij} s_{ij} = 2k^2, \quad (3.3)$$

$$\dot{\varepsilon}_{ij} = \mu s_{ij} \quad \text{where } s_{ij} s_{ij} = 2k^2, \quad (3.4)$$

$$\dot{\varepsilon}_{ij} = 0 \quad \text{where } s_{ij} s_{ij} < 2k^2, \quad (3.5)$$

$$\varepsilon_{ij} = \frac{1}{2}(v_{i,j} + v_{j,i}), \quad (3.6)$$

$$\dot{\varepsilon}_{ii} = 0 \quad \text{in } V_T, \quad (3.7)$$

$$v_i = 0 \quad \text{on } S_V \quad (3.8)$$

where

$$s_{ij} = \sigma_{ij} - \delta_{ij} \sigma, \quad (3.9)$$

and
$$\sigma = \frac{1}{3} \sigma_{kk}. \quad (3.10)$$

Equations (3.1) and (3.2) are the equilibrium condition, (3.3) indicates that the stress state is on the yield surface, (3.4) is the plastic potential flow law for the stress state on the yield surface, (3.5) indicates that there is no plastic flow for stress state that lies within the yield surface, (3.6) is the definition for the strain tensor, (3.7) is the incompressibility condition, (3.9) is the definition for the stress deviator tensor and (3.10) is the definition for the mean stress tensor.

In the previous chapter, it was discussed that a stress field σ_{ij}^0 is said to be statically admissible if it satisfies

$$\sigma_{ij}^0{}_{,j} = 0 \quad \text{in } V_T, \quad (3.11)$$

$$\sigma_{ij}^0 n_j = m_s T_i \quad \text{on } S_T, \quad (3.12)$$

$$f(s_{ij}^0) = \frac{1}{2} s_{ij}^0 s_{ij}^0 - k^2 \leq 0 \quad \text{in } V_T \quad (3.13)$$

where superscript “0” indicates statically admissible states. The proportional constant m_s defined in equation (3.12) is termed the statically admissible multiplier.

Furthermore, a velocity field v_i^* is said to be kinematically admissible if it satisfies,

$$\delta_{ij} v_i^*{}_{,j} = 0 \quad \text{in } V_T, \quad (3.14)$$

$$v_i^* = 0, \quad \text{in } V_T, \quad (3.15)$$

$$\int_{S_T} T_i v_i^* dS > 0,$$

The kinematically admissible multiplier m^* is defined as,

$$m^* = \frac{k \int_{V_T} (2 \dot{\epsilon}_{ij}^* \dot{\epsilon}_{ij}^*)^{1/2} dV}{\int_{S_T} T_i v_i^* dS}. \quad (3.16)$$

According to the limit theorems, it can be stated that

$$m_s \leq m \leq m^*. \quad (3.17)$$

Using the calculus of variations, Mura and Lee (1963) have shown that for a perfectly plastic material, the safety factor, m is the extremum value of the functional,

$$F(s_{ij}, v_i) = \int_{V_T} s_{ij} \frac{1}{2} (v_{i,j} + v_{j,i}) dV \quad (3.18)$$

subject to constraint conditions,

$$\delta_{ij} v_{i,j} = 0, \quad (3.19)$$

$$v_i = 0, \quad (3.20)$$

$$\int_{S_T} T_i v_i dS > 0, \quad (3.21)$$

$$\int_{V_T} \mu \{f(s_{ij}) + (\phi)^2\} dV = 0. \quad (3.22)$$

In order to find the extremum value of the functional F in (3.18), it is transformed into $F_1(s_{ij}, v_i)$ by employing a point-function Lagrangian multipliers σ , R_i , μ and a constant Lagrangian multiplier m as follows.

$$\begin{aligned} F_1[v_i, s_{ij}, \sigma, R_i, m, \mu, \phi] = & \int_{V_T} s_{ij} \frac{1}{2} (v_{i,j} + v_{j,i}) dV + \int_{V_T} \sigma \delta_{ij} v_{i,j} dV \\ & - \int_{S_V} R_i v_i dS - m \left(\int_{S_T} T_i v_i dS - 1 \right) - \int_{V_T} \mu [f(s_{ij}) + \phi^2] dV \end{aligned} \quad (3.23)$$

Setting the variation of the functional F_1 equal to zero yields the following conditions,

$$\frac{1}{2} (v_{i,j} + v_{j,i}) = \mu \frac{\partial f}{\partial s_{ij}} \quad \text{in } V_T, \quad (3.24)$$

$$\mu \geq 0,$$

$$(s_{ij} + \delta_{ij} \sigma)_{,j} = 0 \quad \text{in } V_T, \quad (3.25)$$

$$(s_{ij} + \delta_{ij} \sigma) n_j = m T_i \quad \text{on } S_T, \quad (3.26)$$

$$(s_{ij} + \delta_{ij} \sigma) n_j = R_i \quad \text{on } S_V, \quad (3.27)$$

$$f(s_{ij}) + \varphi^2 = 0 \quad \text{in } V_T, \quad (3.28)$$

$$\mu \varphi = 0 \quad \text{in } V_T, \quad (3.29)$$

$$\delta_{ij} v_{i,j} = 0 \quad \text{in } V_T, \quad (3.30)$$

$$v_i = 0 \quad \text{on } S_V, \quad (3.31)$$

$$\int_{S_T} T_i v_i dS = 1. \quad (3.32)$$

Equation (3.24) is the plastic potential flow law, (3.25) to (3.27) are the equilibrium conditions and (3.30) to (3.32) define a kinematically admissible velocity field. Equations (3.28) and (3.29) define the admissible domain of the stress space, i.e.,

$$f(s_{ij}) = 0 \quad \text{if } \mu > 0, \quad (3.33)$$

$$f(s_{ij}) \leq 0 \quad \text{if } \mu = 0. \quad (3.34)$$

Apparently, equations (3.25) to (3.32) are the conditions of the incipient plastic flow which are the same as (3.1) to (3.8). It should also be noted that equation (3.32) is no more than restrictive than the requirement

$$\int_{S_T} T_i v_i dS > 0.$$

Setting the integral equal to unity only determines the scale of the otherwise arbitrary size of the velocity vector.

3.3 The Extended Lower Bound Theorem

Mura et al. (1965) developed an extended lower bound theorem, in an attempt to develop an alternative approach to classical limit analysis. In classical limit analysis, the statically admissible stress field cannot lie outside the hypersurface of the yield criterion and the stress field obtained from the kinematically admissible velocity field should lie on the hypersurface. Mura and coworkers circumvented such a criterion and replaced it by the ‘integral mean of yield criterion’. Mura’s extended lower bound theorem is stated as an inequality

$$m' = \frac{m^0}{1 + \frac{\max[f(s_{ij}^0) + (\phi^0)^2]}{2k^2}} \leq m \quad (3.35)$$

holds for any set of s_{ij}^0 , σ^0 , m^0 , μ^0 and ϕ^0 satisfying

$$(s_{ij}^0 + \delta_{ij} \sigma^0)_{,j} = 0 \quad \text{in} \quad V_T, \quad (3.36)$$

$$(s_{ij}^0 + \delta_{ij} \sigma^0) n_j = m^0 T_i \quad \text{on} \quad S_T, \quad (3.37)$$

$$\int_{V_T} \mu^0 [f(s_{ij}^0) + (\phi^0)^2] dV = 0, \quad (3.38)$$

$$\mu^0 \geq 0. \quad (3.39)$$

where the “0” indicates statically admissible states and the condition (3.38) is the integral mean of yield criterion.

Mura’s lower bound theorem is proven as follows. Consider the arbitrary arguments,

$$v_i^0 = v_i + \delta v_i, \quad s_{ij}^0 = s_{ij} + \delta s_{ij}, \dots, \quad (3.40)$$

Substituting the arguments (3.40) in the functional F_1 in (3.23) and with regards to conditions (3.24) to (3.32), F_1 is modified to F_2 as

$$\begin{aligned} F_2[v_i^0, s_{ij}^0, \sigma^0, R_i^0, m^0, \mu^0, \varphi^0] = & m + \int_{V_T} \delta s_{ij} \frac{1}{2} (\delta v_{i,j} + \delta v_{j,i}) dV + \int_{V_T} \delta \sigma \delta_{ij} \delta v_{i,j} dV \\ & - \int_{S_V} \delta R_i \delta v_i dS - \delta m \left(\int_{S_T} T_i \delta v_i dS - 1 \right) \\ & - \int_{V_T} \mu \left[\frac{1}{2} \delta s_{ij} \delta s_{ij} + (\delta \varphi)^2 \right] dV - \int_{V_T} \delta \mu [f(s_{ij}^0) + (\varphi^0)^2] dV . \end{aligned} \quad (3.41)$$

Integrating second and third term by parts and using conditions (3.25) to (3.27), (3.36) and (3.37) and setting,

$$(s_{ij}^0 + \delta_{ij} \sigma^0) n_j = R_i^0 \quad \text{on} \quad S_V, \quad (3.42)$$

equation (3.41) can be further simplified to

$$F = m - \int_{V_T} \mu \left[\frac{1}{2} \delta s_{ij} \delta s_{ij} + (\delta \varphi)^2 \right] dV - \int_{V_T} \delta \mu [f(s_{ij}^0) + (\varphi^0)^2] dV . \quad (3.43)$$

Also, integrating equation (3.23) with arbitrary arguments $v_i^0, s_{ij}^0, \sigma^0, R_i^0, m^0, \mu^0$ and φ^0 subject to constraint conditions (3.36), (3.37) and (3.42) gives

$$F = m^0 - \int_{V_T} \mu^0 [f(s_{ij}^0) + (\varphi^0)^2] dV . \quad (3.44)$$

Using equation (3.38), (3.43) and (3.44) yield

$$m^0 \leq m - \int_{V_T} \delta\mu [f(s_{ij}^0) + (\phi^0)^2] dV \quad (3.45)$$

since $\int_{V_T} \mu [\frac{1}{2} \delta s_{ij} \delta s_{ij} + (\delta\phi)^2] dV$ is positive definite. Constraint condition (3.38) can

be rewritten to give

$$- \int_{V_T} \delta\mu [f(s_{ij}^0) + (\phi^0)^2] dV = \int_{V_T} \mu [f(s_{ij}^0) + (\phi^0)^2] dV \quad (3.46)$$

since $\mu^0 = \mu + \delta\mu$. Substituting equation (3.46) into (3.45) and taking the maximum value of the integrand we have

$$m^0 \leq m + \max [f(s_{ij}^0) + (\phi^0)^2] \int_{V_T} \mu dV \quad (3.47)$$

Using equation (3.32), it is observed that,

$$m = m \int_{S_T} T_i v_i dS = 2k^2 \int_{V_T} \mu dV, \quad (3.48)$$

which upon rearranging yields,

$$\int_{V_T} \mu dV = \frac{m}{2k^2} \quad (3.49)$$

Substituting (3.49) into (3.47) proves the Mura's lower bound theorem defined in equation (3.35).

It is evident from Mura's variational formulation that the formulation is limited to structures with elastic-perfectly-plastic material and does not account for the strain hardening effect. Furthermore, the strain distribution in equation (3.6) is limited to small deformation and does not include large deformations.

3.4 Finite Element Implementation of Mura's Formulation

Mura et al. (1965) have shown that m^0 , μ^0 and ϕ^0 can be determined by setting the variation of functional,

$$F = m^0 - \int_{V_T} \mu^0 [f(s_{ij}^0) + (\phi^0)^2] dV \quad (3.50)$$

with respect to m^0 , μ^0 and ϕ^0 to zero. i.e.,

$$\frac{\partial F}{\partial m^0} = 0; \quad \frac{\partial F}{\partial \mu^0} = 0; \quad \frac{\partial F}{\partial \phi^0} = 0. \quad (3.51)$$

Making use of equation (3.13), equation (3.50) can be further expanded as

$$F = m^0 - \int_{V_T} \mu^0 \left[\frac{1}{2} (m^0)^2 \tilde{s}_{ij}^0 \tilde{s}_{ij}^0 - k^2 + (\phi^0)^2 \right] dV. \quad (3.52)$$

where $s_{ij}^0 = m^0 \tilde{s}_{ij}^0$ and \tilde{s}_{ij}^0 corresponds to the applied traction T_i . The von-Mises equivalence for a uniaxial state of stress can be written as

$$\frac{1}{2} \tilde{s}_{ij}^0 \tilde{s}_{ij}^0 = \frac{(\sigma_e^0)^2}{3} \quad (3.53)$$

and
$$k^2 = \frac{\sigma_y^2}{3}. \quad (3.54)$$

Substituting equations (3.53) and (3.54) in (3.52), we get,

$$F = m^0 - \int_{V_T} \frac{\mu^0}{3} [(m^0)^2 (\sigma_e^0)^2 - \sigma_y^2 + 3 (\phi^0)^2] dV. \quad (3.55)$$

By setting the variation of F to zero, Seshadri and Mangalaramanan (1997) obtained an upper bound multiplier m^0 as

$$m^0 = \frac{\sigma_y \sqrt{V}}{\sqrt{\int_{V_T} \sigma_e^2 dV}}. \quad (3.56)$$

In a finite element discretization scheme, equation (3.56) is written as,

$$m^0 = \frac{\sigma_y \sqrt{V_T}}{\sqrt{\sum_{k=1}^N (\sigma_{ek})^2 \Delta V_k}} \quad (3.57)$$

where N is the total number of elements, σ_{ek} and ΔV_k are the effective stress and volume of the k^{th} element respectively. Likewise, Mura's lower bound multiplier can be expressed as,

$$m' = \frac{2 m^0 \sigma_y^2}{\sigma_y^2 + (m^0)^2 (\sigma_M)^2} \quad (3.58)$$

where σ_M is the maximum effective stress in a structure.

Using EMAP in concurrence with linear elastic FEA, statically admissible stress distributions and kinematically admissible strain distributions can be generated. For successive iterations, the elastic modulus is modified according to the equation,

$$E_{i+1} = \left(\frac{\sigma_{arb}}{\sigma_e} \right)^q E_i \quad (3.59)$$

where the subscript i is the iteration number and q is the modulus adjustment parameter and is usually taken as unity. A typical variation of m^0 and m' with iteration ζ for well

designed components will be as shown in the Figure 3.2. For the sake of comparison, the classical upper bound m_u and lower bound m_L are also shown in the figure.

It is noted that m^0 is an upper bound and m' is a lower bound and their proofs are presented in the forthcoming sections. Essentially, such bounds are obtained from statically admissible states and they do not have to lie within the yield surface.

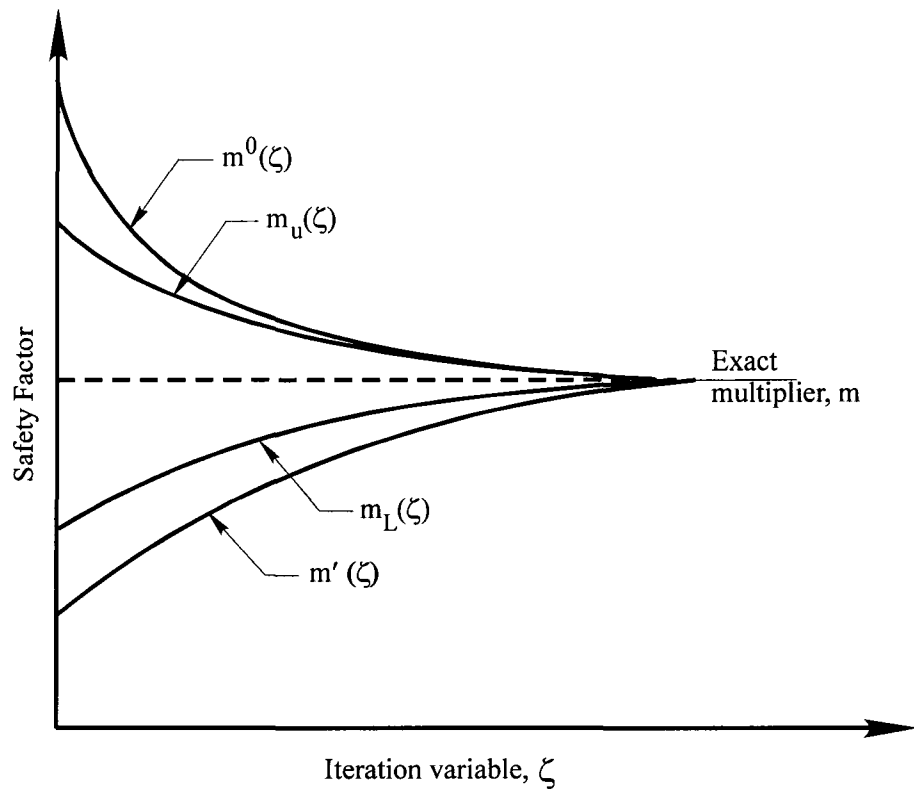


Figure 3.2. Variation of m^0 and m' with iteration ζ

3.5 m-alpha Multiplier Method

It is seen from the previous section that the Mura's lower bound multiplier m' , produce lower bounds that are no better than m_L . In an objective of achieving a superior lower bound, Seshadri and Mangalaramanan (1997) proposed the m_α -method. The method is akin to the reduced modulus method in which, m_α , a statically admissible multiplier, is determined on the basis of two linear elastic finite element analyses by leapfrogging to the limit state. The first linear elastic FEA corresponds to conventional linear elastic analysis whereas in the second linear elastic FEA, the elastic modulus of each element is modified according to the equation (3.59). The derivation of m_α -multiplier is discussed below.

The m_α - method is proposed to be used in conjunction with EMAP. Therefore, to start with, it is convenient to express m' in terms of an iteration variable ζ . Rewriting equation (3.58),

$$m'(\zeta) = \frac{2m^0(\zeta)\sigma_y^2}{\sigma_y^2 + [m^0(\zeta)]^2 [\sigma_M(\zeta)]^2} \quad (3.60)$$

In the above equation, the multipliers m^0 , m' and the maximum stress σ_M are expressed in terms of ζ . Differentiating equation (3.60) with respect to ζ ,

$$\frac{dm'}{d\zeta} = \frac{\partial m'}{\partial m^0} \frac{\partial m^0}{\partial \zeta} + \frac{\partial m'}{\partial \sigma_M^0} \frac{\partial \sigma_M^0}{\partial \zeta} \quad (3.61)$$

Equation (3.61) can be expressed in terms of finite differences as

$$\Delta m' = \left. \frac{\partial m'}{\partial m^0} \right|_{\zeta_i} (\Delta m^0) + \left. \frac{\partial m'}{\partial \sigma_M} \right|_{\zeta_i} (\Delta \sigma_M) \quad (3.62)$$

where $\zeta = \zeta_i$ corresponds to the i th iteration. Although equation (3.62) holds good for any iteration, it is intended to estimate m_α only from two iterations. In other words, the multipliers m^0 and m' are expected to converge to m_α at the subsequent iteration. Therefore, the following quantities can be defined.

$$\Delta m' = m_\alpha - m_i' \quad (3.63a)$$

$$\Delta m^0 = m_\alpha - m_i^0 \quad (3.63b)$$

and

$$\Delta \sigma_M = \frac{\sigma_y}{m_\alpha} - \sigma_{Mi} \quad (3.63c)$$

Substituting equations (3.63) in (3.62) results in a quadratic equation to be solved for m_α . The greatest root of the quadratic equation is adjudged as the solution for m_α , which is expressed as

$$m_\alpha = 2m^0 \frac{2 \left(\frac{m^0}{m_L} \right)^2 + \sqrt{\frac{m^0}{m_L} \left(\frac{m^0}{m_L} - 1 \right)^2 \left(1 + \sqrt{2} - \frac{m^0}{m_L} \right) \left(\frac{m^0}{m_L} - 1 + \sqrt{2} \right)}}{\left(\left(\frac{m^0}{m_L} \right)^2 + 2 - \sqrt{5} \right) \left(\left(\frac{m^0}{m_L} \right)^2 + 2 + \sqrt{5} \right)} \quad (3.64)$$

With reference to the equation (3.64), it is seen that m_α depends on quantities, m^0 and m^0/m_L and it is also evident that we get imaginary roots for $m^0/m_L > 1 + \sqrt{2}$. This is typically the case for the components that contain sharp cracks or notches.

The procedure involved in the determination of m_α multiplier is straightforward. For a prescribed loading, a linear elastic FEA is performed. Subsequent iterations can be carried out by adjusting the elastic modulus of each element according to the equation (3.59).

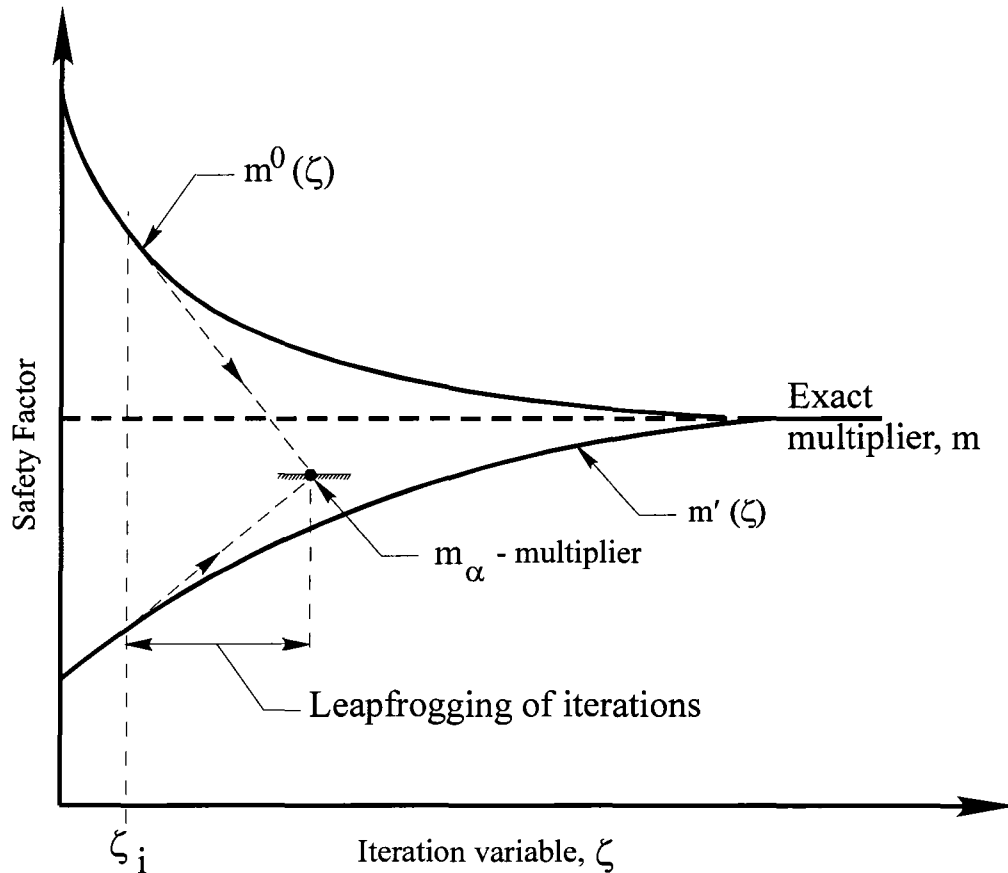


Figure 3.3. Leapfrogging to the Limit State

It was suggested by Seshadri (2000) that m_α can be determined from the successive iterations in an elastic modulus adjustment procedure (EMAP) and the estimate was found to be better as the iterations proceed. The multiplier m_α is determined from

partially converged stress distribution and therefore the convergence rate of m_α is faster than the classical limit multiplier. The idea of leap-frogging of iterations is shown in the Figure 3.3. The m_α determination procedure can be automated by a subroutine built into commercially available finite element software.

3.6 Upper Bound Multiplier – m^0

For components that undergo localized plastic collapse, the method was found to produce overestimated m^0 (upper bounds) and underestimated m_L and m' (lower bounds) when the calculations were based on the total volume. In such cases, the concept of reference volume was proposed to be effective.

3.6.1 Local Plastic Collapse – Notion of Reference Volume (V_R)

The concept of reference volume is useful to identify the “kinematically active” portion of the structure that participates in the plastic action. If V_R is the reference volume, such that $V_R \leq V$, then m^0 - multiplier in equation (3.57) is expressed as

$$m^0(V_R) = \frac{\sigma_y \sqrt{V_R}}{\sqrt{\sum_{k=1}^R (\sigma_{ek})^2 \Delta V_k}} \quad (3.65)$$

where $V_R = \sum_{k=1}^R (\Delta V_k)$ and $R < N$.

To identify the reference volume, first the elements are arranged in descending order of energy dissipation, i.e.,

$$(\sigma_{e1}^0)^2 \Delta V_1 > (\sigma_{e2}^0)^2 \Delta V_2 > \dots > (\sigma_{eN}^0)^2 \Delta V_N \quad (3.66)$$

For any given iteration, the value of m^0 in equation (3.65) will increase with the addition of volumes. The variation of m^0 for the first and second iteration is shown in the Figure 3.4. The volume corresponding to the intersection of two curves is adjudged the reference volume V_R .

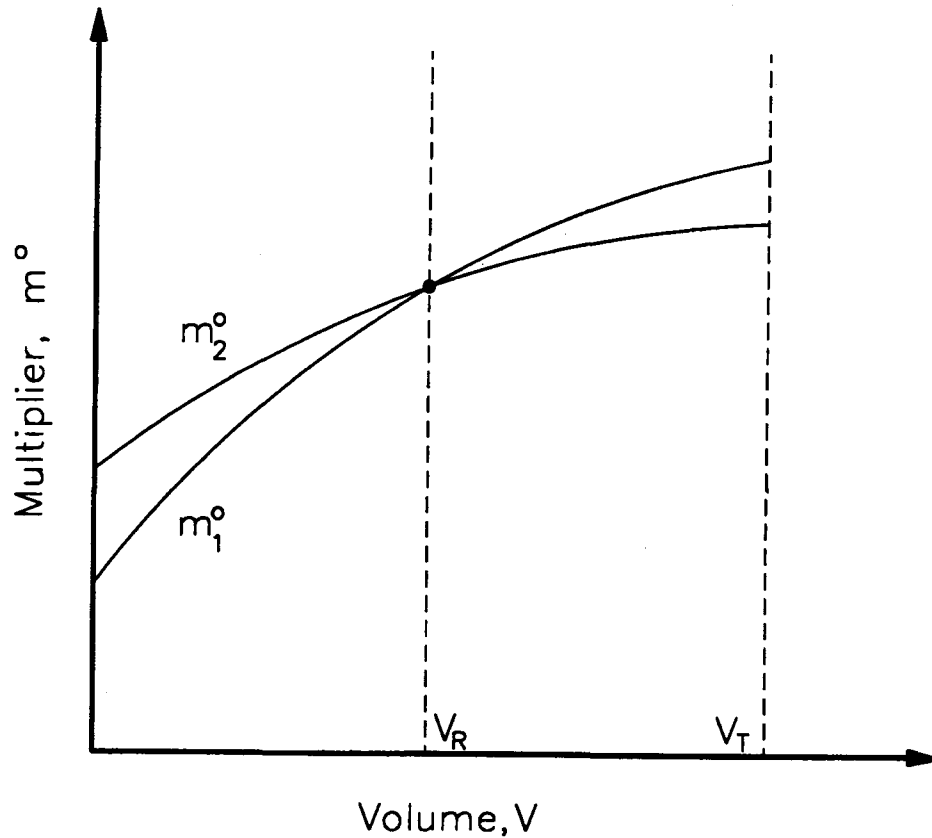


Figure 3.4. Identification of the Reference Volume, V_R

The notion of reference volume enables better bounds by identifying the kinematically active volumes separated from the total volume of the structure. The introduction of reference volume facilitates the narrowing of the spread between the upper and lower bounds m^0 and m' respectively. It is apparent that the sub-volumes are also in static equilibrium as long as internal forces and moments are in equilibrium with the external tractions. Although, the reference volume concept was found to give better bounds for the first two iterations, the performance is not guaranteed for successive iterations.

3.6.2 Plastic Flow Parameter

Using the concepts of Mura's variational formulation, Pan and Seshadri (2002) derived an upper bound multiplier by distributing the plastic flow parameter throughout the structure. The formulation is based on the fact that the plastic flow differs at locations at the state of collapse. Therefore, the plastic flow parameter μ^0 is distributed to the degree of plastic flow at a given location, that is, for a highly plastic region, higher flow parameter is allotted and vice versa. Conceptually, the secant modulus of each element in a finite element discretization is adjusted in a weighted average sense.

In order to derive an upper bound multiplier by distributing the flow parameter, consider the integral mean of yield criterion,

$$\int_{V_T} \mu^0 \{ f(s_{ij}^0) + (\phi^0)^2 \} dV = 0. \quad (3.67)$$

Realizing that,

$$f(s_{ij}^0) = \frac{1}{3}(m^0 \sigma_e^2 - \sigma_y^2) \quad (3.68)$$

equation (3.62) is expanded as

$$\int_{V_T} \frac{\mu^0}{3} [(m^0 \sigma_e^2 - \sigma_y^2) + 3(\phi^0)^2] dV = 0. \quad (3.69)$$

It is implied that ϕ^0 is zero if the stress state lies on the yield surface and $\phi^0 > 0$ for stress states that lie within the yield surface. As the flow parameter μ^0 is very low in the elastic regions and it is reasonable to neglect the product $\mu^0 \phi^0$ in equation (3.69).

Equation (3.69) can be rewritten to evaluate the multiplier m^0 , re-defined as m_2^0

$$m_2^0 = \frac{\sigma_y \sqrt{\int_{V_T} \mu^0 dV}}{\sqrt{\int_{V_T} \mu^0 \sigma_e^2 dV}}. \quad (3.70)$$

In the above equation m^0 is re-defined as m_2^0 .

Identifying that,

$$\mu^0 = \frac{C}{E_s} \quad (3.71)$$

where C is a constant whose value depends on the geometry and loading on the structure. Substituting equation (3.70) in (3.71), the upper bound multiplier m_2^0 , which is based on distributed flow parameter is expressed as

$$m_2^0 = \frac{\sigma_y \sqrt{\int_{V_T} \frac{1}{E_s} dV}}{\sqrt{\int_{V_T} \frac{1}{E_s} (\sigma_{ek})^2 dV}}. \quad (3.72)$$

Unlike the constant flow parameter formulation, expressed in equation (3.57), the upper bound multiplier m_2^0 was found to converge close to the exact solution with successive iterations in modulus adjustment scheme. Furthermore, the m_α -multiplier can be determined using the notion of leap-frogging to the limit state. The method was applied to generic pressure vessel configurations and it was noted that the convergence rate of m_α was faster.

For any stress distribution other than limit state, the flow parameter is μ^0 and at the limit state it is μ . It is vital to note that for successive iterations, the stress distribution converges to limit state stress distribution. Therefore the distribution of plastic flow parameter μ^0 will be closer to the distribution of the actual flow parameter μ at the limit state.

3.7 Bounds on the Limit Load Multipliers

Reinhardt and Seshadri (2003) examined the theoretical proofs for m^0 as an upper bound multiplier (based on both constant flow parameter and distributed flow parameter formulation), m' as lower bound multiplier and bounding nature of m_α as a lower bound multiplier. The details of the proofs are presented below.

3.7.1 Mura's Lower Bound Multiplier - m'

Mura's lower bound multiplier, m' , in equation (3.58) can be shown to be equivalent to,

$$m' = \frac{2m^0}{1 + \left(\frac{m^0}{m_L}\right)^2} \leq m. \quad (3.73)$$

The following variables can now be defined by normalizing them with the exact collapse load multiplier, m .

$$R_L = \frac{m_L}{m}, \quad R_U = \frac{m_U}{m}, \quad R' = \frac{m'}{m} \quad \text{and} \quad R_0 = \frac{m^0}{m}. \quad (3.74)$$

By the definition of limit load theorems, it is realized that,

$$R_L \leq 1, \quad R_U \geq 1 \quad (3.75)$$

Therefore, using equations (3.74), (3.73) can be expressed in normalized form,

$$R' = \frac{2R_0}{1 + \left(\frac{R_0}{R_L}\right)^2} \leq 1 \quad (3.76)$$

Since $\frac{R_0}{R_L} \geq 1$, it is realized that Mura's lower bound multiplier, m' is a lower bound.

Furthermore, it can be shown that $m' \leq m_L$ by assuming that the L.H.S of equation (3.76)

is less than or equal to R_L . That is,

$$R' = \frac{2R_0}{1 + \left(\frac{R_0}{R_L}\right)^2} \leq R_L \Leftrightarrow 2\frac{R_0}{R_L} \leq 1 + \left(\frac{R_0}{R_L}\right)^2 \Leftrightarrow 0 \leq 1 - 2\frac{R_0}{R_L} + \left(\frac{R_0}{R_L}\right)^2 = \left(1 - \frac{R_0}{R_L}\right)^2. \quad (3.77)$$

Therefore, it is verified that $R' \leq R_L \leq 1$, whether or not R_0 is an upper bound. At the limit state, $R' = R_L = 1$.

3.7.2 Upper Bound Multiplier - m_1^0

It is shown below that the multiplier m_1^0 , is greater than m_L , that is,

$$m_1^0 = \frac{\sigma_y \sqrt{V_T}}{\sqrt{\int_{V_T} (\sigma_{eq})^2 dV}} = \frac{\frac{\sigma_y}{\sigma_{\max}} \sqrt{V_T}}{\sqrt{\int_{V_T} \left(\frac{\sigma_{eq}}{\sigma_{\max}}\right)^2 dV}} = m_L \frac{\sqrt{\int_{V_T} 1^2 dV}}{\sqrt{\int_{V_T} \left(\frac{\sigma_{eq}}{\sigma_{\max}}\right)^2 dV}} \geq m_L . \quad (3.78)$$

The term in the square root is always greater than one as $\sigma_{eq} \leq \sigma_{\max} = \max(\sigma_{eq})$, and

therefore $\int_{V_T} 1^2 dV \geq \int_{V_T} \left(\frac{\sigma_{eq}}{\sigma_{\max}}\right)^2 dV$. The multiplier m_1^0 may not converge to limit

multiplier m , $R_1^0 \geq 1$ and the equality holds at the limit state. It is vital to note that

$R_1^0 = 1$ can occur as long as the stress distribution in all parts of the structure reaches the σ_{\max} . In other words, the condition $\sigma_{eq} = \sigma_{\max}$ must be satisfied everywhere in the structure.

It can also be shown that m_1^0 is an upper bound. Use is made of the Schwarz inequality, according to which the inner product of linear operators of a fairly general class satisfies

$$(x, y) \leq \|x\| \|y\| \quad (3.79)$$

where (x, y) is the inner product of x and y , and $\|x\|$ is the norm of x . Integrals for which the integrand is bounded are operators suitable for the application of the Schwarz inequality, and $(x, y) = \int x y dz$, $\|x\| = \sqrt{\int x^2 dz}$. Therefore, using Schwarz inequality, the following relationship can be written.

$$\sqrt{\int_{V_T} (\sigma_{eq})^2 dV} \sqrt{\int_{V_T} 1^2 dV} \geq \int_{V_T} \sigma_{eq} \cdot 1 dV \Leftrightarrow \sqrt{V_T} \geq \frac{\int_{V_T} \sigma_{eq} dV}{\sqrt{\int_{V_T} (\sigma_{eq})^2 dV}}. \quad (3.80)$$

Substituting the right most expression from equation (3.80) into equation (3.56), it is shown that

$$m_1^0 = \frac{\sigma_y \sqrt{V_T}}{\sqrt{\int_{V_T} (\sigma_{eq})^2 dV}} \geq \frac{\sigma_y \int_{V_T} \sigma_{eq} dV}{\sqrt{\int_{V_T} (\sigma_{eq})^2 dV}} = \frac{\sigma_y \int_{V_T} E \varepsilon_{eq} dV}{\sqrt{\int_{V_T} E \sigma_{eq} \varepsilon_{eq} dV}}. \quad (3.81)$$

For a homogeneous material, the elastic modulus is constant and therefore can be cancelled. Also, if the material is isotropic-elastic, the principal axes of stress coincides with the principal axes of strain, and therefore, $\sigma_{eq} \varepsilon_{eq} = \sigma_{ij} \varepsilon_{ij}$. Essentially, the rightmost expression of (3.81) equals m_u , and it follows that $m_1^0 \geq m_u$.

3.7.3 Upper Bound Multiplier - m_2^0

Applying the Schwarz inequality in a similar way as in the previous section, the multiplier, m_2^0 is shown to be an upper bound. Only exception is that the linear operator

$\int_V \frac{1}{E_s} \dots dV$ is used, with the requirement $0 < \frac{1}{E_s} < \infty$, which is always valid in practical

applications. Therefore, applying the Schwarz inequality,

$$\sqrt{\int_{V_T} \frac{1}{E_s} \sigma_{eq}^2 dV} \sqrt{\int_{V_T} \frac{1}{E_s} 1^2 dV} \geq \int_{V_T} \frac{1}{E_s} \sigma_{eq} \cdot 1 dV \Leftrightarrow \sqrt{\frac{1}{E_s} 1^2 \cdot V_T} \geq \frac{\int_{V_T} \frac{1}{E_s} \sigma_{eq} dV}{\sqrt{\int_{V_T} \frac{1}{E_s} \sigma_{eq}^2 dV}}. \quad (3.82)$$

Substituting the rightmost expression in (3.82) into equation (3.72) gives,

$$m_2^0 = \frac{\sigma_y \sqrt{\int_{V_T} \frac{1}{E_s} dV}}{\sqrt{\int_{V_T} \frac{1}{E_s} \sigma_{eq}^2 dV}} \geq \frac{\sigma_y \int_{V_T} \frac{1}{E_s} \sigma_{eq} dV}{\sqrt{\int_{V_T} \frac{1}{E_s} \sigma_{eq}^2 dV}} = \frac{\sigma_y \int_{V_T} \varepsilon_{eq} dV}{\sqrt{\int_{V_T} \sigma_{eq} \varepsilon_{eq} dV}}. \quad (3.83)$$

In the above expression, the material is assumed to be inhomogeneous. In other words, the elastic modulus E_s varies throughout the structure. Furthermore, for an isotropic-elastic behavior, the equation (3.83) determines that $m_2^0 \geq m_u$. In other words, the multiplier m_2^0 is proved to be an upper bound.

3.7.4 Multiplier – m-alpha

It is proposed that the multiplier m_α was determined on the basis of two linear elastic FEA. This means that m_α is evaluated as a final limit multiplier when stress distribution obtained by the EMAP is only partly converged to the collapse state of the structure. To

explore the confidence level of m_α evaluated in this approach as a lower bound, it is

convenient to express m_α in a normalized manner as $R_\alpha = \frac{m_\alpha}{m}$, and

$$R_\alpha = 2 R_0 \frac{2 \left(\frac{R_0}{R_L} \right)^2 + \sqrt{\frac{R_0}{R_L} \left(\frac{R_0}{R_L} - 1 \right)^2 \left(1 + \sqrt{2} - \frac{R_0}{R_L} \right) \left(\frac{R_0}{R_L} - 1 + \sqrt{2} \right)}}{\left(\left(\frac{R_0}{R_L} \right)^2 + 2 - \sqrt{5} \right) \left(\left(\frac{R_0}{R_L} \right)^2 + 2 + \sqrt{5} \right)}. \quad (3.84)$$

By normalizing, it is obvious that $R_\alpha < 1$ indicates that m_α - multiplier is a lower bound,

$R_\alpha > 1$ indicates that m_α - multiplier is an upper bound and finally $R_\alpha = 1$, indicates that

exact limit multiplier. Therefore, various curves for R_α can be plotted in a two-

dimensional space with axes $\frac{R_0}{R_L}$ and R_0 as shown in the Figure 3.5.

It is realized from the equation (3.84) that real roots for m_α are not possible for

$\frac{R_0}{R_L} > 1 + \sqrt{2}$. Therefore, the range for $\frac{R_0}{R_L}$ varies from one (at limit state) and $1 + \sqrt{2}$.

Similarly, for a given stress distribution, the possible values for R_0 are R_L and R_0 .

Hence a 45 degree line is drawn as shown in the Figure 3.5, connecting the points

$R_0 = 1$ and $R_0 = \frac{R_0}{R_L}$.

With reference to the Figure 3.5, it is apparent that the probability of m_α to be a lower bound is high for higher ratios of $\frac{R_0}{R_L}$ and likelihood of overestimating m with m_α is high when $\frac{R_0}{R_L}$ is close to unity. For such cases, it is suggested that $m_\alpha/1.05$ gives acceptable estimates as a lower bound.

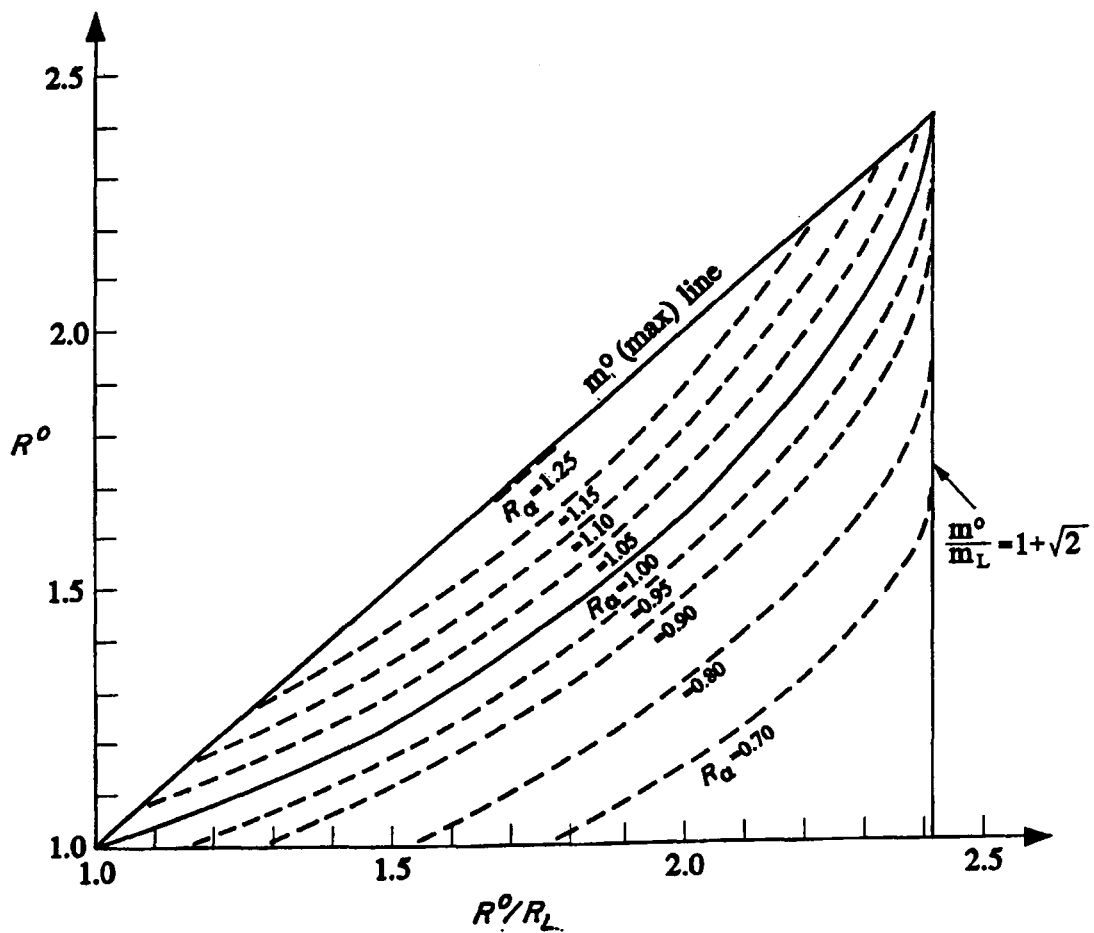


Figure 3.5. Region of Lower and Upper Boundedness of m_α

3.8 Closure

The fundamental concepts relating Mura's variational formulation and methods that are based on variational concepts in plasticity have been presented in this chapter. Further explanations, investigations and related proofs for the m^0 , m' and m_α multipliers have also been discussed.

It is well documented that the multipliers such as m_L , m' and m_α depend on the maximum elastic stress in a component or a structure. In EMAP, these multipliers can provide oscillatory and unsatisfactory lower bound limit load values. This is typically the case for components with cracks and notches. It is realized that if a lower bound multiplier can be evaluated by implementing the entire stress distribution of the structure, such oscillations can be avoided and may lead to quicker convergence to exact limit multiplier. In the following chapters, further explorations on such aspects have been made and a multiplier m_β based on the entire stress distribution on the structure is determined.

CHAPTER 4: LOWER BOUND LIMIT LOAD DETERMINATION – THE M-BETA MULTIPLIER METHOD

4.1 Introduction

The elastic modulus adjustment procedures are based on a series of linear elastic finite element analyses with non-homogeneous elastic properties, that is, spatial variations in elastic moduli. It was seen in Chapter 2 that using EMAP, numerous sets of statically admissible and kinematically admissible distributions can be generated and lower and upper bounds on limit loads can be obtained.

The previous chapter dealt with Mura's development of alternate limit load determination methods that are based on variational principles in plasticity. As the method does not provide better lower bounds than the classical lower bound, Seshadri and Mangalaramanan (1997) extended Mura's variational procedure and developed m_α -method in which a multiplier m_α is determined from partly converged stress distributions.

It is recognized that both the classical and the m_α -multipliers exhibit dependence on the maximum elastic stress in a component or a structure. For components with cracks and notches, these multipliers can provide unsatisfactory lower bound limit load values. For

slender or shape-sensitive components and structures, the maximum stress locations could “move around” leading to possible oscillatory behavior in the values of m_L and m_α with successive elastic iterations.

In this chapter, a multiplier m_β is determined, that relies on the entire stress distribution rather than the maximum stress, leading to good lower bound values for components and structures especially with notches and cracks. The method is applied to simple configurations and the results are compared with exact limit load solutions.

4.2 Theoretical Considerations

The theoretical considerations pertaining to Mura’s variational formulation and several limit load multipliers both classical and the ones based on variational formulation in plasticity are relevant in the development of the m_β -multiplier method. These concepts are summarized in this section.

4.2.1 Integral Mean of Yield Criterion

In classical limit analysis, statically admissible stress states cannot lie outside the hypersurface of the yield criterion. Mura et al. (1965) circumvented such a requirement and allowed the elastically calculated stress fields to exceed the yield stress provided they satisfy the “integral mean of yield” criterion, which can be expressed as

$$\int_{V_T} \mu^0 [f(s_{ij}^0) + (\phi^0)^2] dV = 0 \quad (4.1)$$

The superscript “0” corresponds to a statically admissible state, s_{ij}^0 is the deviatoric stress corresponding to impending limit state, whereby $s_{ij}^0 = m^0 \tilde{s}_{ij}^0$. The deviatoric stresses \tilde{s}_{ij}^0 equilibrates the applied set of loads. ϕ^0 is a point function that takes on a value zero if s_{ij}^0 is at yield and remains positive below yield. The function $f(s_{ij}^0)$ represents a yield criterion. For instance, the von-Mises yield criterion can be expressed as

$$f(s_{ij}^0) = \frac{1}{2} s_{ij}^0 s_{ij}^0 - k^2. \quad (4.2)$$

The value of k is taken as $\sigma_y / \sqrt{3}$.

The associated flow rule is expressed as,

$$\dot{\epsilon}_{ij} = \mu \left(\frac{\partial f}{\partial s_{ij}} \right) \quad (4.3)$$

where $\dot{\epsilon}_{ij}$ is the strain rate tensor and μ is the flow parameter.

4.2.2 Upper and Lower Bound Limit Load Multipliers

Seshadri and Mangalaramanan (1997) derived an upper bound multiplier m_1^0 , which is based on constant flow parameter formulation and is given by

$$m_1^0 = \frac{\sigma_y \sqrt{V_T}}{\sqrt{\int_{V_T} \sigma_e^2 dV}}. \quad (4.4)$$

Pan and Seshadri (2002) derived an upper bound multiplier m_2^0 in order to account for a variable flow parameter, μ^0 , and is expressed as

$$m_2^0 = \frac{\sigma_y \sqrt{\int_{V_T} \frac{dV}{E_s}}}{\sqrt{\int_{V_T} \frac{\sigma_e^2 dV}{E_s}}} \quad (4.5)$$

where E_s is the secant modulus at a given location in the component.

The classical upper bound multiplier m_u is defined as:

$$m_u = \frac{\sigma_y \int_{V_T} \varepsilon_e dV}{\int_{V_T} \sigma_e \varepsilon_e dV} \Leftrightarrow \frac{\sigma_y \int_{V_T} \frac{1}{E_s} \sigma_e dV}{\int_{V_T} \frac{1}{E_s} \sigma_e^2 dV} \quad (4.6)$$

It is recognized that during initial iterations in EMAP, m_u leads to upper bounds that are closer to the exact multiplier, m , than m_2^0 . Furthermore, Reinhardt and Seshadri (2003) proved that m_1^0 and m_2^0 are upper bounds, and $m_1^0 \geq m_u$ and $m_2^0 \geq m_u$.

The classical lower bound (m_L) is defined as

$$m_L = \frac{\sigma_y}{(\sigma_e)_{\max}} \quad (4.7)$$

where $(\sigma_e)_{\max}$ is the maximum equivalent stress in the component under consideration.

Mura's lower bound multiplier, m' can be expressed as,

$$m' = \frac{2m^0}{1 + \left(\frac{m^0}{m_L}\right)^2} \quad (4.8)$$

In the previous chapter, it was shown that $m' \leq m_L$.

The m_α - multiplier is given by the expression,

$$m_\alpha = 2m^0 \frac{2\left(\frac{m^0}{m_L}\right)^2 + \sqrt{\frac{m^0}{m_L}\left(\frac{m^0}{m_L} - 1\right)^2 \left(1 + \sqrt{2} - \frac{m^0}{m_L}\right)\left(\frac{m^0}{m_L} - 1 + \sqrt{2}\right)}}{\left(\left(\frac{m^0}{m_L}\right)^2 + 2 - \sqrt{5}\right)\left(\left(\frac{m^0}{m_L}\right)^2 + 2 + \sqrt{5}\right)} \quad (4.9)$$

It can be verified that $m_\alpha > m_L$ for all iterations except at the converged state. Reinhardt and Seshadri (2003) discussed the issue of lower boundedness of m_α , which was presented in the previous chapter. With reference to the equations (4.7) to (4.9), it is clear that the multipliers m_L , m' and m_α depend on $(\sigma_e)_{\max}$ which oscillates with iteration in EMAP. To avoid this problem, it may be useful to evaluate a lower bound limit load multiplier called m_β - multiplier that incorporates the entire stress distribution. The derivation of m_β - multiplier is carried out in the next section.

4.3 M-Beta Multiplier Method

4.3.1 Derivation of m_β - multiplier

To obtain the m_β - multiplier, consider the inequality derived by Mura et al. (1965) in equation (3.47). If the maximum value of $f(s_{ij}^0)$ is not considered, the inequality can be rewritten as

$$m^0 \leq m + \int_{V_T} \mu \{f(s_{ij}^0) + (\phi^0)^2\} dV. \quad (4.10)$$

Equation (4.10) can be rewritten as

$$m^0 \leq m + \int_{V_T} \mu f^0 dV. \quad (4.11)$$

Multiplying and dividing the term $\int_{V_T} \mu f^0 dV$ by $\int_{V_T} \mu dV$ in the right hand side of equation (4.11) and by making use of equation (3.49), a lower bound multiplier (m'') can be obtained from equation (4.11) as:

$$m'' = \frac{m^0}{1+G} \leq m \quad (4.12)$$

$$\text{where } G = \frac{1}{2k^2} \left[\frac{\int_{V_T} \mu f^0 dV}{\int_{V_T} \mu dV} \right].$$

In equation (4.12), μ corresponds to the flow parameter at the exact limit state which is not known a priori. In order to decouple the effect of μ , use is made of the Schwarz inequality in the numerator and denominator of the expression G as

$$\int_{V_T} \mu f^o dV \leq \sqrt{\int_{V_T} \mu^2 dV} \sqrt{\int_{V_T} (f^o)^2 dV} \quad (4.13a)$$

$$\int_{V_T} \mu dV \leq \sqrt{\int_{V_T} \mu^2 dV} \sqrt{\int_{V_T} 1^2 dV} \quad (4.13b)$$

Equations (4.13a) and (4.13b) are substituted into equation (4.12), and the term G is now defined as

$$G = \frac{1}{2k^2} \left[\frac{\sqrt{\int_{V_T} (f^o)^2 dV}}{V_T} \right]. \quad (4.14)$$

Substituting equation (4.14) in equation (4.12), we can now evaluate a multiplier m'' that accounts for the entire stress distribution in the structure. Due to the application of Schwarz inequality in equation (4.13), the multiplier m'' may not be a lower bound. Therefore, a parameter β is introduced in G so that a multiplier m_β is defined as

$$m_\beta = \frac{m^o}{1 + \beta G}. \quad (4.15)$$

Using EMAP, for a particular β , the multiplier m_β can be evaluated using equation (4.15) for a series of linear elastic analysis iterations. Also, evaluating equation (4.15) for

different β 's leads to a set of $m_\beta(\zeta)$ trajectories as shown in the Figure 4.1. Here ζ is the iteration variable.

Among the several β evaluated, it is necessary to choose a reference $\beta = \beta_R$ so that $m_\beta \leq m$. The "reference trajectory" corresponding to $\beta = \beta_R$ would concurrently satisfies the following requirements:

$$\begin{aligned}
 (1) \quad & m^o \geq m \geq m_\beta \quad \text{for } \zeta \geq 0 \\
 (2) \quad & \frac{dm_\beta}{d\zeta} \geq 0 \quad \text{for } \zeta \geq 0 \\
 (3) \quad & \frac{dm^o}{d\zeta} \leq 0 \quad \text{for } \zeta \geq 0
 \end{aligned} \tag{4.16}$$

$$\text{and, } (4) \quad m^o = m_\beta = m \quad \text{as } \zeta \rightarrow \zeta_L \text{ (limit state)}$$

In effect, $\beta = \beta_R$ would be the lowest possible value of β that would generate a m_β trajectory that satisfies equations (4.16).

4.3.2 Significance of G

Identifying that $f^0 = \frac{1}{3}[(m^0 \sigma_e)^2 - \sigma_y^2]$ and $k^2 = \sigma_y^2 / 3$, the parameter G in equation (4.14) can be expressed as

$$G = \frac{1}{2} \sqrt{\frac{\int_{V_T} [(m^0 \sigma_e)^2 - \sigma_y^2]^2 dV}{\sigma_y^4 V_T}} \tag{4.17}$$

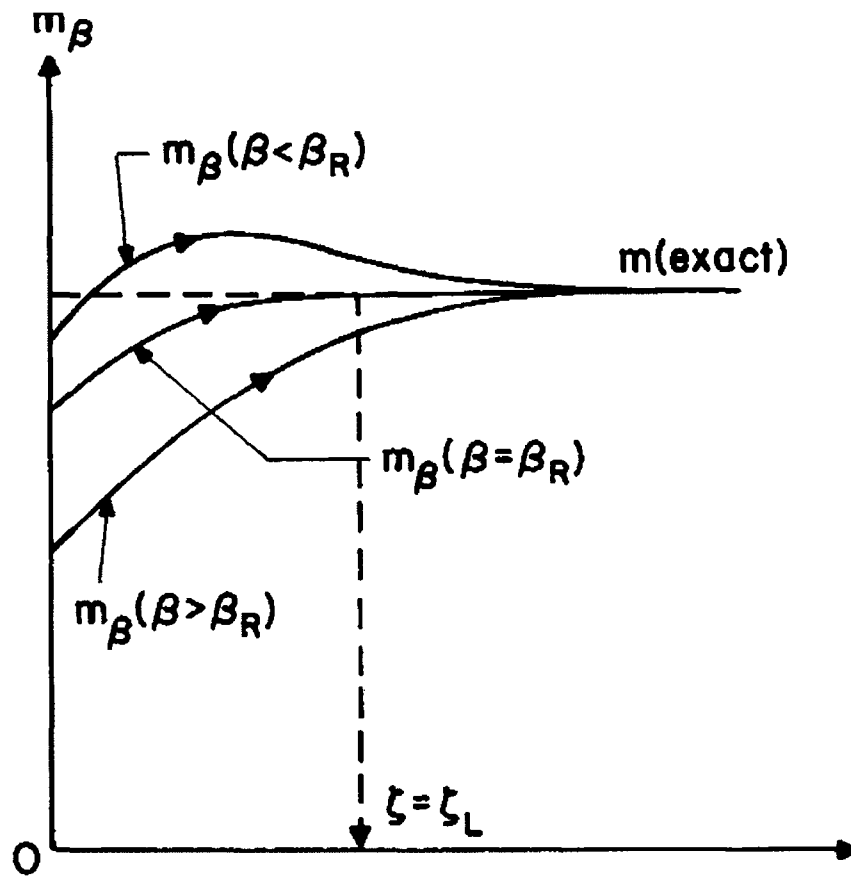


Figure 4.1. m_β - multiplier : Reference Curve ($\beta = \beta_R$)

By defining $R^0 = \frac{m^0}{m}$ and substituting into equation (4.12), it can be verified that $G \geq 0$

since $R^0 \geq 1$. It is recognized that G depends on the statically admissible stress distribution in a structure, and G is always greater than zero except at the limit state. As the stress distribution converges to the state of impending plastic collapse, G equates to zero, i.e.

$$\int_{V_T} (m^0 \sigma_e^0)^2 dV \rightarrow \sigma_y^2 V_T \quad (4.18)$$

Consequently, $m^0 = m_u = m_\beta = m_L = m' = m$. This infers that the limit load multipliers converge to exact multiplier as the stress distribution in entire volume of the structure converges to the limit type distribution.

4.4 Numerical Examples

The objective of the m_β - multiplier method is to establish better lower bounds by incorporating the entire stress distribution in a structure. This is illustrated using two simple problems: a thick-walled cylinder subjected to internal pressure and a beam subjected to pure bending moment. The non-linear stress redistribution is carried out by systematically modifying the elastic modulus at various locations in the structure.

4.4.1 Thick-walled Cylinder under Internal Pressure

Consider a thick-walled cylinder with inner radius a and outer radius b subjected to uniform internal pressure p_i . The cylinder is assumed to be sufficiently long such that plain strain conditions apply.

The equilibrium condition is:

$$\frac{d\sigma_r}{dr} = \frac{\sigma_\theta - \sigma_r}{r} \quad (4.19)$$

The stress boundary conditions are:

$$\begin{aligned}\sigma_r^I &= -p_i & \text{at} & \quad r=a \\ \sigma_r^I &= 0 & \text{at} & \quad r=b\end{aligned}\quad (4.20)$$

The elastic stress distribution that satisfies the equilibrium and the boundary conditions is given by

$$\sigma_r^I = \frac{a^2 p_i}{b^2 - a^2} \left(1 - \frac{b^2}{r^2} \right) \quad (4.21)$$

$$\sigma_\theta^I = \frac{a^2 p_i}{b^2 - a^2} \left(1 + \frac{b^2}{r^2} \right) \quad (4.22)$$

where σ_r^I and σ_θ^I are the radial stress and the hoop stress acting on the cylinder and the superscript I indicates that the quantities correspond to the first iteration.

The material constitutive law is given by

$$\sigma_e^I = E^I \varepsilon_e^I \quad (4.23)$$

where σ_e^I and ε_e^I are the equivalent stress and the equivalent strain at the first iteration.

The von-Mises equivalent stress that incorporates the plane strain condition and the incompressibility condition for the thick cylinder is given by

$$\sigma_e = \frac{\sqrt{3}}{2} (\sigma_\theta - \sigma_r) \quad (4.24)$$

Substituting equations (4.21) and (4.22) in equation (4.24) gives

$$\sigma_e^I = \frac{\sqrt{3} p_i a^2 b^2}{(b^2 - a^2) r^2} \quad (4.25)$$

The upper and lower bound multipliers for the thick cylinder under internal pressure are evaluated below using the equivalent stress σ_e^I for the first iteration defined in equation (4.25).

The upper bound multiplier m^0 is evaluated as

$$m^0 = \frac{\sigma_y (b^2 - a^2)}{\sqrt{3} p_i a b} \quad (4.26)$$

where the denominator in equation (4.4) is estimated as

$$\int_{V_r} \sigma_e^2 dV = \frac{3 \pi p_i a^2 b^2}{b^2 - a^2}. \quad (4.27)$$

The classical upper bound multiplier m_u is evaluated as

$$m_u = \frac{2 \sigma_y \ln\left(\frac{b}{a}\right)}{\sqrt{3} p_i} \quad (4.28)$$

where the term in the numerator in equation (4.6) evaluates to

$$\int_{V_r} \sigma_e dV = \frac{2 \pi \sqrt{3} p_i a^2 b^2}{(b^2 - a^2)} \ln\left(\frac{b}{a}\right). \quad (4.29)$$

It is verified that $m^0 > m_u$ as stated in Section 4.2.2.

The classical lower bound multiplier m_L is evaluated as

$$m_L = \frac{\sigma_y (b^2 - a^2)}{\sqrt{3} p_i b^2} \quad (4.30)$$

where the maximum elastic stress σ_{\max} can be obtained by substituting $r=a$ in equation (4.25),

$$\sigma_{\max} = \frac{\sqrt{3} p_i b^2}{(b^2 - a^2)}. \quad (4.31)$$

Mura's lower bound multiplier m' is evaluated as

$$m' = \frac{2m^0 a^2}{(a^2 + b^2)} \quad (4.32)$$

where the term $\frac{m^0}{m_L} = \frac{b}{a}$.

Knowing $\frac{m^0}{m_L}$ and m^0 in equation (4.26), m_α as in equation (4.9) can be evaluated from

the expression

$$m_\alpha = 2m^0 \frac{\left[2\left(\frac{b}{a}\right)^2 + \sqrt{\left(\frac{b}{a}\right)\left(\frac{b}{a}-1\right)^2 \left(1+\sqrt{2}-\frac{b}{a}\right)\left(\frac{b}{a}-1+\sqrt{2}\right)} \right]}{\left(\left(\frac{b}{a}\right)^2 + 2 - \sqrt{5}\right)\left(\left(\frac{b}{a}\right)^2 + 2 + \sqrt{5}\right)} \quad (4.33)$$

It is noted that m_α multiplier in equation (4.33) does not provide a solution if $\frac{m^0}{m_L} = \frac{b}{a}$ is greater than $1 + \sqrt{2}$.

The m_β - multiplier derived in Section 4.3 can be estimated by evaluating the term G in equation (4.17), as

$$G = \frac{1}{2} \sqrt{\frac{(b^6 - a^6)}{3b^2 a^2 (b^2 - a^2)}} - 1 \quad (4.34)$$

where the term

$$\int_{V_r} \sigma_e^4 dV = \frac{3\pi p_i^4 a^2 b^2 (b^6 - a^6)}{(b^2 - a^2)^4} \quad (4.35)$$

Using the parameter G in equation (4.34), the multiplier m_β can be evaluated using the equation,

$$m_\beta = \frac{m^0}{1+G} \quad (4.36)$$

The limit load multipliers (defined in Section 4.2) at the first iteration are evaluated for a thick walled cylinder with yield strength of 300 N/mm² and an internal pressure of 50 N/mm². The variation of limit load multipliers with $\frac{b}{a}$ ratio is plotted in Figure 4.2. It is seen from the figure that the m_β -multiplier is a better lower bound multiplier than the other lower bound multipliers. Also, it is seen from equation (4.28) that the m_u -multiplier evaluates the exact limit multiplier and therefore the curves of m_u and exact multiplier are embedded into one curve in Figure 4.2.

In order to simulate the inelastic behavior of the thick cylinder, second linear elastic analysis is carried out by systematically modifying the elastic modulus that is based on the stress distribution obtained in the first iteration. The inelastic redistribution of a thick-walled cylinder using EMAP has been demonstrated by Mangalaramanan and Reinhardt (2001) and the same procedure is adopted here.

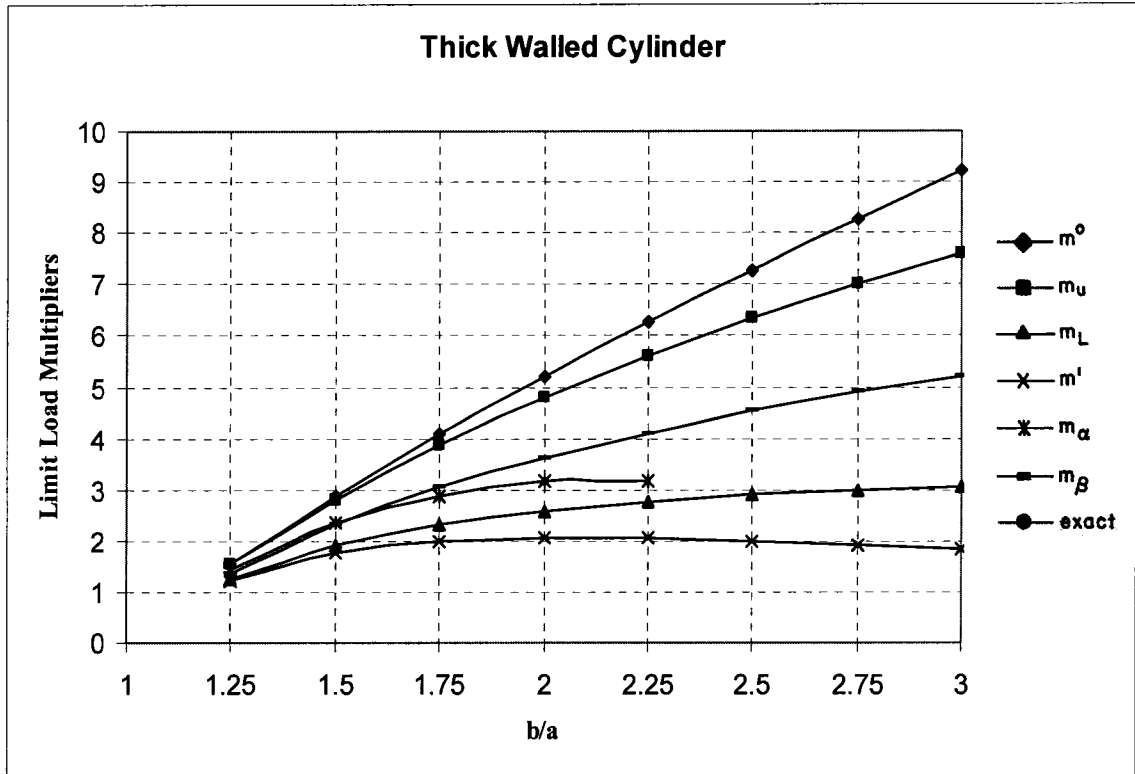


Figure 4.2. Variation of Limit Load Multipliers - Thick Walled Cylinder

The elastic modulus in the second iteration is modified as

$$E^{II} = E^I \left(\frac{\sigma_{arb}^I}{\sigma_e^I} \right)^q \quad (4.37)$$

where the superscript *II* indicates the quantity corresponding to the second iteration.

Substituting equation (4.25) in equation (4.37) gives

$$E^{II} = E^I \left(\frac{1}{\sqrt{3}} \sigma_{arb}^I \frac{b^2 - a^2}{-p_i b^2 a^2} \right)^q r^{2q} \quad (4.38)$$

which, for the sake of simplicity, can be expressed as

$$E^{II} = \kappa r^{2q}. \quad (4.39)$$

The material constitutive relationship is given by

$$\sigma_e^{II} = E^{II} \varepsilon_e^{II} \quad (4.40)$$

where the equivalent strain ε_e^{II} is given by

$$\varepsilon_e = \frac{2}{\sqrt{3}} \frac{C_1}{r^2}. \quad (4.41)$$

Substituting equations (4.24) and (4.41) in equation (4.40) gives

$$\sigma_\theta^{II} - \sigma_r^{II} = \frac{4}{3} \kappa C_1 r^{2(q-1)} \quad (4.42)$$

Substituting the above equation into the equilibrium condition (4.19) gives

$$\frac{d\sigma_r^{II}}{dr} = \frac{4}{3} \kappa C_1 r^{2(q-1)-1} \quad (4.43)$$

The radial stress corresponding to the second iteration is obtained by integrating equation (4.43),

$$\sigma_r^{II} = \frac{4}{3} \kappa C_1 \frac{r^{2q-2}}{q-2} + C_2 \quad (4.44)$$

Applying boundary conditions defined in equation (4.20) evaluates the constant C_1 ,

$$C_1 = \frac{3}{4} \frac{[2p_i(1-q)]}{\kappa} \frac{b^{2(1-q)} a^{2(1-q)}}{b^{2(1-q)} - a^{2(1-q)}} \quad (4.45)$$

Using equations (4.19), (4.43) and (4.45), the equivalent stress for the second iteration can be evaluated as

$$\sigma_e^{II} = \frac{\sqrt{3} p_i (1-q)}{r^{2(1-q)}} \frac{b^{2(1-q)} a^{2(1-q)}}{b^{2(1-q)} - a^{2(1-q)}} \quad (4.46)$$

Imposing $q=1$, equation (4.46) becomes,

$$\lim_{q \rightarrow 1} \sigma_e^{II} = \lim_{q \rightarrow 1} \frac{\sqrt{3} p_i (1-q)}{r^{2(1-q)}} \frac{b^{2(1-q)} a^{2(1-q)}}{b^{2(1-q)} - a^{2(1-q)}} = \frac{\sqrt{3} p_i}{2 \ln\left(\frac{b}{a}\right)} \quad (4.47)$$

using L' Hospital's rule and represents limit stress distribution, which is constant through the thickness of the thick walled cylinder. When σ_e^{II} reached the yield value, the applied pressure (p_i) would equal the collapse pressure, i.e.,

$$m^0 = m_u = m_\beta = m_L = m' = m = \frac{2}{\sqrt{3}} \frac{\sigma_y}{p_i} \ln\left(\frac{b}{a}\right). \quad (4.48)$$

4.4.2 Beam under Pure Bending

Consider a beam of rectangular cross-section with depth t and unit width subjected to pure bending moment M as shown in Figure 4.3. The bending moment can be expressed in terms of equivalent stress distribution as

$$M = \int_{-t/2}^{t/2} \sigma^I z dz \quad (4.49)$$

where σ^I is beam axial stress in the first iteration and for this case is the equivalent stress and z is the position through the beam thickness as shown in Figure 4.3. The material constitutive relationship is expressed as

$$\sigma^I = E^I \varepsilon^I \quad (4.50)$$

where E^I is the elastic modulus and ε^I is the axial strain in the first iteration. The axial strain ε^I can be expressed in terms of curvature κ as

$$\varepsilon^I = \kappa^I z^I \quad (4.51)$$

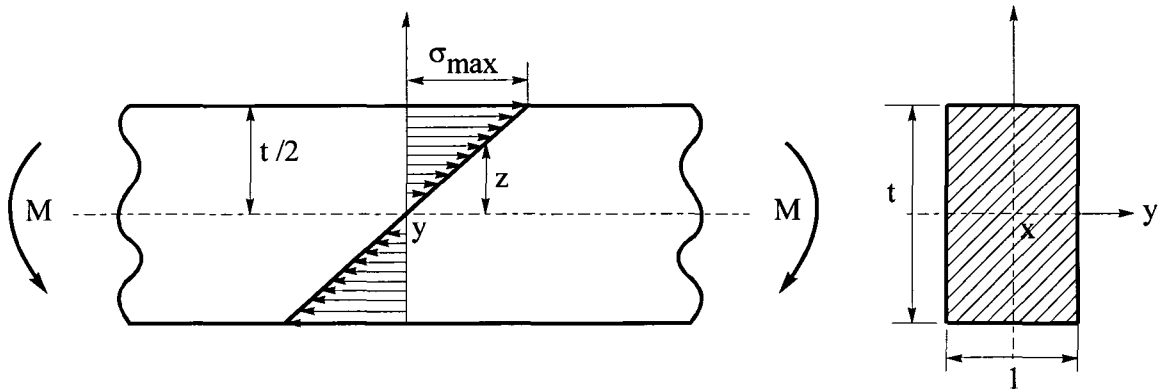


Figure 4.3. Beam Subjected to Pure Bending

Substituting equations (4.50) and (4.51) in equation (4.49) gives

$$M = 2 \int_0^{t/2} E^I \kappa^I z^2 dz = \kappa^I E^I \frac{t^3}{6} \quad (4.52)$$

Making use of constitutive and strain-displacement relationships in (4.50) and (4.51), equation (4.52) defines the elastic stress distribution,

$$\sigma^I = \frac{M z}{I} \quad (4.53)$$

where I is the moment of inertia of the beam cross-section shown in Figure 4.3.

The lower and upper bound limit load multipliers (defined in Section 4.2.2) for a beam subjected to pure bending moment is estimated next using the stress distribution σ^I for the first iteration, defined in equation (4.53).

The upper bound multiplier m^0 is evaluated as

$$m^0 = \frac{\sigma_y I \sqrt{12}}{M t} \quad (4.54)$$

where the denominator in equation (4.4) is estimated as

$$\int_{V_T} \sigma_e^2 dV = \frac{1}{12} \left(\frac{M t}{I} \right)^2. \quad (4.55)$$

The classical upper bound multiplier m_u is evaluated as

$$m_u = \frac{3 \sigma_y I}{M t} \quad (4.56)$$

where the term in the numerator in equation (4.6) evaluates to

$$\int_{V_T} \sigma_e dV = \frac{M t}{4 I}. \quad (4.57)$$

It is verified that $m^0 > m_u$ as stated in Section 4.4.2.

The classical lower bound multiplier m_L is evaluated as

$$m_L = \frac{2 \sigma_y I}{M t} \quad (4.58)$$

where the maximum elastic stress σ_{\max} can be evaluated by substituting $z = t/2$ in equation (4.53),

$$\sigma_{\max} = \frac{M t}{2 I}. \quad (4.59)$$

Mura's lower bound multiplier m' is evaluated as

$$m' = \frac{m^0}{2} \quad (4.60)$$

where the term $\frac{m^0}{m_L} = \sqrt{3}$.

Knowing $\frac{m^0}{m_L}$ and m^0 in equation (4.54), m_α in equation (4.9) is estimated as

$$m_\alpha = 2 m^0 \frac{\left[2(\sqrt{3})^2 + \sqrt{(\sqrt{3})(\sqrt{3}-1)^2 (1+\sqrt{2}-\sqrt{3})(\sqrt{3}-1+\sqrt{2})} \right]}{\left((\sqrt{3})^2 + 2 - \sqrt{5} \right) \left((\sqrt{3})^2 + 2 + \sqrt{5} \right)} = 0.716 m^0 \quad (4.61)$$

The m_β - multiplier derived in Section 4.4 can be estimated by evaluating the term G in equation (4.16), as

$$G = \frac{1}{2} \sqrt{\left(\frac{144}{80} - 1 \right)} \quad (4.62)$$

where the term

$$\int_{V_T} \sigma_e^4 dV = \frac{1}{80} \left(\frac{M t}{I} \right)^4 \quad (4.63)$$

Therefore, the multiplier m_β in equation (4.15) is evaluated as

$$m_\beta = 0.691 m^0 \quad (4.64)$$

In order to simulate the inelastic behavior of the beam, second linear elastic analysis is carried out by systematically modifying the elastic modulus that is based on the stress distribution obtained in the first iteration. The bending moment M in terms of equivalent stress at the second iteration is expressed as

$$M = \int_{-t/2}^{t/2} \sigma^{II} z dz \quad (4.65)$$

with the constitutive relationship, $\sigma^{II} = E^{II} \varepsilon^{II}$ and strain-displacement relationship, $\varepsilon^{II} = \kappa^{II} z$. The superscript II in the above relationships indicate the quantities corresponding to the second iteration. Therefore the bending moment is rewritten as

$$M = \int_{-t/2}^{t/2} \kappa^{II} E^{II} z^2 dz \quad (4.66)$$

The second elastic analysis is carried out by modifying the elastic modulus E^I in the first iteration as

$$E^{II} = E^I \left(\frac{\sigma_{arb}^I}{\sigma^I} \right)^q \quad (4.67)$$

where σ_{arb} is the arbitrary stress and q is the iteration index. Substituting equations (4.53) and (4.67) in equation (4.66), and after performing necessary integration and algebraic manipulations, the curvature κ^{II} can be obtained as

$$\kappa^{II} = \frac{(3-q)M^{(q+1)}}{2E^I (\sigma_{arb}^I)^q I^q \left(\frac{t}{2} \right)^{(3-q)}} \quad (4.68)$$

Using the constitutive and strain-displacement relationships for the second iteration and equation (4.67) in equation (4.68), the redistributed stress corresponding to the second iteration, σ^{II} can be obtained as

$$\sigma^{II} = \frac{(3-q)z^{(1-q)} M}{2 \left(\frac{t}{2}\right)^{(3-q)}} \quad (4.69)$$

Imposing $q=1$, equation (4.69) becomes,

$$\sigma^{II} = \frac{4M}{t^2} \quad (4.70)$$

which is a constant through thickness stress distribution, independent of z , and hence limit type stress distribution. Therefore, the limit load multipliers defined in Section 4.2, are evaluated to be equal to the exact multiplier, i.e.,

$$m^0 = m_u = m_\beta = m_L = m' = m = \frac{3\sigma_y I}{M t} \quad (4.71)$$

It is interesting to note that the multiplier m_u evaluates the limit multiplier in the first iteration itself.

4.5 Discussions

In this chapter, the m_β -multiplier method is developed for limit load determination. The method is based on variational principles that make use of the “integral mean of yield” criterion. It takes into consideration the entire statically admissible stress distribution into

Mura's lower bound formulation rather than simply the maximum stress, leading to improved lower bounds.

It may be worthwhile to note that the simple examples dealt in this chapter correspond to structures exhibiting global collapse and the total volume contributed to the plastic action. In the first iteration, the parameter $G > 0$ as the converged stress distribution was not attained, whereas, in the second iteration, the stress distribution converged to the limit type and hence $G = 0$. Consequently, all the limit load multipliers converged to the exact limit multiplier.

Practically, in most components, the total volume of the component does not contribute to the plastic action. For such components, the statically admissible stress distributions obtained from EMAP may not represent a converged limit type of distribution even after several iterations. Furthermore, the m_β -multiplier when evaluated based on total volume may be overestimated and may not represent a lower bound. Effective means of evaluating a lower bound m_β -multiplier for components do not undergo global collapse are dealt with in the next chapter.

CHAPTER 5: THE M-BETA MULTIPLIER METHOD FOR LIMIT LOAD DETERMINATION OF COMPONENTS WITH LOCAL PLASTIC COLLAPSE

5.1 Introduction

It is obvious that in most real life structures, plastic yielding occurs only in part of structure that results in local plastic collapse. Pressure vessel assemblies constructed with cylinders, ellipsoidal or torispherical dished ends, flat heads, nozzles with reinforcing pads etc. are subjected to local plastic collapse. Pressure vessel components with defects such as pipes and vessels with circumferential or longitudinal flaws are also typical applications that involve local plastic action. The integrity assessment of such components is often performed to ascertain safety and to prevent them against catastrophic failure.

Knowledge of load carrying capacity of cracked components is of immense importance in assessing the component's serviceability. The characteristics of limit loads of cracked components are as below.

- The information of limit loads becomes relevant in order to estimate the inelastic fracture parameters such as the inelastic energy release rate, J – Integral and the creep crack growth parameter, C^* .

- A survey of limit loads for structures with defects was carried out by Miller (1988). In United Kingdom, Milne et al., (1988) performed a two-criteria failure assessment of the R6 method that addresses components that are subjected to both fracture and plastic collapse.
- Webster and Ainsworth (1994) used the reference stress method to evaluate inelastic fracture parameters such as J or C^* . In the reference stress approach, an estimate of elastic-plastic fracture parameter solution is obtained from known elastic and fully plastic fracture parameter solutions. Consequently, fully plastic fracture parameter solutions are related to limit load solutions.
- The characteristic of reference stress is a load controlled stress and is similar to primary stress in ASME stress classification framework. As the fundamental concepts of reference stress, limit loads and redistribution nodes (r-nodes) can be related, Seshadri et al. (1990, 2001) evaluated inelastic fracture parameters using the concept of r-nodes.

It is evident from the formulation of the m_β - multiplier method that the method requires a converged stress distribution in order to evaluate a value of G close to zero. However, for structures subjected to local plastic collapse, the stress distributions obtained from EMAP will not converge to a limit type distribution. Therefore, it becomes difficult to attain a value of G close to zero if it is evaluated by taking into account the total volume of the structure. The concept of reference volume, discussed next, will be useful to explore the methods of obtaining suitable values of the parameter G .

5.2 Concept of Reference Volume

For structures that exhibit local plastic collapse, plastic action may be confined only to a sub-region of the total volume, called the reference volume (refer Figure 5.1). In the context of local collapse, the concept of reference volume is useful in identifying the 'kinematically active' portion that participates in plastic action.

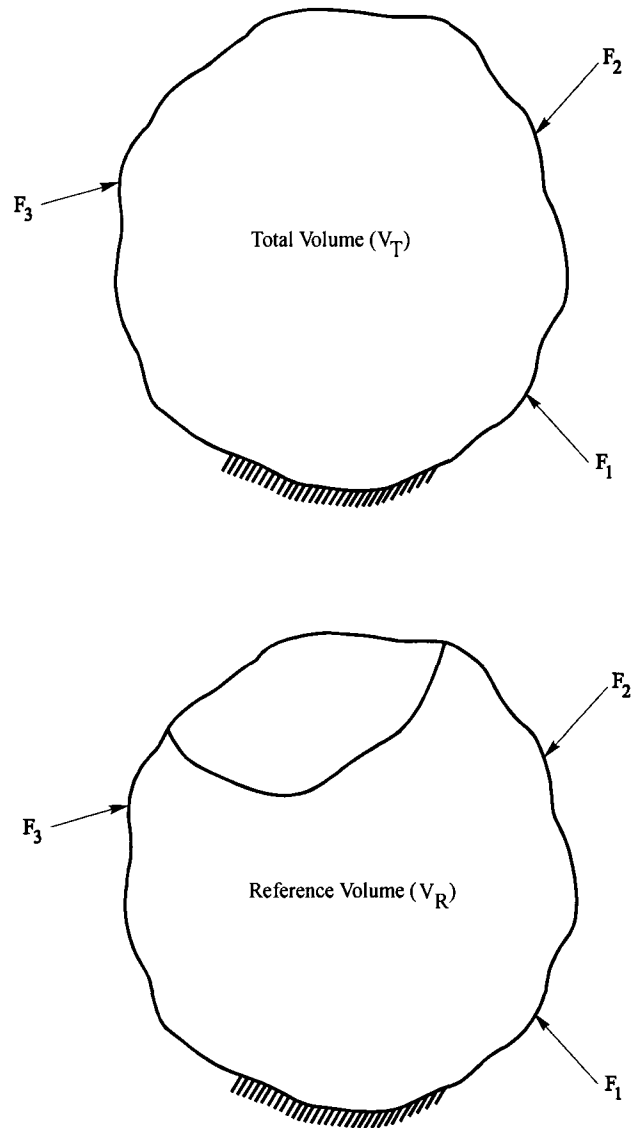


Figure 5.1. Total and Reference Volumes

For components subjected to local plastic collapse, the multipliers, m_1^0 and m'' are overestimates of the limit load (Figure 5.2) if they are based on the total volume. This is due to the fact that only part of the total volume contributes to local plastic collapse and taking into account the total volume in evaluating the multipliers results as an overestimate. Therefore, it is reasonable to base their evaluation on the reference volume concept.

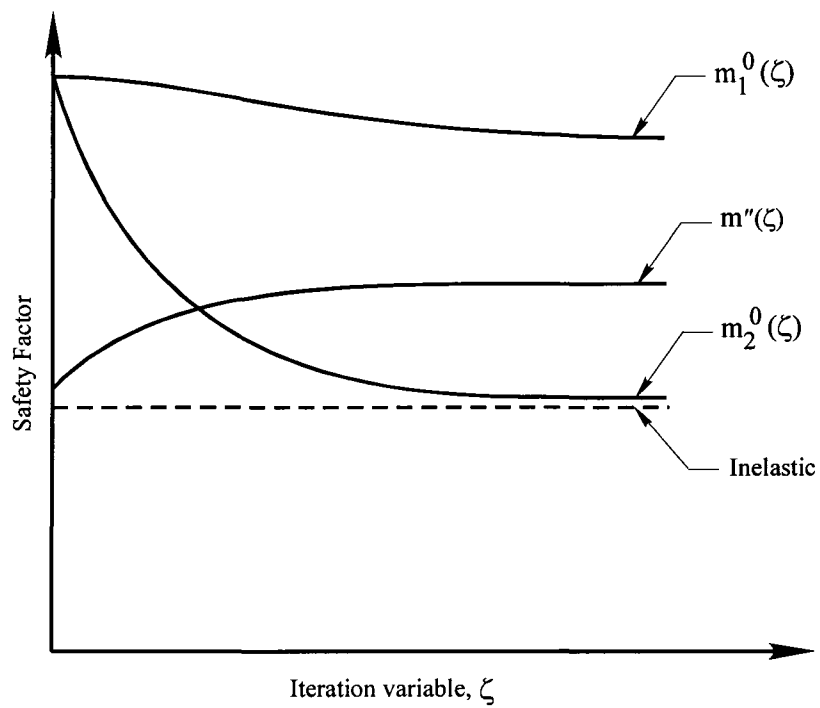


Figure 5.2. Overestimation of m_1^0 , m''

As well, it is clearly seen that the parameter G depends on m_1^0 and the statically admissible stress distribution, σ_e^0 . When evaluating G for components subjected to local plastic collapse, the multipliers m_1^0 and σ_e^0 has to be based on the reference volume V_R , instead of total volume V_T .

It can be shown that the upper bound multiplier m_2^0 is implicitly based on the reference volume concept even though it mathematically integrates the total volume of the structure. It was indicated in the Chapter 3 that m_2^0 is estimated by identifying the extent of plastic flow at each point in a structure. In other words, the highly stressed location is considered to posses a higher degree of plastic flow by reducing the secant modulus and vice versa.

The inclusion of the concept of reference volume in the multiplier m_2^0 is explained as follows. On the basis of Figure 5.1, the structure can be divided into a reference volume V_R , which is the ‘kinematically’ active volume and a dead zone V_D , which does not contribute to plastic flow. i.e., $V_T = V_R + V_D$. Therefore, the multiplier m_2^0 in equation (4.5) is rewritten as,

$$m_2^0(V_T) = \sigma_y \sqrt{\frac{\int_{V_R} \frac{1}{E_s} dV + \int_{V_D} \frac{1}{E_s} dV}{\int_{V_R} \frac{1}{E_s} \sigma_e^2 dV + \int_{V_D} \frac{1}{E_s} \sigma_e^2 dV}} \quad (5.1)$$

Recognizing that the secant modulus E_s is lower in the regions of plastic flow and much higher in the dead zone, the equation (5.1) can be simplified as

$$m_2^0(V_T) = \sigma_y \sqrt{\frac{\int_{V_R} dV}{\int_{V_R} \sigma_e^2 dV}} = m_1^0(V_R) \quad (5.2)$$

In the above process of simplification, it is assumed that the degree of plastic flow is constant over the reference volume V_R . It is useful to note that the difference in magnitude of the multipliers $m_1^0(V_T)$ and m_2^0 will enable an analyst to obtain insight into relative proportion of the reference volume and the total volume.

Furthermore, $G(V_R)$ is expressed as

$$G(V_R) = \frac{1}{2} \sqrt{\frac{\int_{V_R} [(m^0 \sigma_e)^2 - \sigma_y^2]^2 dV}{\sigma_y^4 V_R}} \quad (5.3)$$

Therefore, the multiplier $m''(V_R)$ can be further calculated using

$$m''(V_R) = \frac{m^0(V_R)}{1 + G(V_R)} \quad (5.4)$$

The procedure to identify the reference volume using m_2^0 is straightforward.

- In EMAP, the stress distribution corresponding to the least m_2^0 is chosen.
- The stress distribution obtained from a finite element analysis is arranged in the following sequence

$$\sigma_{e1} > \sigma_{e2} > \sigma_{e3} > \dots > \sigma_{eN}$$

Corresponding to the stresses $\sigma_{e1}, \sigma_{e2}, \dots, \sigma_{eN}$ are the volumes

$$\Delta V_1, \Delta V_2, \dots, \Delta V_N.$$

- The multiplier $m_1^0(V_R)$ is now estimated by accumulating the volumes ΔV_k as per the previous step. The sum of accumulated volumes $\sum_{k=1}^R \Delta V_k$ is adjudged as reference volume V_R when $m_1^0(V_R) = m_2^0$.

Having identified V_R , $G(V_R)$ can be calculated and the resulting $m''(V_R)$ evaluated using the equation (5.4) would be a lower bound. It can be verified that the value of parameter $G(V_T)$ may be of higher magnitude whereas the value of $G(V_R)$ may be reduced to a significant lower magnitude; i.e., the lower the value of G the better.

Finally, the reference parameter β_R is obtained by equating $m'(V_R)$ and right hand side of the equation (4.15). The purpose of evaluating β_R is to adjust the m' curve based on total volume by specifying β_R , which is tantamount to estimating m' based on reference volume.

It is seen in the previous chapter that the m_β - multiplier method provided better estimates of limit loads than the classical method for structures that exhibit global collapse. Given the significance of limit load solutions associated with components subjected to local plastic collapse, in this chapter, the performance of the method is verified for components subjected to local plastic collapse using the concept of reference volume. The m_β - multiplier method is applied to typical pressure vessel and cracked component configurations. Furthermore, when analyzing cracks, it is important to note that the strain singularity lies at the crack-tip. The key aspects related to simulating crack-tip singularity using finite elements are considered next.

5.3 Finite Element Modeling of Cracks

While modeling the cracked components using FEA, it is necessary to use singular elements around the crack-tip to simulate singularity of the strain field at the crack-tip. Use of singular elements enhances numerical accuracy even when very few elements are used whereas a great deal of mesh refinement would be required when ordinary elements are used to capture the crack tip fields.

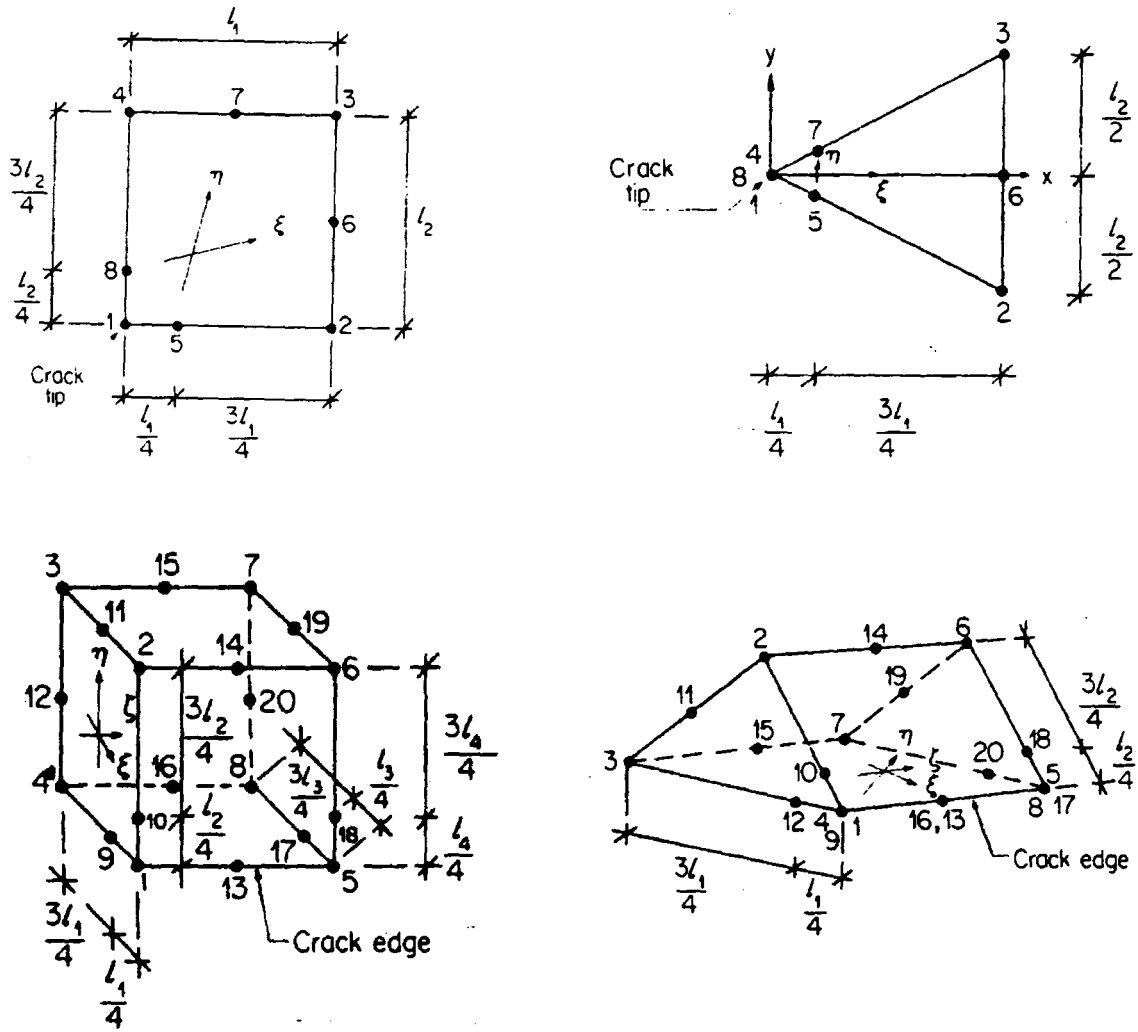


Figure 5.3. Singular Elements in FEA

In linear elastic fracture mechanics, the theoretical crack-tip singularity of $1/\sqrt{r}$ is achieved by using a six-noded isoparametric triangular elements and moving the mid-side nodes to the quarter points (Barsoum, 1976 and 1977) as shown in Figure 5.3. Such an element can also be obtained by collapsing one side of an eight noded quadrilateral element to a six-noded triangular element and nodes at the crack-tip are tied.

An eight noded quadrilateral element with mid-side nodes moved to the quarter points can also be used to model the cracks. However, it is recommended to use triangular elements as it was shown that triangular elements give better results than quadrilateral elements, as stiffness is singular when integrated exactly. Furthermore, singularity exists within the element as well as on the edges for the triangular element whereas the singularity only exists on the element edges for the quadrilateral element.

When the plastic zone forms, $1/\sqrt{r}$ singularity no longer exists at the crack tip. For elastic-perfectly-plastic behavior, Rice and Rosengren (1968) have shown that $1/r$ crack-tip singularity exists at the crack-tip. This is achieved by using triangular quadratic isoparametric elements, formed by collapsing one side and placing mid-side node near the crack tip at the quarter point. The plastic singularity of $1/r$ is obtained by having multiple independent nodes or untied nodes at the crack tip (Barsoum, 1976 and 1977).

For three-dimensional cracked components, a 20-noded quadrilateral isoparametric brick element is collapsed to obtain a wedge with mid-side nodes near the crack front moved to the quarter points as shown in Figure 5.3

5.4 Numerical Examples

The m_β - multiplier method in conjunction with the concept of reference volume described in Section 5.2 applied to benchmark pressure vessel and cracked component configurations. These include a thick unwelded flat head, welded-in flat head, plate with a center crack, a compact tension specimen, a plate with multiple cracks. The pressure vessel configurations are subjected to internal pressure loading whereas the cracked specimens are subjected to tensile loading. The problems are modeled using ANSYS (2001) software (educational version).

5.4.1 Elastic Modulus Adjustment Scheme

Successive linear elastic finite element iterations are carried out by modifying the elastic modulus of the various elements as follows:

$$E_{s,i+1} = \left(\frac{\sigma_{ref}}{\sigma_e} \right)^q E_{s,i} \quad (5.5)$$

where σ_{ref} is a reference stress, q is the elastic modulus adjustment parameter, and “ i ” is the iteration index. The limit load multipliers obtained from EMAP are compared with those of inelastic finite element analyses.

5.4.2 Evaluation of m-beta multiplier

A procedure to evaluate a m_β - multiplier for any given structure subjected to local plastic collapse is discussed in Section 5.2. Clearly, the procedure involves identification of reference volume at any given iteration by arranging the centroidal stresses of numerous finite elements in descending order. Due to computational efficiency, it is suggested that the m_β - multiplier be evaluated when the stress distribution attains a converged state. A converged stress distribution may be attained when the upper bound multiplier m_2^0 reaches a converged state. Therefore, in this thesis, m_β - multiplier is evaluated only at the last iteration and for convenience, the variation of m" (m_β - multiplier $\beta=1$) with each iteration is not plotted in the graphs.

5.4.3 Thick Unwelded Flat Head under internal pressure

A thick unwelded flat head configuration is as shown in Figure 5.4. It has a cylinder thickness $t_c = 101.6$ mm, flat head thickness $t_f = 101.6$ mm, overall length $L_o = 406.4$ mm, fillet radius $r_f = 101.6$ mm is considered. The modulus of elasticity considered is 207,000 N/mm² and the yield strength is 207 N/mm².

The finite element model of a thick flat head is modelled using four noded isoparametric plane element PLANE182 with axisymmetric option. The element has two translational degrees of freedom in the x and y directions at each node. The finite element mesh used

in analyzing the geometry is shown in Figure 5.5. The flat head part is meshed with 12 elements through the thickness and 34 elements along its length. The cylinder part is meshed with 12 elements through the thickness and 36 elements along its length. The fillet region is meshed with 32 elements along the radius. The flat head is supported in the vertical (y) direction at the cylinder side and the internal pressure of 50 N/mm^2 is applied as surface loads on the inside surfaces of the cylinder and the flat head.

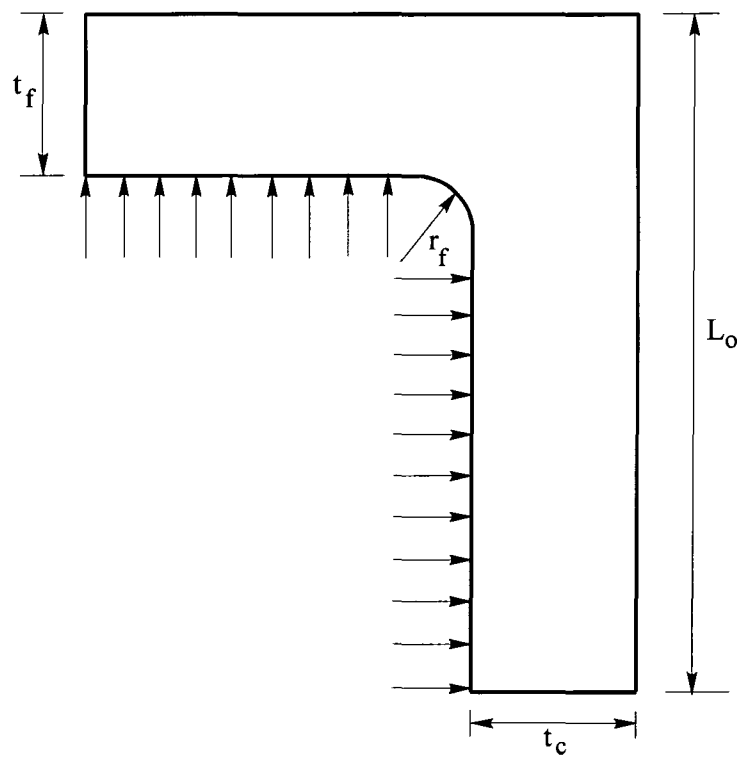


Figure 5.4. Thick Unwelded Flat Head under Internal Pressure

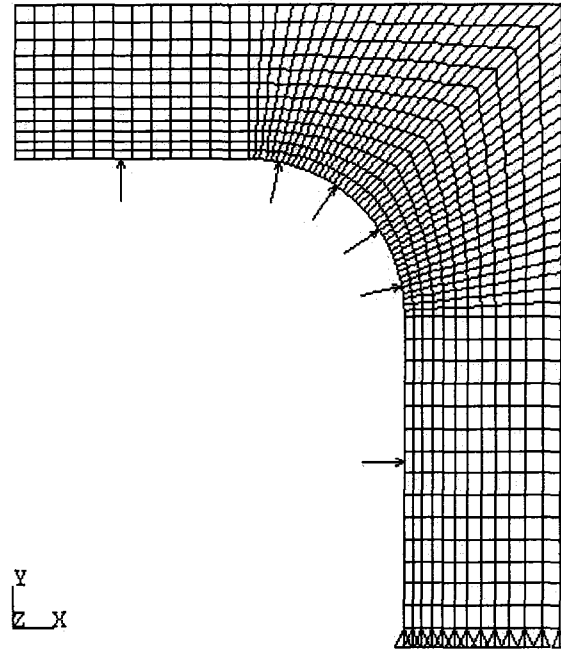


Figure 5.5. FE Mesh of Thick Unwelded Flat Head under Internal Pressure

The variation of limit load multipliers for ten iterations is shown in Figure 5.6. It is seen from the figure that the limit load multipliers does not converge even after ten iterations. The reference volume for the thick flat head under internal pressure is identified as per the procedure outlined in Section 5.2. At 10th iteration, for $V_R/V_T = 0.619$, $m_1^0(V_R) = m_2^0(V_T)$ (defined in equation (5.2)) is satisfied and the value of G is found to be 0.024. The best results of various limit load multipliers after 10 iterations with $q = 1.0$ (equation (4.23)) and the comparison with the result of inelastic FEA are tabulated in Table 5.1. A reference β_R for which $m_\beta = m'(V_R)$ is estimated as 0.988.

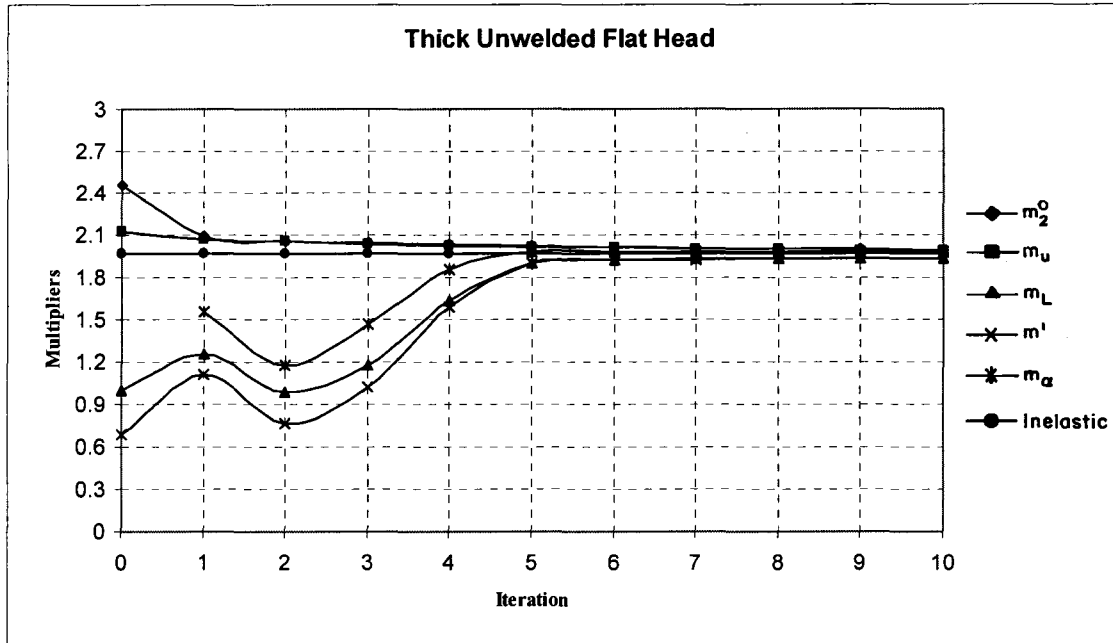


Figure 5.6. Variation of Limit Load Multipliers – Thick Unwelded Flat Head

5.4.4 Welded-in flat head under internal pressure

A welded-in flat head configuration is as shown in Figure 5.7. The dimensions of the welded-in flat head are: cylinder thickness $t_c = 21.5$ mm, flat head thickness $t_f = 43$ mm, overall length $L_o = 243$ mm and weld groove $w_g = 18$ mm. The yield strength is 300 N/mm^2 ; and the modulus of elasticity is $200,000 \text{ N/mm}^2$.

A four noded isoparametric plane element PLANE42 with axisymmetric option is used to model the welded-in flat head. The PLANE42 element has two translational degrees of

freedom in the x and y directions at each node. Figure 5.8 shows the finite element mesh used to analyze the welded-in flat head.

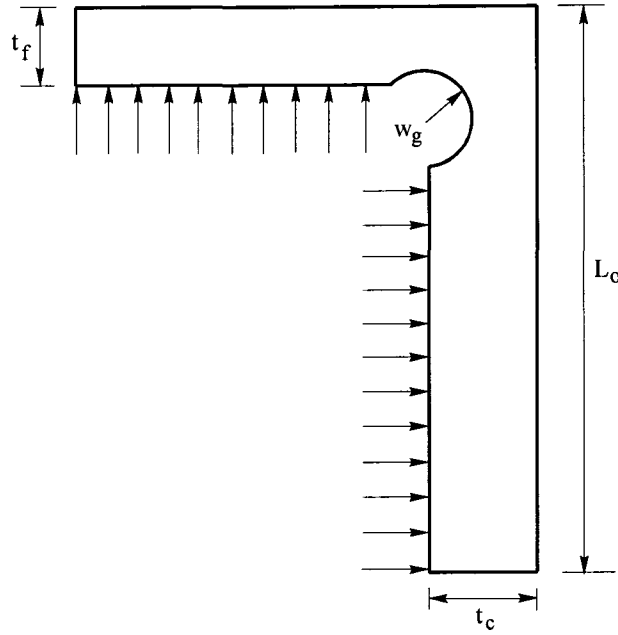


Figure 5.7. Welded-in Flat Head under Internal Pressure

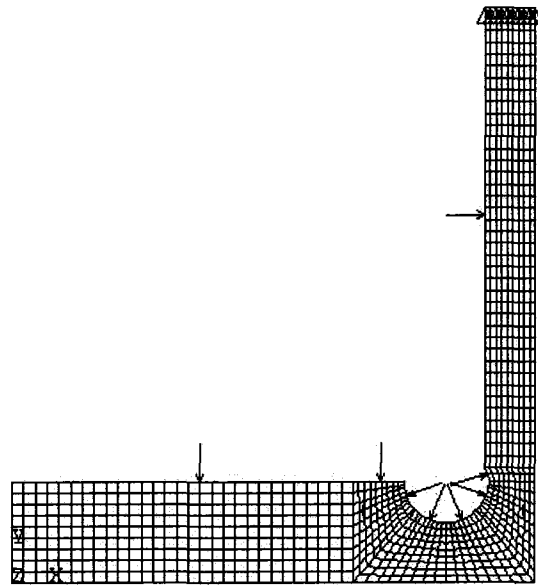


Figure 5.8. FE Mesh of Welded-in Flat Head under Internal Pressure

The flat head part is meshed with 9 elements through the thickness and 38 elements along its length. The cylinder part is meshed with 9 elements through the thickness and 38 elements along its length. The groove region is meshed with 36 elements along the groove. The flat head is supported in the vertical (y) direction at the cylinder side and the internal pressure of 10 N/mm² is applied as surface loads on the inside surfaces of the cylinder, flat head and the groove.

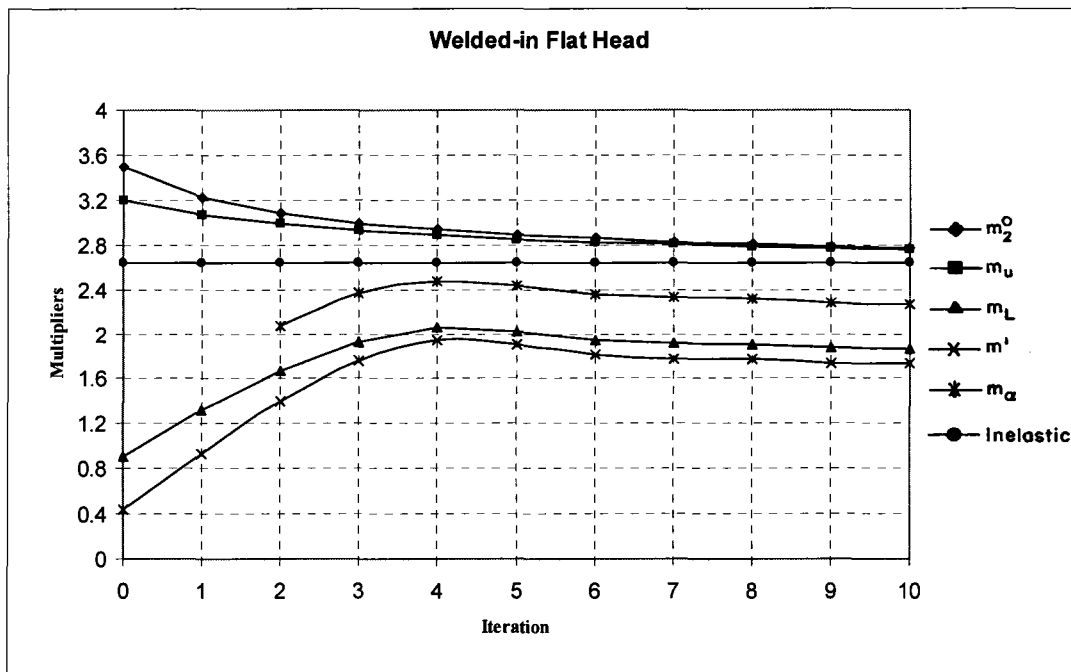


Figure 5.9. Variation of Limit Load Multipliers – Welded-in Flat Head

The variation of limit load multipliers for ten iterations is shown in Figure 5.9. The reference volume for the welded-in flat head under internal pressure is identified as per the procedure outlined in Section 5.2. At 10th iteration, for $V_R/V_T = 0.653$, $m_1^0(V_R) = m_2^0(V_T)$ is satisfied and the value of G is found to be 0.077. The best results

of various limit load multipliers after 10 iterations with $q = 0.5$ and the comparison with the result of inelastic FEA are tabulated in Table 5.1. A reference β_R for which $m_\beta = m''(V_R)$ is estimated as 1.225.

5.4.5 Plate with a center crack

A plate with a center crack shown in Figure 5.10, has a width $W = 254$ mm (10 inch), thickness $B = 3.175$ mm (0.125 inch) and crack length $2a = 50.8$ mm (2 inch). The material properties are, Young's modulus $E = 206.85$ GPa (3×10^7 psi) and yield stress $\sigma_y = 174$ MPa (25,000 psi) with a Poisson's ratio of $\nu = 0.3$.

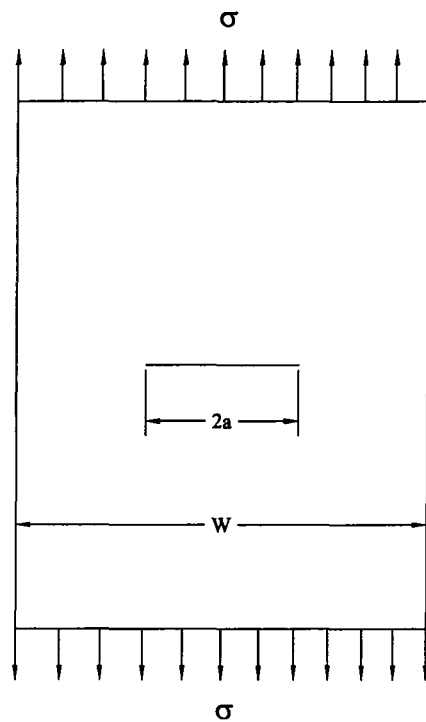


Figure 5.10. Plate with a Center Crack

An eight noded isoparametric plane element PLANE82 with plane stress option is used to model the plate with a center crack. The PLANE82 element has two translational degrees of freedom in the x and y directions at each node. Only one quarter of the specimen is modelled due to its symmetry in geometry and loading. Figure 5.11 shows the finite element mesh used to analyze the center-cracked plate. The specimen is meshed with 12 elements through the uncracked thickness portion and 5 elements through the cracked thickness portion. The crack tip region is meshed with eight crack tip elements. The center-cracked plate is constrained in the horizontal (x) and vertical (y) direction at the uncracked thickness portion and a tensile stress $\sigma = 137.90$ MPa is applied as a surface load to the specimen.

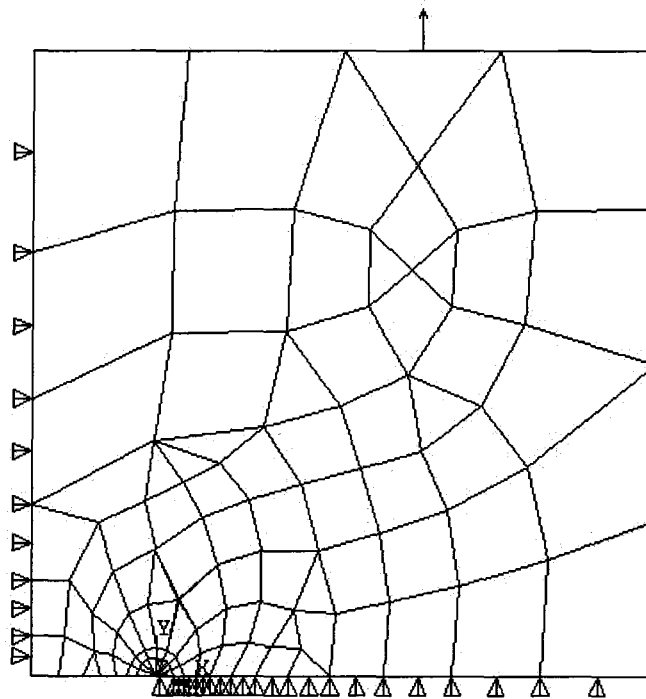


Figure 5.11. FE Mesh of Plate with a Center Crack

The variation of limit load multipliers for twenty iterations is shown in Figure 5.12. The reference volume for center-cracked specimen is identified as per the procedure outlined in Section 5.2. At 20th iteration, equation (5.2), which is defined as $m_1^0(V_R) = m_2^0(V_T)$ is satisfied for $V_R/V_T = 0.587$ and $G(V_R)$ is found to be 0.031. The best results of various limit load multipliers after 20 iterations with $q = 0.5$ and the comparison with the result of inelastic FEA are tabulated in Table 5.1. A reference β_R for which $m_\beta = m''(V_R)$ is estimated as 0.963.

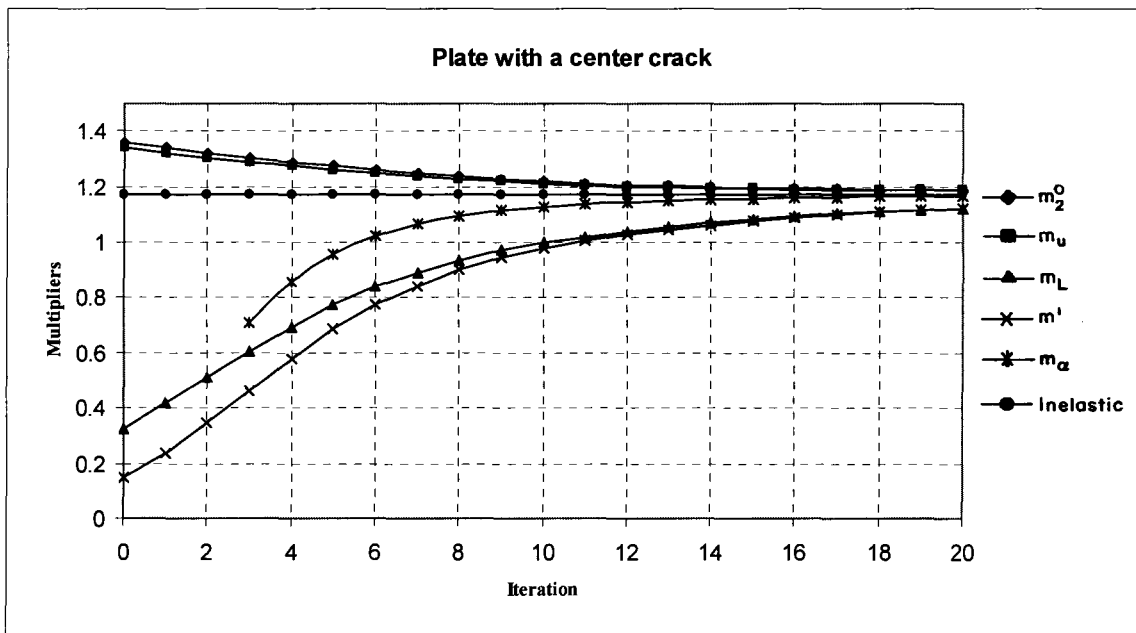


Figure 5.12. Variation of Limit Load Multipliers – Plate with a Center Crack

5.4.6 Compact Tension Specimen

A compact tension specimen with width $W = 100$ mm, height $H = 120$ mm, thickness $B = 3$ mm and crack length $a = 46$ mm is considered as shown in the Figure 5.13. The Young's modulus $E = 211$ GPa and the yield stress $\sigma_y = 488.43$ MPa with a Poisson's ratio of $\nu = 0.3$.

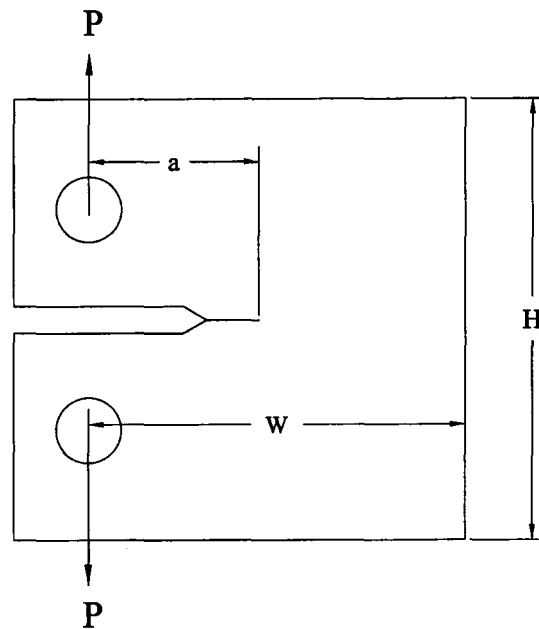


Figure 5.13. Compact Tension Specimen

The finite element model of a compact tension specimen is modelled using six noded isoparametric plane element PLANE2 with plane stress option. The element has two translational degrees of freedom in the x and y directions at each node. Only one half of the specimen is modelled owing to its symmetry in geometry and loading. The finite element mesh used in analyzing the geometry is shown in Figure 5.14. The specimen is meshed with 10 elements through the uncracked thickness portion and 6 elements

through the cracked thickness portion. The crack tip region is meshed with nine crack tip elements. The compact tension specimen is constrained in the vertical (y) direction at the uncracked thickness portion and a tensile load of $P = 20$ KN is applied to the specimen.

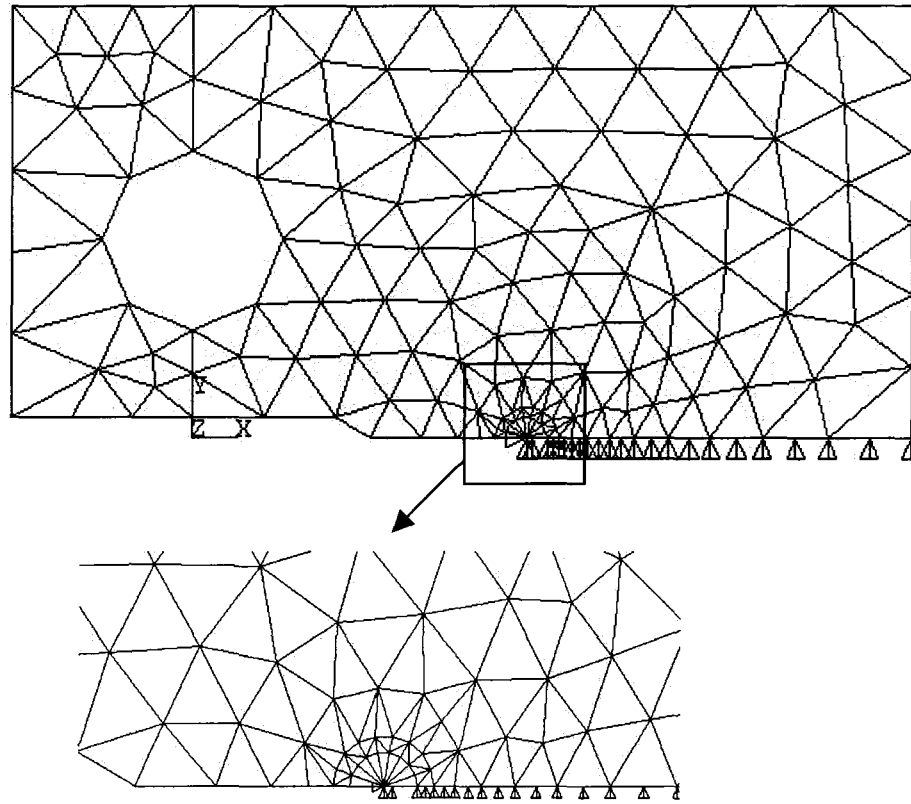


Figure 5.14. FE Mesh of Compact Tension Specimen

The variation of limit load multipliers for fifteen iterations is shown in Figure 5.15. It is seen that the limit load multipliers do not converge even after fifteen iterations. Therefore, reference volume concept is invoked for the compact tension specimen. At

15th iteration, for $V_R/V_T = 0.173$, $m_1^0(V_R) = m_2^0(V_T)$ is satisfied and the value of G is found to be 0.073. The best results of various limit load multipliers after 15 iterations with $q = 0.5$ and the comparison with the result of inelastic FEA are tabulated in Table 5.1. A reference β_R for which $m_\beta = m''(V_R)$ is estimated as 1.788.

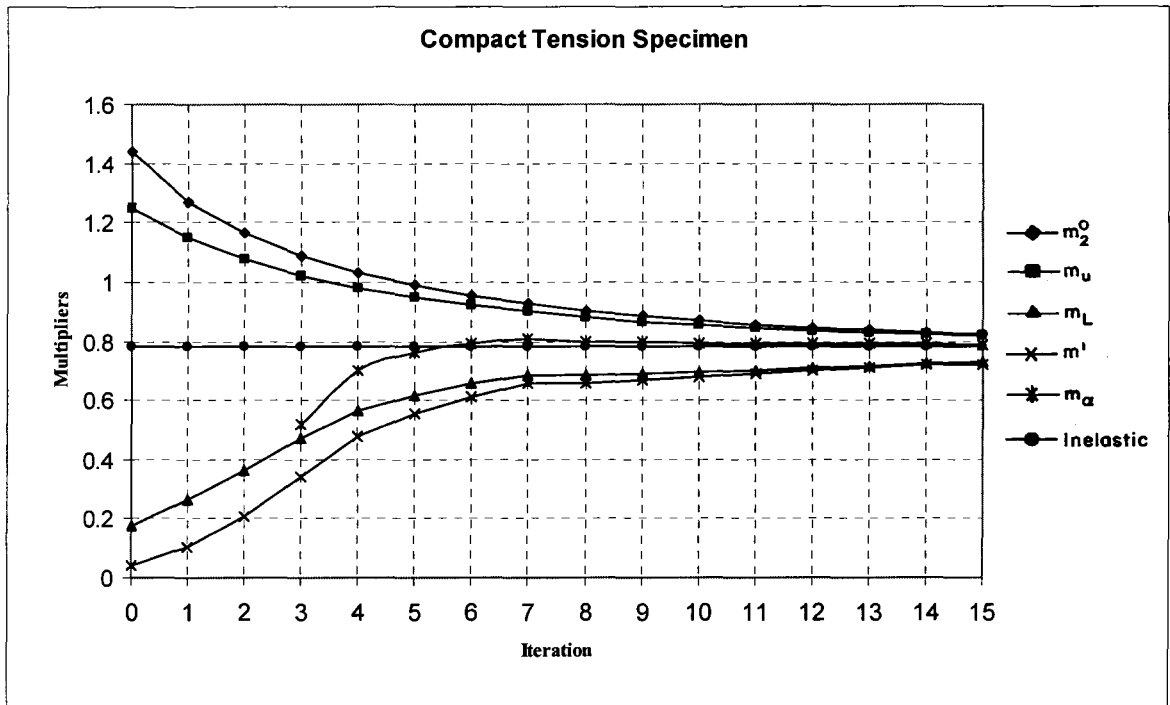


Figure 5.15. Variation of Limit Load Multipliers – Compact Tension Specimen

5.4.7 Plate with Multiple Cracks

A plate with multiple cracks as shown in the Figure 5.16 has a width $W = 100$ mm and a height $H = 200$ mm. The plate has one horizontal crack (length $2a = 20$ mm) at the center, and four 45 degree inclined cracks (length $2b = 21.2$ mm) symmetrically located on both sides of the horizontal and vertical center lines. The crack tips are separated horizontally by 20 mm (dimension c) and vertically by 40 mm (dimension d). The plate is subjected to a tensile stress of $\sigma_y = 300$ MPa. The elastic modulus $E = 210$ GPa, yield strength $\sigma_y = 480$ MPa with a Poisson's ratio $\nu = 0.3$.

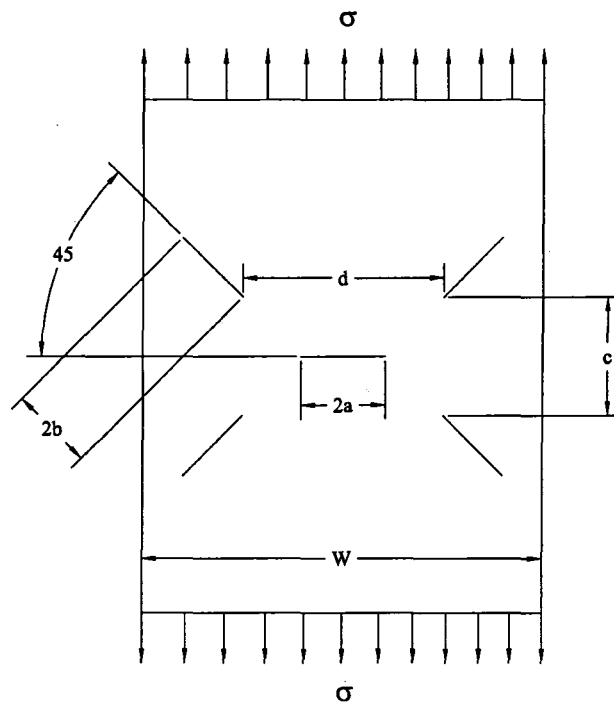


Figure 5.16. Plate with Multiple Cracks

The finite element model of a plate with multiple cracks is modelled using six noded isoparametric plane element PLANE2 with plane stress option. The element has two translational degrees of freedom in the x and y directions at each node. Only one quarter of the specimen is modelled owing to its symmetry in geometry and loading. The finite element mesh used in analyzing the geometry is shown in Figure 5.17. It can be seen that smaller sized elements are used to model the region near the three crack fronts than region away from the cracks. Each of the crack tip regions is meshed with twelve crack tip elements. The plate with multiple cracks is constrained in the horizontal (x) and vertical (y) direction at the uncracked thickness portion and a tensile stress of $\sigma_y = 300$ MPa is applied as a surface load to the specimen.

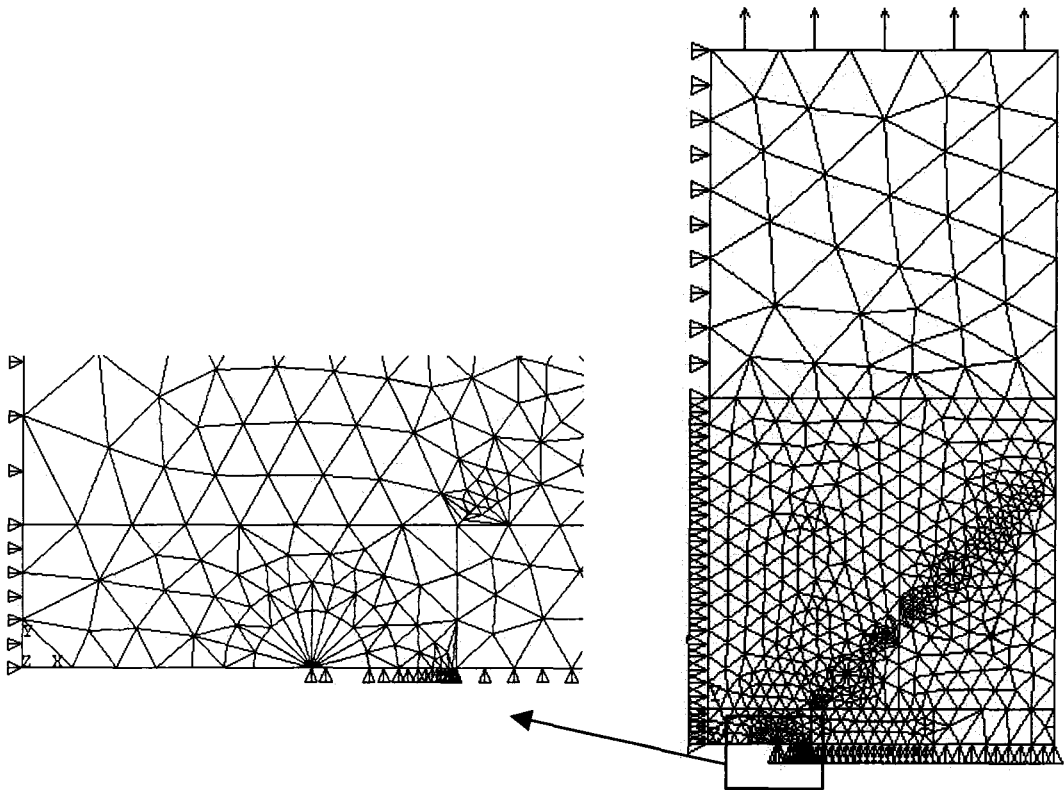


Figure 5.17. FE Mesh of Plate with Multiple Cracks

The variation of limit load multipliers for thirty iterations is shown in Figure 5.18. The reference volume for center-cracked specimen is identified as per the procedure outlined in Section 5.2. At 30th iteration, equation (5.2), which is defined as $m_1^0(V_R) = m_2^0(V_T)$ is satisfied for $V_R/V_T = 0.064$ and $G(V_R)$ is found to be 0.036. The best results of various limit load multipliers after 30 iterations with $q = 0.5$ and the comparison with the result of inelastic FEA are tabulated in Table 5.1. A reference β_R for which $m_\beta = m''(V_R)$ is estimated as 2.496.

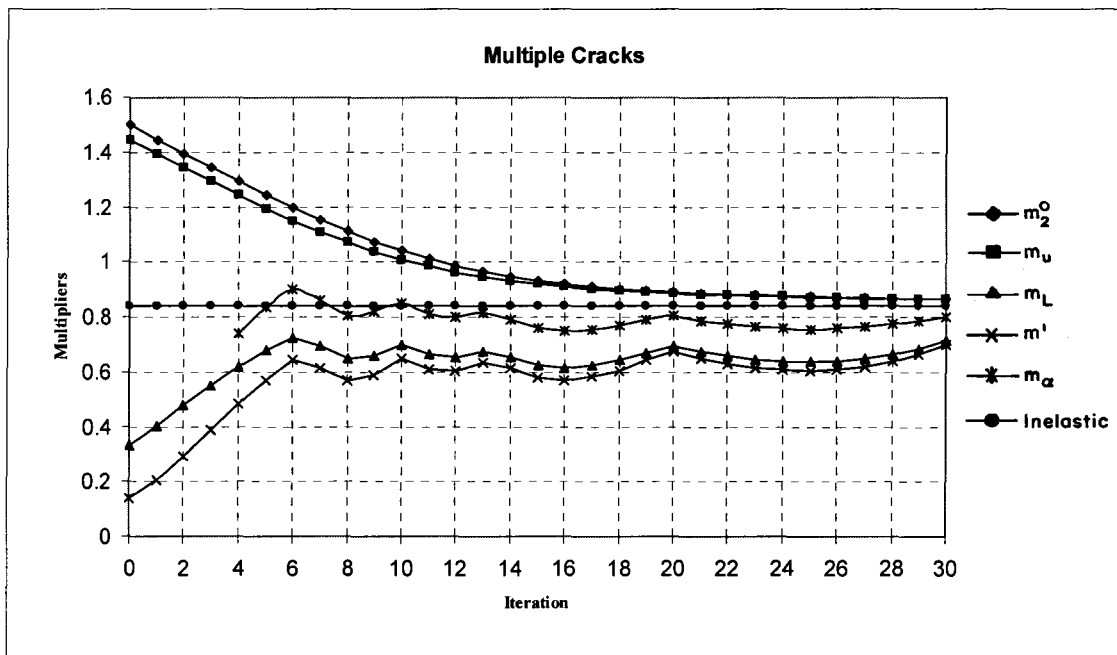


Figure 5.18. Variation of Limit Load Multipliers – Plate with Multiple Cracks

Table 5.1. Values of V_R/V_T , m_1^0/m_2^0 and G for Cracked Components

Application	m_2^0	m_u	$\frac{m_1^0}{m_2^0}$	$\frac{V_R}{V_T}$	G	m_β	m_L	Inelastic FEA
Thick Unwelded Flat Head	1.991	1.989	1.061	0.619	0.024	1.943	1.938	1.967
Welded-in Flat Head	2.772	2.759	1.069	0.653	0.077	2.574	2.061	2.642
Plate with a Center Crack	1.187	1.185	1.104	0.587	0.031	1.150	1.122	1.171
Compact Tension Specimen	0.825	0.819	1.419	0.173	0.073	0.766	0.728	0.780
Plate with Multiple Cracks	0.865	0.864	1.608	0.064	0.036	0.834	0.726	0.840

5.5 Closure

In this chapter, the behavior of m_β -multiplier method is applied for typical pressure vessel and cracked components configurations. The concept of reference volume is invoked for the investigation of such components as they are subjected to local plastic collapse.

It is realized that for structures that are not subjected to global collapse, the statically admissible stress distributions obtained from EMAP may not represent a converged limit type of distribution even after several iterations. For such problems, the concept of reference volume is introduced and the m_β -multiplier is evaluated by taking into account the elements that contributes to plasticity. Furthermore, a parameter G is evaluated that acts as a convergence criterion and is indicative of the deviation of any statically stress distribution from limit type.

It was found that the m'' - multiplier when estimated using the total volume of the structure, evaluated a higher G , thereby significantly overestimating m'' . When the concept of reference volume was invoked for such problems, a significantly lower G was obtained, thereby evaluating a m'' - multiplier that was better than the classical lower bound multiplier and compared well with the inelastic analysis results.

For the problems considered, as low as 0.08 is obtained for the parameter G . This indicates that an improved convergence of stress distribution is achieved using the concept of reference volume, thereby estimating limit loads that are in good comparison with the inelastic analysis results.

For the problems considered so far, the m_β -multiplier using the concept of reference volume is found to be a lower bound. Since more than one stress is accounted for in the estimation of m_β , the results are better than the classical lower bound multiplier m_L .

CHAPTER 6: LIMIT LOAD OF ANISOTROPIC COMPONENTS USING THE M-BETA MULTIPLIER METHOD

6.1 Introduction

Anisotropic properties are usually exhibited by materials due to the dependence of their material properties with respect to the orientation. Components with anisotropic properties such as rolled steel plate, layered cylinders, composites etc. are commonly used in pressure vessel construction. Low cost, lightweight, good stiffness and strength and satisfactory product design are some of the key factors that demand the use of anisotropic materials.

The previous two chapters demonstrated that m_β -multiplier method estimated good lower bounds for typical pressure vessel and cracked component configurations with isotropic material behavior. It may be observed that the formulation of m_β -method to limit analysis is such that it is applicable to a general class of yield criterion. Therefore, in this chapter, attempts are made to investigate the applicability of m_β -multiplier method to anisotropic materials. Of several anisotropic yield criteria, emphasis is oriented towards Hill's yield criterion and the “fourth-order” yield criterion, which is suitable to characterize the plastic behavior of perforated heat exchanger tubesheets.

Limit analysis of heat exchanger tubesheet also addresses the use of repeated elastic analyses technique by implicitly incorporating the fourth-order yield criterion in commercially available FE softwares. The tubesheet material is of isotropic, however its anisotropic model arises in a different manner. For computational efficiency purposes, it is customary to model large, ordered pattern of perforated heat exchanger tubesheets and tube support plates as having equivalent solid material properties.

The perforated tubesheet example considered in this chapter is analyzed as an equivalent solid with anisotropic properties, as it is not feasible to represent a large number of perforations (~ 12000) explicitly in FE model. Hill's yield criterion is often used to characterize the anisotropic plastic behavior. However, the compressibility and rotational symmetry requirements of a triangular perforations pattern makes the use of Hill's criterion problematic. Reinhardt (1998) addressed these problems by deriving a fourth-order yield criterion. Furthermore, approximate associated flow rules were developed by Reinhardt (1999) that led to a complete perfectly plastic model for perforated tubesheet. In this chapter, the limit analysis of the tubesheet is carried out using the m_β -method, in conjunction with both Hill's and fourth-order yield criteria.

Details on Hill's yield criterion and the associated anisotropic constitutive relationships suitable for EMAP are discussed first. Explanations on the limit analysis of heat exchanger tubesheet using fourth-order yield criterion are provided next.

6.2 Anisotropic Constitutive Relationships

6.2.1 Hill's Yield Criterion

An anisotropic yield criterion suggested by Hill (1971) is given by

$$C_{ijkl} \sigma_{ij} \sigma_{kl} = 1 \quad (6.1)$$

where C_{ijkl} is the symmetric material tensor and σ_{ij} is the stress tensor.

Due to symmetry of the material tensor, the equation (6.1) can be rewritten as

$$\sigma_J M_{JK} \sigma_K = 1 \quad (6.2)$$

where σ_K is the stress "vector" composed of the three normal and three shear stresses.

For a general anisotropic material the matrix M has 21 independent constants. For an orthotropic material, M can be reduced to have 9 independent constants, and can be expressed as

$$M_{JK} = \begin{bmatrix} M_{11} & M_{12} & M_{13} & 0 & 0 & 0 \\ M_{12} & M_{22} & M_{23} & 0 & 0 & 0 \\ M_{13} & M_{23} & M_{33} & 0 & 0 & 0 \\ 0 & 0 & 0 & M_{44} & 0 & 0 \\ 0 & 0 & 0 & 0 & M_{55} & 0 \\ 0 & 0 & 0 & 0 & 0 & M_{66} \end{bmatrix} \quad (6.3)$$

Shih and Lee (1978) have shown that assumption of zero volumetric strains in plasticity leads to additional relationships for off-diagonal elements, i.e.,

$$\begin{aligned}
M_{12} &= \frac{1}{2}(M_{33} - M_{11} - M_{22}) \\
M_{13} &= \frac{1}{2}(M_{22} - M_{11} - M_{33}) \\
M_{23} &= \frac{1}{2}(M_{11} - M_{22} - M_{33})
\end{aligned} \tag{6.4}$$

Therefore, the diagonal elements can be determined by performing three uniaxial tests in the x, y and z directions, and three corresponding pure shear experiments.

6.2.2 Non-Dimensionalized form of Hill's Yield Criterion

Valliappan et al. (1976) have described the Hill's criterion in a non-dimensional coefficient form as

$$F = \bar{\sigma} = \frac{1}{2} \{ [\alpha_{12} (\sigma_x - \sigma_y)^2 + \alpha_{23} (\sigma_y - \sigma_z)^2 + \alpha_{31} (\sigma_z - \sigma_x)^2] + 3[\alpha_{44} \tau_{xy}^2 + \alpha_{55} \tau_{yz}^2 + \alpha_{66} \tau_{zx}^2] \}^{1/2} \tag{6.5}$$

where $\bar{\sigma}$ is the reference effective stress, x, y and z are three orthogonal axes of anisotropy. The non-dimensional anisotropic parameters α_{ij} can be related to the uniaxial yield stresses as

$$\begin{aligned}
\alpha_{12} &= \bar{\sigma}_0^2 \left(\frac{1}{\sigma_{0x}^2} + \frac{1}{\sigma_{0y}^2} - \frac{1}{\sigma_{0z}^2} \right); \\
\alpha_{23} &= \bar{\sigma}_0^2 \left(-\frac{1}{\sigma_{0x}^2} + \frac{1}{\sigma_{0y}^2} + \frac{1}{\sigma_{0z}^2} \right); \\
\alpha_{31} &= \bar{\sigma}_0^2 \left(\frac{1}{\sigma_{0x}^2} - \frac{1}{\sigma_{0y}^2} + \frac{1}{\sigma_{0z}^2} \right) \\
\alpha_{44} &= \frac{\bar{\sigma}_0^2}{3} \left(\frac{1}{\tau_{0xy}^2} \right); \quad \alpha_{55} = \frac{\bar{\sigma}_0^2}{3} \left(\frac{1}{\tau_{0yz}^2} \right); \quad \alpha_{66} = \frac{\bar{\sigma}_0^2}{3} \left(\frac{1}{\tau_{0xz}^2} \right)
\end{aligned} \tag{6.6}$$

where σ_{0x} , σ_{0y} and σ_{0z} are the tensile yield stresses in x, y and z directions respectively, τ_{0xy} , τ_{0yz} and τ_{0xz} are the shear yield stresses in xy, yz and xz planes respectively and $\bar{\sigma}_0$ is the reference yield stress which is adopted as one of the six yield stresses. The parameters $\alpha_{ij}, i \neq j$, are the off-diagonal elements in equation (6.3) and therefore, equations (6.4) and (6.6) are similar.

6.3 M-Beta Method for Anisotropic Materials

6.3.1 Integral Mean of Yield Criterion

The variational approach in limit analysis was extended to anisotropic materials by Mura et al. (1968) and Rimawi et al. (1966) in which the integral mean of yield criterion is given by

$$\int_{V_T} \mu^0 [f(s_{ij}^0) + (\phi^0)^2] dV = 0 \tag{6.7}$$

The above equation is similar to equation (4.1) except that $f(s_{ij}^0)$ is replaced by a suitable form of the anisotropic yield criterion.

6.3.2 Flow Rule

The associated flow rule can be expressed as

$$\dot{\varepsilon}^P_{ij} = d\lambda \left(\frac{\partial f}{\partial \sigma_{ij}} \right) \quad (6.8)$$

where $d\lambda$ is a proportionality constant, and using equation (6.5)

$$\frac{\partial f}{\partial \sigma_{ij}} = \frac{1}{2\bar{\sigma}} \begin{bmatrix} \alpha_{12} (\sigma_x - \sigma_y) + \alpha_{31} (\sigma_x - \sigma_z) \\ \alpha_{12} (\sigma_y - \sigma_x) + \alpha_{23} (\sigma_y - \sigma_z) \\ \alpha_{31} (\sigma_z - \sigma_x) + \alpha_{23} (\sigma_z - \sigma_y) \\ 6\alpha_{44} \tau_{xy} \\ 6\alpha_{55} \tau_{yz} \\ 6\alpha_{66} \tau_{zx} \end{bmatrix} \quad (6.9)$$

6.3.3 Upper Bound Multiplier - m^0

Pan and Seshadri (2003) have derived an expression for m^0 using the concept of distributed anisotropic flow parameter μ . The anisotropic flow parameter μ^0 in each iteration of repeated elastic finite element analyses was considered to be a function of the secant modulus in the reference direction of each element. The upper bound multiplier, m^0 , can be expressed as

$$m^0 = \sigma_{0x} \sqrt{\frac{\int_{V_T} \frac{dV}{E_{sx}}}{\int_{V_T} \frac{\bar{f}^2 dV}{E_{sx}}}} \quad (6.10)$$

where \bar{f} is the equivalent stress, E_{sx} is the secant modulus in x-direction and x is taken as the reference direction. The classical upper bound multiplier, m_u , defined in equation (4.5) can be used to estimate upper bound limit loads for anisotropic materials by substituting E_{sx} for the secant modulus and \bar{f} for the equivalent stress.

The derivation for m_β -multiplier described in Chapter 4 applies to anisotropic materials as well, except that the yield function $f(s_{ij}^0)$ has to be replaced by an anisotropic yield criterion.

6.4 Numerical Examples Based on Hill's Criterion

6.4.1 Elastic Modulus Adjustment Scheme

The repeated elastic finite element analyses for orthotropic materials are carried out by modifying the elastic modulus of various elements, after each iteration (elastic solution) as follows:

$$(E_{ij})_{i+1} = \left[\frac{\sigma_{arb}}{\bar{f}_i} \right]^q (E_{ij})_i \quad (6.11)$$

where E_{ij} is the elastic modulus of the material in three orthogonal directions, σ_{arb} is an arbitrary stress, \bar{f} is the effective stress of an element, q is the modulus adjustment index, and i is the iteration number.

6.4.2 Initial Elastic Properties

When implementing EMAP, the stress distributions obtained from successive linear elastic FEA iterations should follow the orthotropic yield surface. This is done by selecting the initial elastic parameters in a proper proportion that is derived from the associated flow rule (Reinhardt and Mangalaramanan, 1999, 2000). Therefore, the initial elastic moduli and Poisson's ratios are determined by comparing the elastic and plastic strains. The elastic stress-strain relationship is given by

$$\{\varepsilon\}=[C]\{\sigma\} \quad (6.12)$$

where $\{\varepsilon\}$ is the strain tensor, $\{\sigma\}$ is the stress tensor and $[C]$ is the compliance matrix which is given by

$$C = \begin{bmatrix} \frac{1}{E_x} & \frac{-\nu_{yx}}{E_y} & \frac{-\nu_{zx}}{E_z} & 0 & 0 & 0 \\ \frac{-\nu_{xy}}{E_x} & \frac{1}{E_y} & \frac{-\nu_{zy}}{E_z} & 0 & 0 & 0 \\ \frac{-\nu_{xz}}{E_x} & \frac{-\nu_{yz}}{E_y} & \frac{1}{E_z} & 0 & 0 & 0 \\ 0 & 0 & 0 & G_{xy} & 0 & 0 \\ 0 & 0 & 0 & 0 & G_{yz} & 0 \\ 0 & 0 & 0 & 0 & 0 & G_{xz} \end{bmatrix} \quad (6.13)$$

Comparing equations (6.8) and (6.12), the elastic properties of initial elastic analysis are given by

$$\begin{aligned}
 E_x &= \sigma_{0x}^2; & E_y &= \sigma_{0y}^2; & E_z &= \sigma_{0z}^2; \\
 G_{xy} &= \tau_{0xy}^2; & G_{yz} &= \tau_{0yz}^2; & G_{xz} &= \tau_{0xz}^2 \\
 \nu_{xy} &= 0.5 E_y \left(\frac{1}{\sigma_{0x}^2} + \frac{1}{\sigma_{0y}^2} - \frac{1}{\sigma_{0z}^2} \right) \\
 \nu_{yz} &= 0.5 E_z \left(\frac{1}{\sigma_{0y}^2} + \frac{1}{\sigma_{0z}^2} - \frac{1}{\sigma_{0x}^2} \right) \\
 \nu_{xz} &= 0.5 E_z \left(\frac{1}{\sigma_{0z}^2} + \frac{1}{\sigma_{0x}^2} - \frac{1}{\sigma_{0y}^2} \right)
 \end{aligned} \tag{6.14}$$

To assure the positive definiteness of stiffness matrix, a factor of 0.47 instead of 0.5 is used for Poisson's ratio in the present analysis.

The m_β -multiplier method for anisotropic materials using Hill's yield is investigated for an orthotropic cylinder under internal pressure, and a transversely isotropic Bridgman notch specimen under tensile load. The problems are modeled using ANSYS (2000) (educational version). The multipliers $m^0, m_u, m_L, m', m_\alpha$ and m_β are calculated automatically using ANSYS APDL language. The results obtained are then compared with inelastic finite element analysis.

6.4.3 Orthotropic Cylinder under Internal Pressure

An orthotropic cylinder under internal pressure with an inner radius is 30 mm and outer radius is 40 mm. The material properties considered are as follows:

$$\sigma_{0x} = 579.2 \text{ MPa}; \sigma_{0y} = 472.3 \text{ MPa}; \sigma_{0z} = 630.9 \text{ MPa}; \tau_{0xy} = 262.9 \text{ MPa};$$

$$E_x = 100993 \text{ MPa}; E_y = 95793.6 \text{ MPa}; E_z = 100593 \text{ MPa};$$

$$G_{xy} = 36147.6 \text{ MPa}; \nu_{xy} = 0.361; \nu_{yz} = 0.345; \nu_{xz} = 0.341;$$

The finite element model of an orthotropic cylinder is modelled using four noded isoparametric plane element PLANE42 with axisymmetric option. The element has two translational degrees of freedom in the x and y directions at each node. The cylinder is meshed with 30 elements through the thickness. In order to simulate the plane strain condition, all the nodes are constrained along the axial direction. An internal pressure of 250 MPa is applied as surface loads on the inside surfaces of the cylinder.

The repeated elastic analysis is carried out with the material properties according to equation (6.14) using the yield stress values listed above. The variation of limit load multipliers with iteration and their comparison with non-linear analysis is plotted in Figure 6.1. It is seen that all the multipliers converge to the limit state value of 0.905. The m_β trajectory shown in the figure corresponds to $\beta_R = 1$ solution and converges to the limit state at the third iteration.

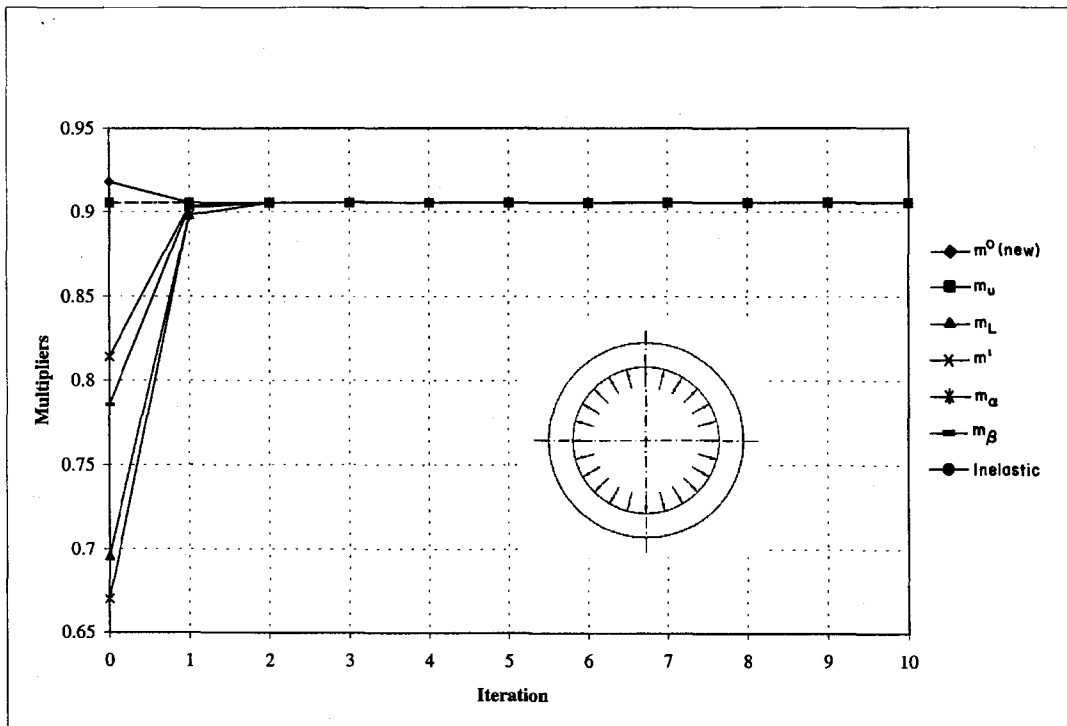


Figure 6.1. Orthotropic Cylinder under Internal Pressure

6.4.4 Transversely Isotropic Bridgman Notch Specimen under Tensile Load

A Bridgman notch specimen subjected to a tensile load has a maximum diameter of 26.416 mm and a minimum diameter of 21.082 mm and a notch radius of 6.858 mm. The specimen is transversely isotropic in the x-z plane. The material properties considered are as below:

$$\sigma_{0x} = 579.2 \text{ MPa}; \sigma_{0y} = 472.3 \text{ MPa}; \sigma_{0z} = 579.2 \text{ MPa};$$

$$\tau_{0xz} = 262.9 \text{ MPa}; \tau_{0yz} = 366.6 \text{ MPa}$$

$$E_x = 100993 \text{ MPa}; E_y = 95793.6 \text{ MPa}; E_z = 100993 \text{ MPa};$$

$$G_{xy} = 36147.6 \text{ MPa}; \nu_{xy} = 0.361; \nu_{yz} = 0.361; \nu_{xz} = 0.341;$$

A four noded isoparametric plane element PLANE182 with axisymmetric option is used to model the bridgman notch specimen. The PLANE182 element has two translational degrees of freedom in the x and y directions at each node. Only one half of the specimen is modelled due to its symmetry in geometry and loading. The specimen is meshed with 20 elements through the thickness and 24 elements along its length. The notch region is meshed with 24 elements along the radius. The bridgman notch specimen is constrained in the horizontal (x) direction along its axis and vertical (y) direction due to symmetry. A tensile stress of 500 MPa is applied as a surface load to the specimen.

The repeated elastic analysis is carried out with the material properties according to equation (6.14) using the yield stress values listed above. The variation of limit load multipliers for twenty iterations and their comparison with non-linear analysis is plotted in Figure 6.2. It is realized that the specimen is subjected to a local plastic collapse. Therefore, the concept of reference volume is invoked for this problem.

The reference volume for the bridgman notch specimen is identified as per the procedure outlined in Chapter 5 for isotropic components. At 20th iteration, for $V_R/V_T = 0.459$, $m_1^0(V_R) = m_2^0(V_T)$ (defined in equation (5.2)) is satisfied and the value of G is found to be 0.013. Corresponding to $V_R/V_T = 0.428$, the m_β -multiplier estimates a value of 0.803 whereas the best value of m_L - multiplier is estimated as 0.795. The m_β -multiplier has a

very good comparison with the inelastic analysis value of 0.807. A reference β_R for which $m_\beta = m''(V_R)$ is estimated as 1.008.

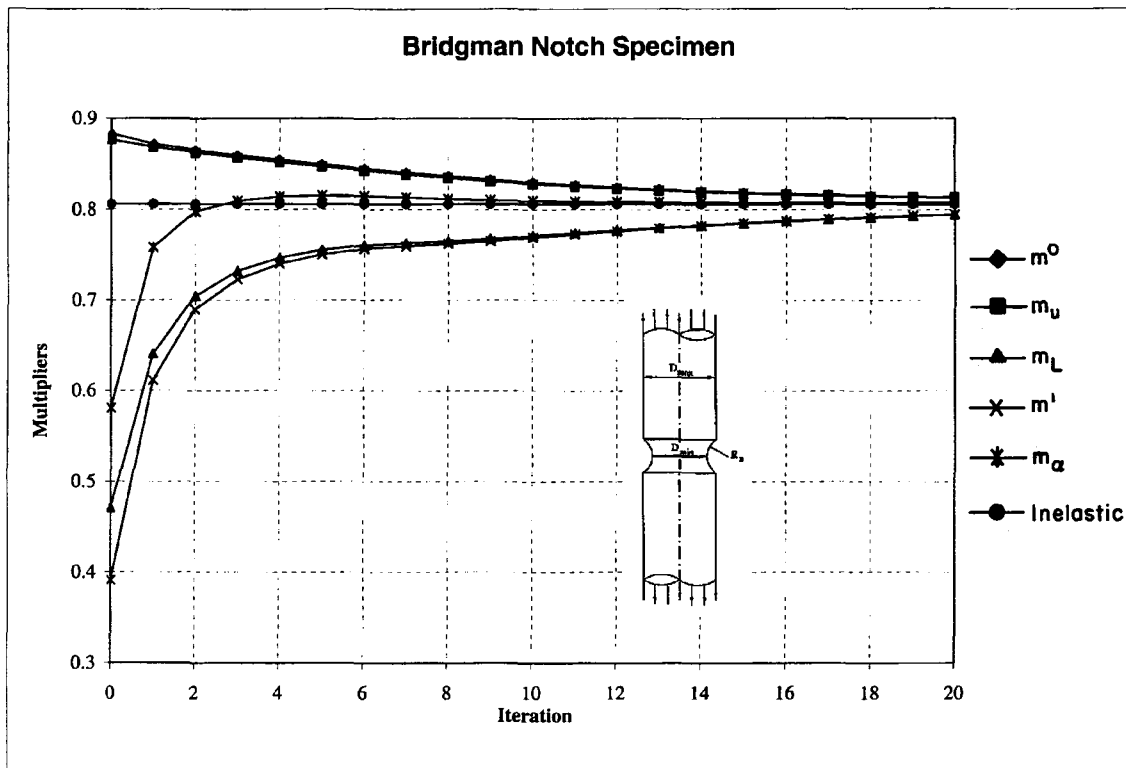


Figure 6.2. Transversely Isotropic Bridgman Notch Specimen

6.5 Heat Exchanger Tubesheet

Heat exchanger tubesheets are often analyzed as an idealized solid (equivalent solid) plate with anisotropic properties, since it is impractical to model the detailed geometry of all perforations. The large number of perforations renders the equivalent solid to exhibit anisotropic properties.

Furthermore, due to presence of perforations, the tubesheet acts as a compressible solid. The inherent assumption of incompressibility in Hill's yield criterion does not predict an accurate response under biaxial loading. Sullivan et al. (1997) investigated the behavior of a tubesheet ligament under a positive biaxial stress state. It was observed that the response was too stiff in the out-of-plane direction, and led to the suggestion that the actual out-of-plane yield stress be replaced with equibiaxial yield stress. As well, the tubesheet with a triangular perforation pattern has a 60° rotational symmetry, and the Hill's criterion does not reflect the 60° symmetry of mechanical properties in the in-plane direction.

6.5.1 Fourth-order Yield Criterion

Reinhardt (1998) derived a fourth-order criterion, and demonstrated that the fourth-order criterion is the lowest order collapse function that describes the behavior required by 60° symmetry of the equilateral perforation pattern. The fourth-order criterion is obtained by squaring the Hill's quadratic yield criterion, and is given by the equation

$$\begin{aligned} & (P s_1^4 + Q (s_2^2 + s_3^2)^2 + R s_1^2 (s_2^2 + s_3^2) + T s_1 s_2 (s_2^2 - 3 s_3^2))^{1/2} \\ & + Y_1 \sigma_{zz}^2 - Y_2 (\sigma_{xx} \sigma_{zz} + \sigma_{yy} \sigma_{zz}) + Y_3 (\sigma_{xz}^2 + \sigma_{yz}^2) = 1 \end{aligned} \tag{6.15}$$

In the above equation, the terms associated with the coefficients P, Q, R and T describe 60° rotational symmetry in the tubesheet plane and the terms associated with Y_1, Y_2 and Y_3 allow compressibility of the perforations.

The in-plane coefficients P, Q, R and T , and the out-of plane coefficients Y_1, Y_2 and Y_3 are defined as:

$$P = \frac{1}{Sy_b^4}; Q = \frac{1}{Sy_s^4}; R = 8 \left(\frac{1}{Sy_{xx}^4} + \frac{1}{Sy_{yy}^4} \right) - \frac{1}{Sy_b^4} - \frac{1}{Sy_s^4};$$

$$T = 8 \left(\frac{1}{Sy_{xx}^4} - \frac{1}{Sy_{yy}^4} \right); Y_1 = Y_2 = \frac{1}{Sy_{zz}^2}; Y_3 = \frac{1}{Sy_{os}^2}$$
(6.16)

where Sy_b is the equibiaxial yield stress, Sy_s is the in-plane yield stress in shear, Sy_{xx} is the tensile yield stress in x-direction, Sy_{yy} is the tensile yield stress in y-direction, Sy_{zz} is the tensile yield stress in z-direction and Sy_{os} is the out-of-plane yield stress in shear.

The fourth-order criterion in equation (6.15), can be rewritten to represent the Hill's yield criterion for a transversely isotropic material with incompressibility assumptions as

$$\sqrt{Q_1 s_2^4 + Q_2 s_3^4 + Q_3 s_2^2 s_3^2} + Y_1 (\sigma_{zz}^2 + \sigma_{xx} \sigma_{yy} - \sigma_{yy} \sigma_{zz} - \sigma_{xx} \sigma_{zz})$$

$$+ Y_3 (\sigma_{xz}^2 + \sigma_{yz}^2) = 1$$
(6.17)

In the above equation, the coefficients in equation (6.15), P, R and T are set to zero and a term $\sigma_{xx} \sigma_{zz}$ is added to the out-of-plane terms. The coefficients Q_1, Q_2, Q_3, Y_1 and Y_2 are defined as

$$Q_1 = \frac{16}{Sy_{xx}^4}; Q_2 = \frac{1}{Sy_s^4}; Q_3 = \left(\frac{8}{Sy_{xx}^2} \right) \left(\frac{1}{Sy_s^2} \right)$$

$$Y_1 = \frac{1}{Sy_{zz}^2}; Y_3 = \frac{1}{Sy_{os}^2}$$
(6.18)

In the next section, the m_β - method is applied to estimate the limit load of a typical tubesheet configuration with Hill's and fourth-order yield criteria. It is revealed that incorporation of compressibility and 60° rotational symmetry of ligaments in the fourth-order function affects the collapse loads. The properties of the tubesheet are listed in the next section.

6.5.2 Geometric Properties

ASME Code Equivalent Radius (R^*) = 72.2549 in (1835.27 mm)

Tubesheet Thickness (t) = 21.4375 in (544.51 mm)

Hole Pattern = Equilateral triangle (60 deg.)

Hole Diameter = 0.758 in (19.25 mm)

Hole Pitch = 1 in (25.4 mm)

Ligament Efficiency (η) = 0.242

6.5.3 Base Material Properties

Young's Modulus = 30E6 psi

Yield Strength = 45E3 psi

Poisson's Ratio = 0.3

Equivalent solid properties are obtained by analyzing a basic ligament model subjected to six basic loading conditions. Jones and Gordon (2001) obtained collapse surfaces for the

fourth-order yield function for thick perforated plates containing triangular perforations for a range of ligament efficiencies, and suggested that the collapse function is reasonable for ligament efficiencies between 0.15-0.50. Therefore, for any ligament efficiency between 0.15-0.50, the in-plane and out-of-plane fourth-order function coefficients can be obtained from the results of Jones and Gordon by linear interpolation. For a considered ligament efficiency of 0.242, the constants are listed as below thereby evaluating the yield stresses in their respective uniaxial loading.

$$\bar{P} = 0.515$$

$$\bar{Q} = 14.394$$

$$\bar{R} = 5.256$$

$$\bar{T} = 10.311$$

where the coefficients \bar{P} , \bar{Q} , \bar{R} and \bar{T} are the coefficients P , Q , R and T normalized with respect to the base yield stress.

Yield stresses for Equivalent Solid (EQS)

$$Sy_x = 9.271 \text{ ksi}$$

$$Sy_z = 12.296 \text{ ksi}$$

$$Sy_y = 21.552 \text{ ksi}$$

$$Sy_b = 12.853 \text{ ksi}$$

$$Sy_s = 5.591 \text{ ksi}$$

$$Sy_{os} = 6.287 \text{ ksi}$$

It is presumed that x is the pitch direction, x - z is the in-plane axes of the tubesheet and y is the out-of-plane direction. It is also presumed that the tubesheet is transversely isotropic in x - z plane.

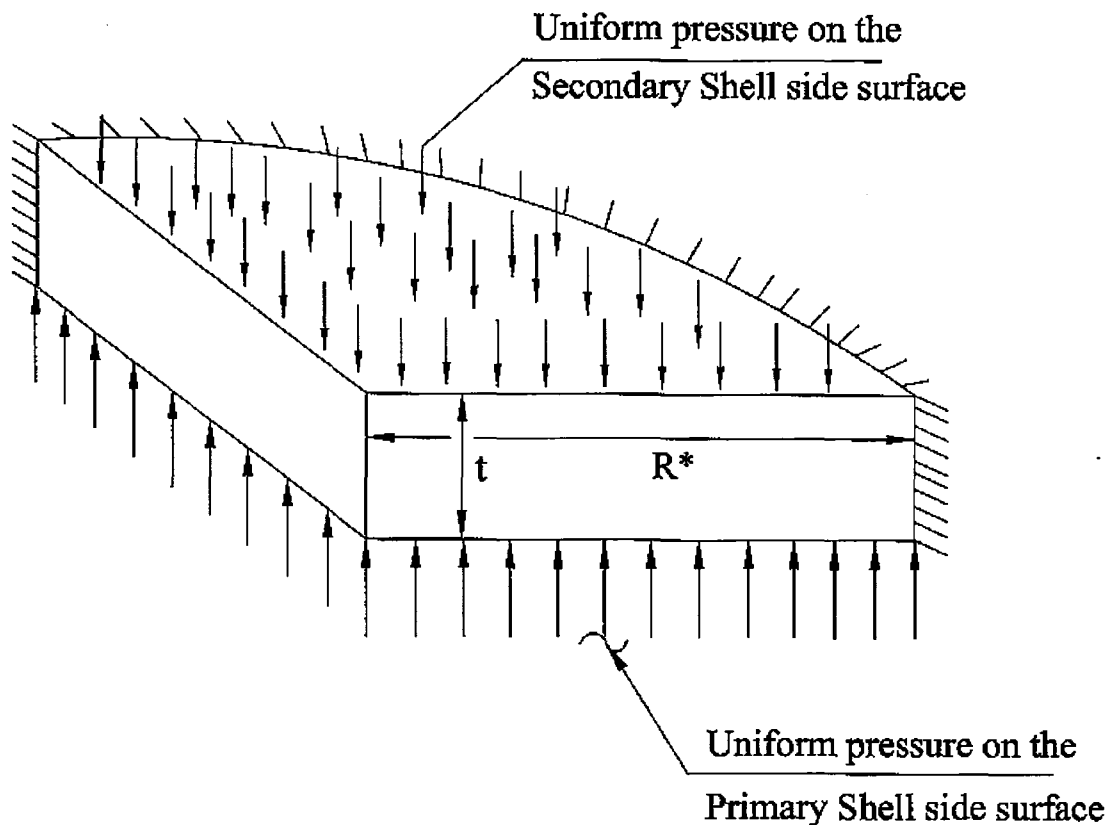


Figure 6.3. Equivalent Solid Model of a Tubesheet

6.5.4 Repeated Elastic Analysis – Hill's Criterion

The finite element model of a heat exchanger tubesheet is modelled using eight noded isoparametric brick element PLANE185. The element has three translational degrees of freedom in the x , y and z directions at each node. Only one quarter of the tubesheet is modelled owing to its symmetry in geometry and loading. The tubesheet is meshed with

20 elements through the thickness, 22 elements along half the diameter and 22 elements along the circumference. The tubesheet thickness face is constrained in the xy and yz planes and is also constrained radially along the outside surface of the circumference. The primary shell side pressure of 2500 psi and secondary shell side pressure of 250 psi are applied as surface loads.

Since Hill's criterion does not reflect 60° rotational symmetry of perforations, $Sy_x = Sy_z = \min(Sy_x, Sy_z)_{actual}$ is considered. Furthermore, as suggested by Sullivan et al. (1997), the out-of-plane yield stress (Sy_y) is replaced with the equibiaxial yield stress (Sy_b) to obtain a more accurate behavior of in-plane plastic behavior under biaxial loading. The elastic constants for the initial elastic run are set according to equation (6.14) so that the stress fields follow the orthotropic yield surface and for the subsequent iterations, the elastic moduli are modified according to the equation (6.11).

The analysis is carried out for 20 iterations. The variation of limit load multipliers with iteration is plotted in Figure 6.4. It is seen that the limit load multipliers almost converge with the inelastic analysis result. In order to assess their nature of convergence, the parameter G is evaluated in conjunction with the concept of reference volume. At 20th iteration, for $V_R/V_T = 0.900$, equation (5.2), $m_1^0(V_R) = m_2^0(V_T)$ is satisfied and the value of G is found to be 0.005. The results of various limit load multipliers at the 20th iteration and the comparison with the result of inelastic FEA are presented in Table 6.1.

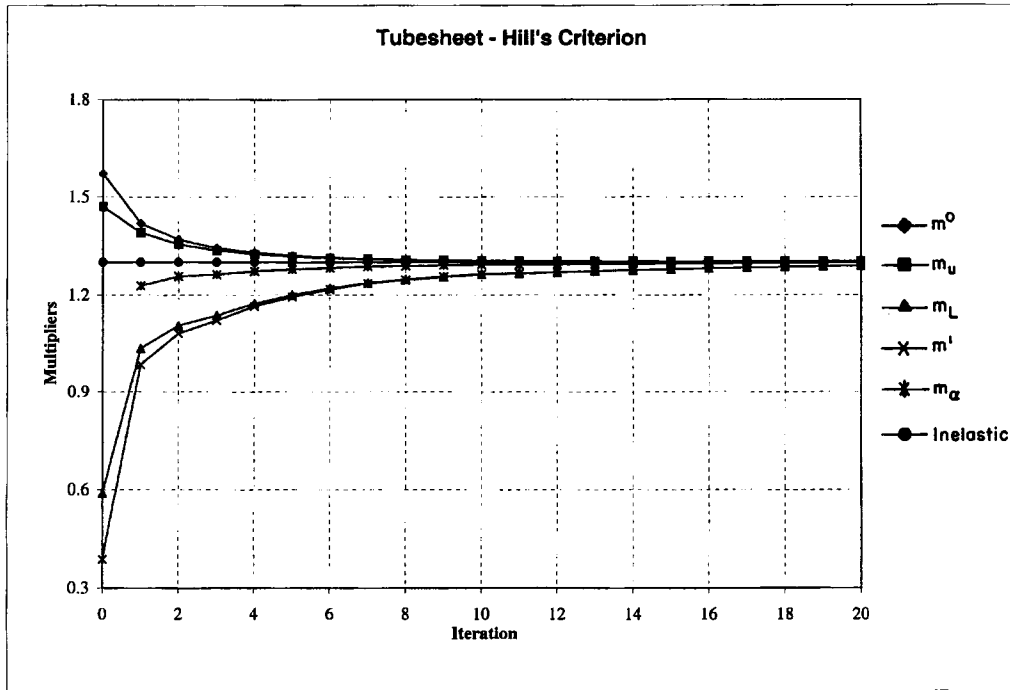


Figure 6.4. Tubesheet – Hill's Criterion

6.5.5 Repeated Elastic Analysis – Fourth Order Criterion

The equivalent solid tubesheet finite element model developed for the Hill's criterion is used for this case. An arbitrary internal pressure of 2500 psi on the primary side and 250 psi on the secondary side is applied. The yield stresses for the equivalent solid derived from fourth-order constants are used except that the out-of-plane yield stress (S_{y_y}) is replaced with the equibiaxial yield stress (S_{y_b}). The elastic properties are modified according to the level 3 approximate flow rule derived by Reinhardt (1999). The elastic properties are

$$\begin{aligned}
 E_x &= Sy_b^2; & E_y &= Sy_s^2; & E_z &= Sy_b^2; \\
 G_{xz} &= \frac{Sy_b^2}{2(1+\nu_{xz})}; & G_{yz} = G_{xy} &= \frac{Sy_b^2 Sy_{os}^2}{2 Sy_s^2 (1+\nu_{xz})} \\
 \nu_{xz} &= \frac{Sy_b^2 - Sy_s^2}{Sy_b^2 + Sy_s^2} \\
 \nu_{xy} &= \nu_{yz} = 0
 \end{aligned}
 \tag{6.19}$$

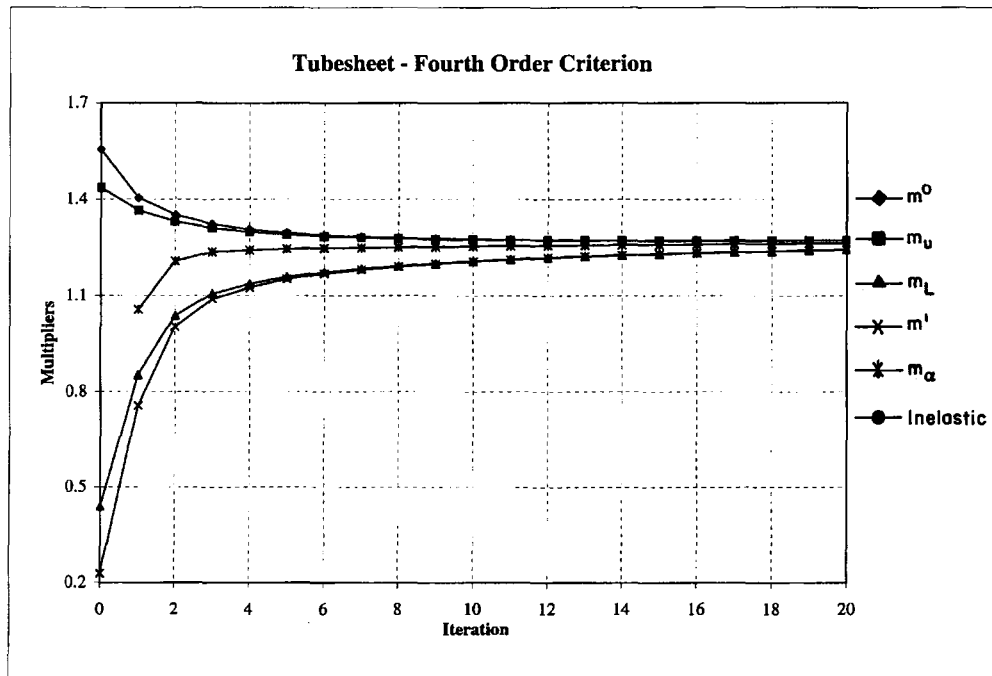


Figure 6.5. Tubesheet – Fourth Order Criterion

The analysis is carried out for 20 iterations. The variation of limit load multipliers with iteration is plotted in Figure 6.5. Similar to the case of the tubesheet analyzed with Hill's criterion, the upper and lower bound limit load multipliers almost converge with a small gap between them. In order to assess their nature of convergence, the parameter G is again evaluated in conjunction with the concept of reference volume. At 20th iteration, for

$V_R/V_T = 0.789$, equation (5.2), $m_1^0(V_R) = m_2^0(V_T)$ is satisfied and the value of G is found to be 0.007. The results of various limit load multipliers at the 20th iteration are presented in Table 6.1.

Table 6.1
Values of V_R/V_T , m_1^0/m_2^0 and G for Tubesheet

Yield Criterion	m_2^0	m_u	$\frac{m_1^0}{m_2^0}$	$\frac{V_R}{V_T}$	G	m_β	m_L	Inelastic FEA
Hill's criterion	1.303	1.303	1.003	0.900	0.005	1.297	1.289	1.301
Fourth-order criterion	1.271	1.271	1.009	0.789	0.007	1.262	1.242	-

6.6 Discussions

The limit loads for anisotropic components are determined using the m_β -multiplier method and the applicability of the m_β -method to a general class of yield criterion is established.

The m_β -method is applied to an orthotropic cylinder and a transversely isotropic Bridgman notch specimen that obey Hill's criterion. In case of orthotropic cylinder, the lower bound limit loads obtained using the m_β -method are improved and converge

rapidly to inelastic analysis results. For the case of Bridgman notch specimen, the specimen collapses across the notch cross-section instead of the whole specimen reaching yield stress. Therefore, use of concept of reference volume evaluated the parameter G of 0.013 and provides a limit load multiplier that is in good agreement with the result of inelastic analysis.

The proposed method is also applied to a heat exchanger tubesheet represented by equivalent solid model with anisotropic properties. Hill's yield criterion assumes plastic incompressibility and does not represent triangular perforation symmetry. The fourth-order criterion is used to account for the compressibility of perforations.

For the equivalent solid tubesheet, the m_β - method estimates better limit loads than the classical lower bound multiplier using the Hill's criterion and fourth-order criterion. Since the fourth-order criterion exhibits compressibility, the results are 3% lower than the Hill's criterion. As well, the EMAP procedures are useful in implementing a plasticity model, which is not currently available in commercial FE softwares.

CHAPTER 7: FITNESS-FOR-SERVICE METHODOLOGY BASED ON VARIATIONAL PRINCIPLES IN PLASTICITY

7.1 Introduction

Fitness-for-service evaluation is performed to ensure safety and economy of an in-service plant that possesses ageing equipments. It also aids in optimizing the maintenance and operation activities of older plants and enhance the long-term viability of the plant. Furthermore, fitness-for-service assessments demonstrate the ability of in-service equipment with defects in preserving the structural integrity of the plant.

Integrity evaluations in the context of engineered facilities involve a systematic and proactive identification of potential modes of failure in engineering plant systems or engineered systems and devices, assessment of the likelihood and consequences of failures; and the devising of appropriate failure avoidance strategies through good design, operational, maintenance and restoration practices.

Oil and gas production facilities, both land-based and offshore, are large financial investments that are valued at millions to billions of dollars. There are well-developed codes and standards in place for new engineered systems and associated equipment; however, there has been a general lack of guidance with respect to the mechanical and structural integrity assessment of aging facilities, although the situation is rapidly

improving (API 579, 2000). The challenge for the industry and educational institutions lies in the logical and effective development and implementation of integrity assessment practice.

Structural integrity assessment in an operating plant is practiced at three levels. Level 1 assessment procedures provide conservative screening criteria that can be used with a minimum quantity of inspection data or information about the component. Level 2 is intended for use by facilities or plant engineers, although some owner-operator organizations consider it more suitable for a central engineering evaluation. Level 3 assessments require sophisticated analysis by experts, where advanced computational procedures are often carried out.

In this chapter, Level 2 integrity assessment methods are developed to evaluate the “Remaining Strength Factor (RSF)” of pressure vessels and piping containing locally thinned areas (LTA) and hot spots. Use is made of a variational formulation in plasticity (Mura et al., 1965) in order to develop simple Level 2 procedures for fitness-for-service evaluation.

7.2 Theoretical Considerations

The integral mean of yield criterion explained in Chapter 3 is used effectively in this chapter to evaluate the RSF of a thin cylinder with LTA and hot spots. Three different damage measures are evaluated in this chapter. These are RSF1, RSF2 and RSF3 and are

based on m^0 , m_L and m_α multipliers respectively. The theory pertaining to the above mentioned multipliers are mentioned again for the sake of clarity.

The “integral mean of yield” is expressed as

$$\int_{V_T} \mu^0 [f(\bar{s}_{ij}^o) + (\phi^o)^2] dV = 0 \quad (7.1)$$

The von-Mises yield criterion, for instance, can be expressed as

$$f(\bar{s}_{ij}) = \frac{1}{2} \bar{s}_{ij} \bar{s}_{ij} - k^2 \quad (7.2)$$

The classical lower bound (m_L) is given by

$$m_L = \frac{\sigma_y}{(\sigma_e)_{\max}} \quad (7.3)$$

The multiplier (m_α) is given by the expression

$$m_\alpha = 2m^0 \frac{2\left(\frac{m^o}{m_L}\right)^2 + \sqrt{\frac{m^o}{m_L}\left(\frac{m^o}{m_L}-1\right)^2\left(1+\sqrt{2}-\frac{m^o}{m_L}\right)\left(\frac{m^o}{m_L}-1+\sqrt{2}\right)}}{\left(\left(\frac{m^o}{m_L}\right)^2 + 2 - \sqrt{5}\right)\left(\left(\frac{m^o}{m_L}\right)^2 + 2 + \sqrt{5}\right)} \quad (7.4)$$

7.3 Integrity Assessment Method – Level 2

7.3.1 Reference Volume for a Thin Cylinder

A thin-walled cylinder with a rectangular LTA is considered as shown in Figure 7.1. In this figure, the dimension $2a$ is the circumferential length and $2b$ is the longitudinal

length of the LTA. Practically, LTA occurs as an irregular shape and it can be represented by an equivalent rectangular LTA. The presence of discontinuities such as a LTA has a localized effect on the cylindrical shell, and such an effect has been discussed in detail by Seshadri (2004). The extent to which this localized effect acts is X_C in the circumferential direction, and X_L in the longitudinal direction.

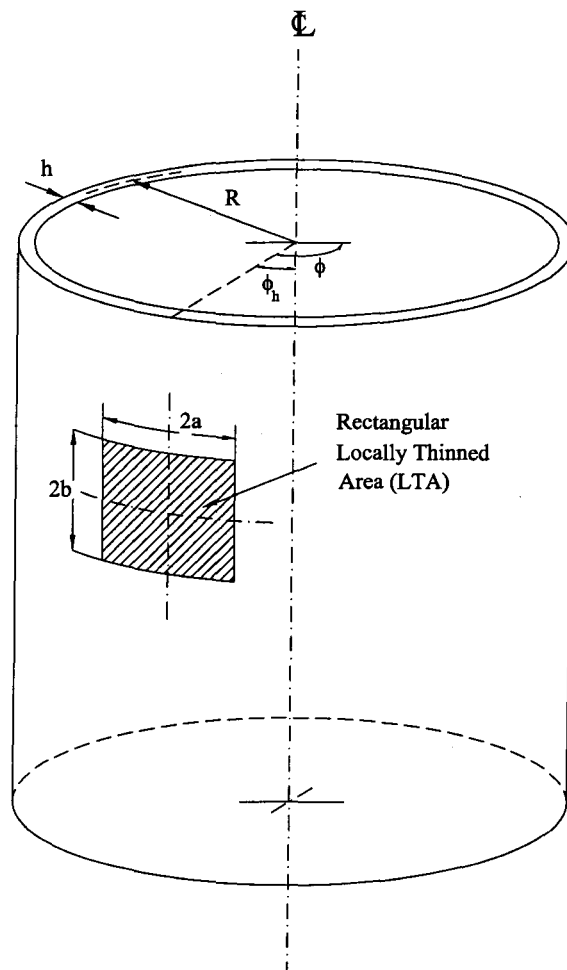


Figure 7.1. A Rectangular LTA in a Cylindrical Vessel

The quantities X_C and X_L can be expressed as:

$$X_C = 6.1(R^3 t)^{1/4} \quad (7.5a)$$

$$X_L = 2.5\sqrt{Rt} \quad (7.5b)$$

where R is taken as the outside radius of the cylindrical shell, and t is the thickness of the shell.

The concept of reference volume suitable for a damaged cylinder has been introduced by Seshadri (2004). The reference volume identifies the ‘kinematically active’ portion of the cylindrical shell that participates in plastic action. During a local plastic collapse, plastic action is assumed to be confined to a local region of the cylinder as shown in Figure 7.2. For example, the reference volume for a cylinder with a single hot spot can be expressed as

$$V_R = 4(X_C + a)(X_L + b)t \quad (7.6)$$

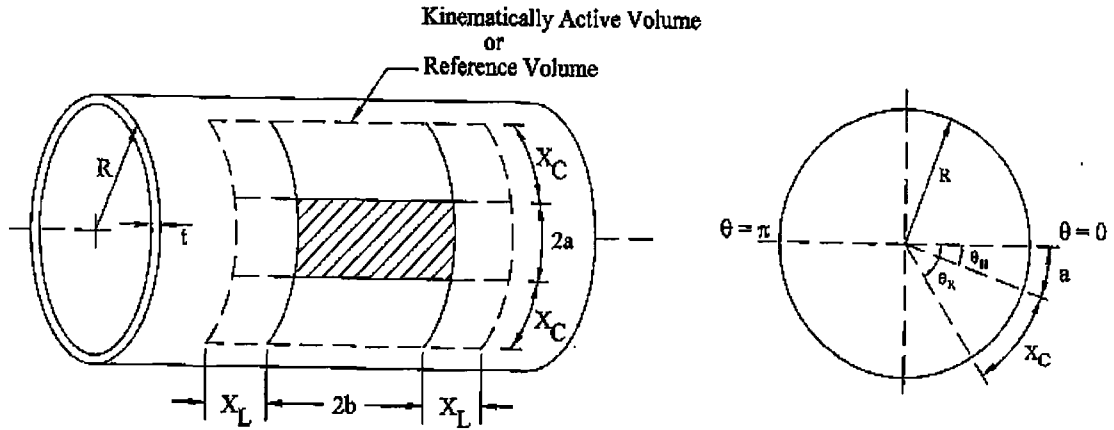


Figure 7.2. Reference Dimensions for Localized Effects

The application of the concept of integral mean of yield for assessment of damaged “local areas” of pressure vessels and piping is considered next.

7.3.2 Locally Thinned Areas (LTA)

A thin walled cylinder with a LTA is shown in the Figure 7.3. The von-Mises criterion, equation (7.2), can be rewritten as,

$$f^0 = (m^0 \sigma_e^0)^2 - \sigma_y^2 = 0 \quad (7.7)$$

where σ_e^0 is the statically admissible uniform equivalent stress.

The integral mean of yield criterion using von-Mises criterion can be expressed as

$$\int_{V_u} \left\{ (m_d^0 \sigma_{eU}^0)^2 - \sigma_y^2 \right\} dV + \int_{V_c} \left\{ (m_d^0 \sigma_{eC}^0)^2 - \sigma_y^2 \right\} dV = 0 \quad (7.8)$$

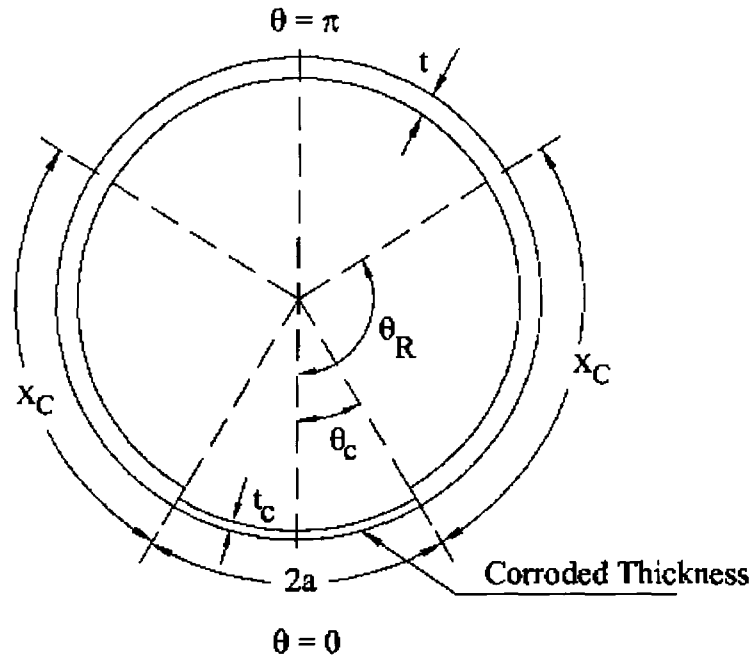


Figure 7.3. LTA in a Thin Cylinder

where the suffix C refers to the LTA and suffix U refers to the region with undamaged thickness.

If stresses are constant within V_U and V_C , integration of (7.8) leads to

$$[(m_d^0 \sigma_{eU}^0)^2 - \sigma_y^2]V_U + [(m_d^0 \sigma_{eC}^0)^2 - \sigma_y^2]V_C = 0 \quad (7.9)$$

where σ_{eU} is the equivalent stress of undamaged cylinder, and σ_{eC} is the equivalent stress in the LTA region. Carrying out the necessary algebraic manipulations, m_d^0 is expressed as

$$m_d^0 = \sqrt{\frac{\sigma_y^2 (V_R)}{\sigma_{eU}^2 V_U + \sigma_{eC}^2 V_C}} \quad (7.10)$$

which in turn can be written as,

$$RSF1 = \frac{m_d^0}{m_u^0} = \sqrt{\frac{V_R}{V_C \left(\frac{\sigma_{eC}^2}{\sigma_{eU}^2} - 1 \right) + V_R}} \quad (7.11)$$

$RSF1$ is the remaining strength factor that is based on m_d^0 and $m_u^0 = \frac{\sigma_y}{\sigma_{eU}}$.

Two additional damage measures, namely $RSF2$ and $RSF3$, based on multipliers m_α and m_L respectively, can be expressed as

$$RSF2 = \frac{m_{ad}}{m_u^0}, \quad (7.12)$$

$$RSF3 = \frac{m_{Ld}}{m_u^0} \quad (7.13)$$

where

$$m_{Ld} = \frac{\sigma_y}{\sigma_{eC}}. \quad (7.14)$$

In the similar manner, the various RSF can be evaluated by making use of the Tresca criterion. The Tresca criterion can be expressed as

$$f^0 = |m^0 \sigma_\theta^0 - \sigma_y| = 0 \quad (7.15)$$

where σ_θ^0 is the hoop stress in the cylinder.

The integral mean of yield criterion using Tresca criterion can be expressed as

$$\int_{V_u} \left\{ (m_d^0 \sigma_{\theta U}^0) - \sigma_y \right\} dV + \int_{V_c} \left\{ (m_d^0 \sigma_{\theta C}^0) - \sigma_y \right\} dV = 0 \quad (7.16)$$

where $\sigma_{\theta C}^0$ and $\sigma_{\theta U}^0$ are the hoop stresses in the LTA and the undamaged sections, respectively. Assuming that the stresses are constant within V_U and V_C , integration of (7.16) leads to

$$[(m_d^0 \sigma_{\theta U}^0) - \sigma_y] V_U + [(m_d^0 \sigma_{\theta C}^0) - \sigma_y] V_C = 0 \quad (7.17)$$

Carrying out necessary algebraic manipulations, the equation for m_d^0 and *RSF1* can be derived as

$$m_d^0 = \frac{\sigma_y V_R}{\sigma_{\theta U} V_U + \sigma_{\theta C} V_C} \quad (7.18)$$

$$RSF1 = \frac{m_d^0}{m_u^0} = \frac{1}{1 - \frac{V_C}{V_R} \left(1 - \frac{\sigma_{\theta C}}{\sigma_{\theta U}} \right)} \quad (7.19)$$

Replacing $\sigma_{\theta C}^0$ and $\sigma_{\theta U}^0$ instead of σ_{eC}^0 and σ_{eU}^0 , *RSF2* and *RSF3* can be evaluated using equations (7.12) and (7.13).

7.3.3 Local Hot Spots

Seshadri (2004) has formulated an assessment procedure for pressure vessels and piping with local hot spots that may undergo yielding. In this thesis, assessment of local hot spots that do not yield is considered.

For a thin cylinder with a single hot spot, for example, the integral mean of yield criterion for a reference volume V_R can be expressed as

$$\int_{V_H} \left\{ \left(m_d^0 \sigma_{eH}^0 \right)^2 - \sigma_{yH}^2 \right\} dV + \int_{V_C} \left\{ \left(m_d^0 \sigma_{eC}^0 \right)^2 - \sigma_{yC}^2 \right\} dV = 0 \quad (7.20)$$

where the suffix H refers to the hot spot region and C refers to the uniform temperature away from the hot spot region. Also, m_d^0 refers to the m^0 - multiplier for the damaged pressure component.

If the stresses are assumed to be uniform within the respective volumes, equation (7.20) can be expressed as,

$$\left[\left(m_d^0 \sigma_{eH}^0 \right)^2 - \sigma_{yH}^2 \right] V_H + \left[\left(m_d^0 \sigma_{eC}^0 \right)^2 - \sigma_{yC}^2 \right] V_C = 0. \quad (7.21)$$

If the thickness is unaltered throughout the reference volume, then,

$$\sigma_{eH}^0 = \sigma_{eC}^0 = \sigma_e^0. \quad (7.22)$$

Using equation (7.22), equation (7.21) can be written as,

$$m_d^0 = \sqrt{\frac{\sigma_{yH}^2 V_H + \sigma_{yC}^2 V_C}{(\sigma_e^0)^2 V_R}}. \quad (7.23)$$

where V_R is the reference volume, and $V_R = V_C + V_H$. Equation (7.23) can further be written as

$$m_d^0 = \sqrt{\frac{\sigma_{yC}^2}{(\sigma_e^0)^2} \left(\frac{\sigma_{yH}^2 V_H}{\sigma_{yC}^2 V_R} + \frac{V_C}{V_R} \right)}. \quad (7.24)$$

Substituting $V_C = V_R - V_H$, equation (7.24) can be rewritten to define *RSF1* as,

$$RSF1 = \frac{m_d^0}{m_u^0} = \sqrt{\frac{\sigma_{yH}^2 V_H}{\sigma_{yC}^2 V_R} + \frac{V_R - V_H}{V_R}} \quad (7.25)$$

where $m_u^0 = \frac{\sigma_{yC}}{\sigma_{eU}}$. Therefore,

$$RSF1 = \frac{m_d^0}{m_u^0} = \sqrt{1 - \frac{V_H}{V_R} \left(1 - \frac{\sigma_{yH}^2}{\sigma_{yC}^2} \right)}. \quad (7.26)$$

Proceeding as in the application of LTA, additional damage measures namely *RSF2* and *RSF3* can also be evaluated for hot spots as follows.

$$RSF2 = \frac{m_{ad}}{m_u^0}, \quad (7.27)$$

$$RSF3 = \frac{m_{Ld}}{m_u^0} \quad (7.28)$$

where,

$$m_{Ld} = \frac{\sigma_{yH}}{\sigma_e}. \quad (7.29)$$

Similarly, expressions for m_d^0 and $RSF1$ using Tresca criterion in equation (7.15) can be derived as

$$m_d^0 = \frac{\sigma_{yH} V_H + \sigma_{yC} V_C}{\sigma_{\theta}^0 V_R}, \quad (7.30)$$

$$RSF1 = \frac{m_d^0}{m_u^0} = 1 + \frac{V_H}{V_R} \left(\frac{\sigma_{yH}}{\sigma_{yC}} - 1 \right). \quad (7.31)$$

Replacing the hoop stress σ_{θ}^0 for σ_e^0 , $RSF2$ and $RSF3$ can be evaluated using equations (7.27) and (7.28).

7.4 Numerical Examples

Level 2 assessment procedures for hot spots and LTA are applied to a typical thin walled cylinder under internal pressure with the following specifications. The values given in the brackets are in SI units.

ASTM Material = SA 516 Gr. 55

Shell Inside Radius (R_i) = 33 in. (0.838 m)

Shell Overall Length (L) = 400 in. (10.16 m)

Operating Pressure (P_o) = 180 psig (1.24 MPa)

Design Pressure (P_d) = 220 psig (1.52 MPa)

Operating Temperature (T_1) = 90 deg. F (32.22 deg. C)

Design Temperature (T_2) = 100 deg. F (37.78 deg. C)

Allowable Stress (S) = 13700 psi. (94.46 MPa)

Corrosion Allowance (CA) = 1/16 in. = 0.063 in. (0.002 m)

Joint Efficiency (E) = 1.0

7.4.1 Required Shell Thickness Calculations

Under Design Conditions:

Design thickness:

$$t_d = \frac{P_d R_i}{S E - 0.6 P_d} = 0.536 \text{ in. (0.014 m)}$$

$$\text{Shell Thickness } (t_s) = t_d + CA = 0.599 \text{ in. (0.015 m)}$$

Therefore, use 5/8 in. (0.016 m) plate.

Using equations (7.5a) and (7.5b), the local parameters X_C and X_L are calculated as,

$$X_C = 6.10 \sqrt[4]{R^3 t} = 75.735 \text{ in. (1.924 m)}$$

$$X_L = 2.5 \sqrt{R t} = 11.461 \text{ in. (0.291 m)}$$

7.4.2 Evaluation of RSF for Locally Thinned Areas (LTA)

Level 2 assessment procedure for LTA is demonstrated for a thin cylinder with the following specifications.

Outside Radius (R) = 33.625 in. (0.854 m)

Shell Thickness (t) = 0.625 in. (0.016 m)

Corroded Thickness (t_c) = 0.375 in. (0.01 m)

Corroded Radius (R_c) = 33.25 in (0.845 m)

Yield Stress (σ_y) = 30 ksi (206.85 MPa)

The dimensions of the LTA (Figure 7.3) are chosen such that,

$\theta_c = 50.95$ degrees

$\theta_R = 180$ degrees

Therefore,

$a = \pi R - X_C = 29.9$ in. (0.759 m)

As well, we choose, $b = 29.9$ in. (Aspect Ratio of 1.0)

Volume of the LTA: $V_C = (2a)(2b)t_c = 1341.02$ in³. (0.022 m³)

Uncorroded volume,

$V_U = [(2X_C + 2a)(2X_L + 2b) - (2a)(2b)]t = 8687.88$ in³. (0.142 m³)

Reference Volume, $V_R = V_C + V_U = 10028.9$ in³. (0.164 m³)

Stresses in the LTA:

Hoop Stress, $\sigma_{tc} = \frac{P_d R_c}{t_c} = 19506.7$ psi (134.50 MPa)

Longitudinal Stress, $\sigma_{lc} = \frac{P_d R_c}{2 t_c} = 9753.4$ psi (67.25 MPa)

Von-Mises Equivalent Stress,

$$\sigma_{ec} = \sqrt{\sigma_{tc}^2 + \sigma_{lc}^2 - \sigma_{tc} \sigma_{lc}} = 16893.27 \text{ psi (116.48 MPa)}$$

Stresses in the uncorroded cylinder:

$$\text{Hoop Stress, } \sigma_t = \frac{P_d R_i}{t} = 11616 \text{ psi (80.09 MPa)}$$

$$\text{Longitudinal Stress, } \sigma_l = \frac{P_d R_i}{2 t} = 5808 \text{ psi (40.05 MPa)}$$

Von-Mises Equivalent Stress,

$$\sigma_{eu} = \sqrt{\sigma_t^2 + \sigma_l^2 - \sigma_t \sigma_l} = 10060 \text{ psi (69.36 MPa)}$$

We have,

$$m_{u}^0 = \frac{\sigma_y}{\sigma_{eu}} = 2.9822$$

$$\text{Using equation (7.23), } m_d^0 = \sqrt{\frac{\sigma_y^2 V_R}{(\sigma_{ec})^2 V_C + (\sigma_{eu})^2 V_U}} = 2.6744$$

$$\text{Using equation (7.29), } m_{Ld} = \frac{\sigma_y}{\sigma_{ec}} = 1.776$$

Using equation (7.4),

$$m_{ad} = \frac{2 \left(\frac{m_d^0}{m_{Ld}} \right)^2 + \sqrt{\frac{m_d^0 \left(\frac{m_d^0}{m_{Ld}} - 1 \right)^2 \left(1 + \sqrt{2} - \frac{m_d^0}{m_{Ld}} \right) \left(\frac{m_d^0}{m_{Ld}} - 1 + \sqrt{2} \right)}}{\left(\left(\frac{m_d^0}{m_{Ld}} \right)^2 + 2 - \sqrt{5} \right) \left(\left(\frac{m_d^0}{m_{Ld}} \right)^2 + 2 + \sqrt{5} \right)} = 2.1677$$

Using equation (7.26), $RSF1 = \frac{m_d^0}{m_u} = 0.8968$

Using equation (7.27), $RSF2 = \frac{m_{\alpha d}}{m_u} = 0.7269$

Using equation (7.28), $RSF3 = \frac{m_{Ld}}{m_u} = 0.5955$

A Level 3 elastic-plastic finite element analysis is carried out with a plastic modulus of 50E4 psi. For 1% membrane strain limit, a *RSF* of 0.7286 is obtained. The proposed *RSF2* when compared with inelastic FEA is conservative.

As indicated before, *RSF1* is based on m^0 - multiplier and is an upper bound, whereas *RSF2* is based on m_{α} - an improved limit load multiplier and is of interest from the structural integrity standpoint. From the above results, it can be seen that *RSF2* is conservative.

The Level 2 assessment method is applied to a thin cylinder with different sizes of LTA and 1/16", 1/8" and 1/4" thickness losses. The results are tabulated below. It is apparent that as the size of the LTA or thickness loss increases, the *RSF* of the structure reduces. Indeed, the proposed Level 2 results reflect this effect. The calculated *RSF2* is found to be conservative and compares well with inelastic finite element analysis.

For LTA, an allowable *RSF* of 0.9 has been shown to be conservative for typical process equipment (API 579, 2000).

Table 7.1.
LTA with 1/16" Corroded Thickness

Case No.	θ_c deg.	θ_R deg.	Aspect Ratio	<i>RSF1</i>	<i>RSF2</i>	<i>RSF3</i>	Inelastic
1	10.22	139.27	1.0	0.9973	0.9622	0.8983	1.0000
2	20.45	149.50	1.0	0.9925	0.9594	0.8983	1.0000
3	30.67	159.72	1.0	0.9875	0.9564	0.8983	0.9999
4	40.90	170.00	1.0	0.9827	0.9535	0.8983	0.9938
5	50.95	180.00	1.0	0.9782	0.9508	0.8983	0.9907
6	50.95	180.00	2.0	0.9828	0.9536	0.8983	1.000
7	25.13	154.18	0.5	0.9872	0.9562	0.8983	1.000

Table 7.2.
LTA with 1/8" Corroded Thickness

Case No.	θ_c deg.	θ_R deg.	Aspect Ratio	<i>RSF1</i>	<i>RSF2</i>	<i>RSF3</i>	Inelastic
1	10.22	139.27	1.0	0.9943	0.9095	0.7970	0.9907
2	20.45	149.50	1.0	0.9841	0.9050	0.7970	0.9389
3	30.67	159.72	1.0	0.9736	0.9001	0.7970	0.9191
4	40.90	170.00	1.0	0.9636	0.8954	0.7970	0.9038
5	50.95	180.00	1.0	0.9543	0.8910	0.7970	0.8978
6	50.95	180.00	2.0	0.9639	0.8956	0.7970	0.9237
7	25.13	154.18	0.5	0.9730	0.8999	0.7970	0.9359

Table 7.3.
LTA with 1/4" Corroded Thickness

Case No.	θ_c deg.	θ_R deg.	Aspect Ratio	<i>RSF1</i>	<i>RSF2</i>	<i>RSF3</i>	Inelastic
1	10.22	139.27	1.0	0.9864	0.7378	0.5955	0.9145
2	20.45	149.50	1.0	0.9630	0.7360	0.5955	0.7728
3	30.67	159.72	1.0	0.9391	0.7335	0.5955	0.7392
4	40.90	170.00	1.0	0.9168	0.7303	0.5955	0.7316
5	50.95	180.00	1.0	0.8968	0.7269	0.5955	0.7286
6	50.95	180.00	2.0	0.9176	0.7304	0.5955	0.7469
7	25.13	154.18	0.5	0.9377	0.7333	0.5955	0.7712

7.4.3 Evaluation of RSF for Hot Spots

A hot spot with dimension $2a$ is chosen such that X_C subtends the entire cylinder in the circumferential direction. i.e.,

$$a = \pi R - X_C = 29.9 \text{ in. (0.759 m)}$$

Also choose, $b = 29.9$ in. (Aspect Ratio of 1.0)

With reference to the Figure 7.2,

$$\theta_h = 50.95 \text{ degrees}$$

$$\theta_R = 180 \text{ degrees}$$

Reference Volume, $V_R = (2X_C + 2a)(2X_L + 2b)t = 10922.9 \text{ in}^3 (0.179 \text{ m}^3)$

Hot Spot Volume, $V_H = (2a)(2b)t = 2235.03 \text{ in}^3 (0.037 \text{ m}^3)$

Remaining Volume, $V_C = V_R - V_H = 8687.88 \text{ in}^3 (0.142 \text{ m}^3)$

Hoop Stress, $\sigma_t = \frac{P_d R_i}{t} = 11616 \text{ psi (80.09 MPa)}$

Longitudinal Stress, $\sigma_l = \frac{P_d R_i}{2t} = 5808 \text{ psi (40.05 MPa)}$

von-Mises Equivalent Stress,

$$\sigma_e = \sqrt{\sigma_t^2 + \sigma_l^2} = 10060 \text{ psi (69.36 MPa)}$$

$\sigma_{yC} (@ T_C = 100 \text{ deg. F}) = 30000 \text{ psi (206.85 MPa)}$

$\sigma_{yH} (@ T_H = 400 \text{ deg. F}) = 25700 \text{ psi (178.00 MPa)}$

$$m_u^0 = \frac{\sigma_{yC}}{\sigma_e} = 2.9822$$

$$\text{Using equation (7.23), } m_d^0 = \sqrt{\frac{\sigma_{yH}^2 V_H + \sigma_{yC}^2 V_C}{(\sigma_e)^2 V_R}} = 2.8998$$

$$\text{Using equation (7.29), } m_{Ld} = \frac{\sigma_{yH}}{\sigma_e} = 2.5547$$

Using equation (7.4),

$$m_{cd} = \frac{2 \left(\frac{m_d^o}{m_{Ld}} \right)^2 + \sqrt{\frac{m_d^o}{m_{Ld}} \left(\frac{m_d^o}{m_{Ld}} - 1 \right)^2 \left(1 + \sqrt{2} - \frac{m_d^o}{m_{Ld}} \right) \left(\frac{m_d^o}{m_{Ld}} - 1 + \sqrt{2} \right)}}{\left(\left(\frac{m_d^o}{m_{Ld}} \right)^2 + 2 - \sqrt{5} \right) \left(\left(\frac{m_d^o}{m_{Ld}} \right)^2 + 2 + \sqrt{5} \right)} = 2.7727$$

$$\text{Using equation (7.26), } RSF1 = \frac{m_d^0}{m_u^0} = 0.9724$$

$$\text{Using equation (7.27), } RSF2 = \frac{m_{cd}}{m_u^0} = 0.9297$$

$$\text{Using equation (7.28), } RSF3 = \frac{m_{Ld}}{m_u^0} = 0.8566$$

A Level 3 elastic-plastic finite element analysis is carried out with a plastic modulus of 50E4 psi. For 1% membrane strain limit, a *RSF* of 0.945 is obtained. The finite element analysis software ANSYS (2000) (educational version) was used to perform the inelastic analysis.

7.4.4 Thermo-elastic Calculations

The material properties of carbon steel for a temperature range of 100 – 600 degree F is listed in the table below.

Table 7.4.
Material Properties of Carbon Steel

Temp °F	100	200	300	400	500	600
E (x10 ⁶) psi	29.3	28.8	28.3	27.7	27.3	26.7
α (x10 ⁻⁶) in./in. °F	5.53	5.89	6.26	6.61	6.91	7.17
σ_y (x10 ³) psi	30.0	27.3	26.6	25.7	24.5	22.2

Temperature in the Hot Spot region (T_H) = 400 deg. F (204.44 deg. C)

Temperature in the other parts of the cylinder (T_C) = 100 deg. F (37.78 deg. C)

Average Temperature (T_{avg}) = 250 deg. F (121.11 deg. C)

Elastic Modulus at T_{avg} (E) = 28.55 E6 psi (196.85 E3 MPa)

Coefficient of Thermal Expansion at T_{avg} (α) = 6.08 E-6 in./ in. deg. F

Temperature Gradient (ΔT) = 300 deg. F (148.89 deg. C)

$$\text{Thermal Stress, } \sigma_{th} = \frac{E \alpha \Delta T}{2}$$

$$\sigma_1 = \frac{P_d R_i}{t} - \frac{E \alpha \Delta T}{2} = -14422 \text{ psi } (-99.44 \text{ MPa})$$

$$\sigma_2 = \frac{P_d R_i}{2t} - \frac{E \alpha \Delta T}{2} = -20230 \text{ psi } (-139.48 \text{ MPa})$$

von-Mises Equivalent Stress, $\sigma_e = \sqrt{\sigma_1^2 + \sigma_2^2 - \sigma_1 \sigma_2} = 18041.34 \text{ psi (124.39 MPa)}$

which is less than 25700 psi, σ_{yh} @ 400 degree F.

Therefore, the local hot spot does not yield and would remain elastic. No bulging will occur.

7.5 Discussions

Level 2 fitness-for-service assessment methods are developed to estimate the remaining strength factor of pressure vessels and piping with locally thinned areas, and hot spots. The procedure is based on variational principles that make use of the “integral mean of yield criterion”.

The Level 2 integrity assessment procedures are applied to rectangular LTA and hotspots, and sample calculations for evaluating the *RSF* is presented. The method is applied to LTA of a range of sizes and corroded thicknesses, and the results are compared with inelastic finite element analysis results. The *RSF2* that is based on m_α - multiplier is found to be conservative, and comparable with the inelastic FEA. Therefore, the use of *RSF2* is recommended for “fitness-for-service” evaluations.

In this thesis, the estimated remaining strength factors namely *RSF1*, *RSF2* and *RSF3* are based on the assumption of a single statically admissible stress distribution. Whereas an

estimation of a RSF based on m_{β} - multiplier may not be possible in this fitness-for-service assessment's present form as the evaluation of m_{β} - multiplier involves several iterations to be performed.

The proposed assessment method is a simple step-by-step procedure that should be attractive to plant engineers and designers, and is straightforward to program using a spreadsheet. The integrity assessment method, which is applied to a cylindrical shell, should provide the impetus for its applicability to other pressure vessel and piping configurations.

CHAPTER 8: CONCLUSIONS AND FUTURE RESEARCH

8.1 Conclusions

By performing limit analysis, the inherent redundancy found in structures like pressurized components, are made use of and therefore, an economic and safe design can be achieved. Plastic design method such as elastic plastic FEA has recently found its existence by the virtue of advanced computer technology. However, they may be perceived as laborious and exhaustive from the designer's viewpoint in estimating only the load-carrying capacity of a structure.

EMAP, a technique predominantly adopted in this thesis, is simple, efficient and based on a series of linear elastic analyses. Using lower and upper bound theorems, in conjunction with EMAP, lower and upper bound multipliers are estimated, and for well-behaved structures, they tend to converge towards the exact multiplier. The procedures based on elastic modulus adjustments used together with linear elastic FEA represent "independent verification" methods of inelastic FEA results.

m_β - multiplier method, a lower bound limit load determination method, developed in this thesis is based on variational principles in plasticity that makes use of the "integral mean of yield" criterion. The entire statically admissible stress distribution is accounted for into Mura's lower bound formulation rather than simply the maximum stress in a

structure, thereby resulting in non-oscillatory bounds for structures with slender and shape-sensitive structures and components with notches and cracks.

Evaluation of lower bound limit load multipliers such as m' , m_L or m_α is based on a maximum elastic stress in a structure. Statically admissible stress distributions obtained from several iterations in EMAP result in maximum stress that moves around at several locations in the structure thereby leading to oscillatory bounds. After several iterations using EMAP, stress distribution in a structure leads to converged type therefore consideration of an entire stress distribution should reduce the tendency of oscillation and lead to quicker convergence to exact limit load.

When components subjected to global plastic collapse are analyzed, the m_β - multiplier converges rapidly to exact limit multiplier and provides better lower bounds than the classical lower bound multiplier. For problems involving local plastic collapse, the parameter G is introduced in the m_β - method formulation. The parameter G , in conjunction with the concept of reference volume, enables the identification of the “kinematically active” regions in a component or structure. Furthermore, parameter G serves as a magnitude in designating the deviation of any statically admissible stress distribution from a limit state. In general, for any given iteration, the (m_β, m_u) pair provides a minimum spread in terms of bounds on the limit load multipliers.

The applicability of the m_β -method to a general yield criterion is established, thereby finding its use in the determination of limit loads for anisotropic components. Specifically, the advantage of the method is utilized in efficiently designing heat exchanger tubesheet, which is represented by equivalent solid model with anisotropic properties and its plastic behavior is appropriately characterized by the fourth-order yield criterion. While the implementation of fourth-order criterion in commercially available inelastic FE codes is difficult, the EMAP procedures provide an effortless way to perform tubesheet collapse analysis with fourth-order criterion.

Besides employing the integral mean of yield criterion to determine the safety factor for as-built equipments, structural and mechanical integrity of operating equipments were also demonstrated. Level 2 fitness-for-service assessment methods suitable for plant engineers were developed to estimate the remaining strength factor of a thin cylinder with locally thinned areas, and hot spots.

Through numerical examples, the efficiency of the m_β -multiplier method to determine lower bound limit loads and its good comparison with inelastic finite element results has been established. Although, the investigation is carried out with a variety of pressurized component configurations with internal pressure loading, the method can be applied to any general configuration and the applicability of the m_β -method to structures subjected to combined loading (for example pressure + moment) is also possible. The analysis can be performed in the same way as performed for heat exchanger tubesheet application that

is subjected to primary and secondary shell side pressures. While the method is proposed as an alternate method to performing inelastic analysis, it may also find its immense importance in the preliminary stages of design and life assessment activities.

8.2 Future Research

The primary advantage of elastic modulus modification technique is its simplicity and efficiency. The concept inherent in EMAP is that the plastic redistribution is simulated by modifying the elastic modulus at various locations in a structure using a series of linear elastic analysis. Each linear elastic analysis makes use of a statically admissible stress distribution and these intermediate statically admissible stress distributions lead to impending collapse state. Whereas an inelastic analysis is performed by applying the total load in increments. For each incremental load, an equilibrating stress distribution is obtained through several iterations. In effect, the total number of iterations performed and its corresponding computing time in an inelastic analysis would be quite more than those performed in EMAP.

The savings in computing time may not be significant for two-dimensional problems, however, for three-dimensional problems, time-saving aspect of EMAP would prevail over the use of inelastic analysis. Therefore, future research should be devoted to applications involving complex three-dimensional pressurized component configurations and configurations involving cracks.

A procedure to identify the reference volume is presented in this thesis. The identified reference volume may not exactly match with the reference volume obtained from the inelastic analysis. It may be worthwhile to direct some research in obtaining a stress distribution that matches with that of inelastic analysis by varying the parameters, for instance, degree of modulus modification. Furthermore, as the parameter G is used to assess the nature of converged stress distribution obtained from EMAP, for comparison purposes, it can also be used to assess the final stress distribution obtained from inelastic analysis.

The m_β - multiplier method in its present form cannot be utilized to analyze for applications involving layered structures or structures made of materials that exhibit isotropic and anisotropic properties. Therefore, extension of the present m_β - method, to be suitable for analyzing such problems may be a valuable research area to pursue.

PUBLICATIONS AND PRESENTATIONS DURING THE PH. D

PROGRAM

1. H. Indermohan and R. Seshadri, "Fitness-for-Service Methodology Based on Variational Principles in Plasticity", *Journal of Pressure Vessel Technology*, Vol. 127, No. 1, Feb. 2005, pp.92-97.
2. H. Indermohan, W.D. Reinhardt and R. Seshadri, "Limit Load of Anisotropic Components Using the m-beta Multiplier Method", *Journal of Pressure Vessel Technology*, Vol. 126, No. 4, Nov 2004, pp. 455-460.
3. R. Seshadri and H. Indermohan, "Lower Bound Limit Load Determination: The m-beta Multiplier Method", *Journal of Pressure Vessel Technology*, Vol. 126, No.2, May 2004, pp.237-240.
4. H. Indermohan and R. Seshadri, "The M-Beta Multiplier Method for Limit Load Determination of Components with Local Plastic Collapse", *Computer Technology: Efficient Computational Methods for Elastic-Plastic and Limit Load Analysis*, Proceedings of the ASME PVP Conference, Denver, Colorado, 2005.
5. H. Indermohan and R. Seshadri, "Fitness-for-Service Methodology Based on Variational Principles in Plasticity", Student Paper Competition, Proceeding of the ASME PVP Conference, San Diego, California, PVP-Vol. 473, 2004.
6. H. Indermohan, W.D. Reinhardt and R. Seshadri, "Limit Load of Anisotropic Components Using the m-beta Multiplier Method", Proceedings of the ASME PVP Conference, San Diego, California, PVP Vol. 482, 2004.
7. R. Seshadri and H. Indermohan, "Lower Bound Limit Load Determination: The m-beta Multiplier Method", *Codes and Standards: Proceedings of the ASME PVP Conference*, Cleveland, Ohio, 2003.

REFERENCES

1. ABAQUS User Manuals, Vol. 1-4, 2002, Hibbitt, Karlson & Sorensen Inc.
2. ANSYS, 2000, Educational Version 6.0, SAS IP, Inc.
3. API 579, 2000, API, Fitness-for-Service, American Petroleum Institute, Washington D. C., USA.
4. ASME Boiler and Pressure Vessel Code", 2001, American Society of Mechanical Engineers, New York, USA.
5. ASME, 1972 "Criteria of the ASME Boiler and Pressure Vessel Code for Design by Analysis in Sections III and VIII, Division 2," The American Society of Mechanical Engineers, New York, 1969. Reprinted in Pressure Vessel Design and Analysis - A Decade of Progress, The American Society of Mechanical Engineers, New York, 1972.
6. Barsoum, R. S., 1976, "On the Use of Isoparametric Finite Elements in Linear Fracture Mechanics," International Journal of Numerical Methods in Engineering, Vol. 10, pp. 25-37.
7. Barsoum, R. S., 1977, "Triangular Quarter-point elements as Elastic and Perfectly-plastic Crack-tip Elements," International Journal of Numerical Methods in Engineering, Vol. 11, pp 85-98.
8. Boyle, J. T., Hamilton, R., Shi, J. and Mackenzie, D., 1997, "A Simple Method of Calculating Lower Bound Limit Loads for Axisymmetric Thin Shells", Journal of Pressure Vessel Technology, Vol. 119, pp. 236-242.
9. Calladine, C. R., 1969, Engineering Plasticity, Pergamon Press, Oxford.
10. Chakrabarty, J., Theory of Plasticity, McGraw-Hill Book Company, New York, USA.
11. Chen, W. F. and Han, D. J., 1988, Plasticity for Structural Engineers, Springer-Verlag, New York, USA.
12. Cloud, R. L., 1972, "Design Criteria: Introduction", Pressure Vessel Design and Analysis - A Decade of Progress, The American Society of Mechanical Engineers, New York.

13. Dhalla, A. K., 1984, "Verification of an Elastic Procedure to Verify Follow-up", Design of Elevated Temperature Piping, Ed. Mallet, R. H., and Mello, R. M., ASME, San Francisco, pp. 367-387.
14. Fernando, C. P. D. and Seshadri, R., 1992, "Limit Loads of Framed Structures and Arches using the GLOSS R-node Method", Proceedings of the 11th Symposium on Engineering Applications of Mechanics, pp. 236-242.
15. Gill, S. S., 1970, The Stress Analysis of Pressure Vessels and Pressure Vessel Components, Pergamon Press.
16. Hechmer, J. L. and Hollinger, G. L., 1986, "Three dimensional stress criteria - a weak link in vessel design and analysis," ASME Special Publication, PVP 109, "A Symposium on ASME Codes and Recent Advances in Pressure Vessel and Valve Technology" Editor J T Fong.
17. Hechmer, J. L. and Hollinger, G. L., 1991, "Three dimensional stress criteria," ASME PVP-Vol. 210-2 Codes and Standards and Applications for Design and Analysis of Pressure Vessel and Piping, ASME PVP-Vol. 161.
18. Hill, R., 1971, The Mathematical Theory of Plasticity, Oxford University Press, New York.
19. Horne, M. R., 1979, Plastic Theory of Structures, 2nd Edition, Pergamon Press.
20. Johnson, W. and Mellor, P. B., 1983, Engineering Plasticity, Ellis Horwood Limited.
21. Jones, G. L. and Dhalla, A. K., 1981, "Classification of Clamp Induced Stresses in Thin-walled pipe", Proceedings of ASME-PVP, New York, Vol. 81.
22. Jones, G. L. and Dhalla, A. K., 1986, "ASME Code Classification of Pipe Stresses: A Simplified Elastic Procedure", International Journal of Pressure Vessel and Piping, Vol. 26, pp. 145-166.
23. Jones, R. M., 1975, Mechanics of Composite Materials, Scripta Book Company, Washington D. C., USA.
24. Jones, D. P. and Gordon, J. L., 2001, "Collapse Surfaces for Perforated Plates with Triangular Penetration Patterns for Ligament Efficiencies Between 0.05 – 0.5", Presented at ASME PVP California, Atlanta.

25. Kizhatil, R. K. and Seshadri, R., 1991, "Inelastic Strain Concentration factors and Low Cycle Fatigue of Pressure Components using GLOSS Analysis", ASME PVP, San Diego, Vol. 210-2, pp. 149-154.
26. Kroenke, W. C., 1973, "Classification of finite element stresses according to ASME Section III stress categories," Proceedings of 94th ASME Winter Annual Meeting.
27. Mackenzie, D., and Boyle, J.T., 1993a, "A Method of Estimating Limit Loads by Iterative Elastic Analysis. I-Simple Examples," International Journal of Pressure Vessels and Piping, Vol. 53, pp. 77-95.
28. Mackenzie, D., Nadarajah, C., Shi, J. and Boyle, J. T., 1993b, "Simple Bounds on Limit Loads by Elastic Finite Element Analysis", Journal of Pressure Vessel Technology, Vol. 115, pp. 27-31.
29. Mackenzie, D. and Boyle, J. T., 1993c, "A Simple Method of Estimating Shakedown Loads for Complex Structures," Proceedings of ASME Pressure Vessels and Piping Conference, PVP-Vol. 265, pp. 89-94.
30. Mackenzie, D., Shi, J. and Boyle, J. T., 1994, "Finite Element Modeling for Limit Analysis by the Elastic Compensation Method", Computers & Structures, Vol. 51, No. 4, pp. 403-410.
31. Mackenzie, D., Boyle, J. T., Hamilton, R. and Shi. J., 1995, "Secondary stress and Shakedown in Axisymmetric Nozzles," Proceedings of ASME Pressure Vessels and Piping Conference, PVP-Vol. 313-1, pp. 409-413.
32. Mackenzie, D., Boyle, J. T. and Hamilton, R., 2000, "The Elastic Compensation Method for Limit and Shakedown Analysis: A Review", Journal of Strain Analysis, Vol. 35, No. 3, 171-188.
33. Mangalaramanan, S. P., 1997a, "Conceptual Models for Understanding the Role of the R-Nodes in Plastic Collapse," Journal of Pressure Vessel Technology, Vol. 119, pp. 374-378
34. Mangalaramanan, S. P., 1997b, "Robust Limit Loads using Elastic Modulus Adjustment Techniques," Ph D Thesis, Faculty of Engineering and Applied Science, Memorial University of Newfoundland.
35. Mangalaramanan, S. P. and Seshadri, R., 1997, "Minimum Weight Design of Pressure Components Using R-nodes", Journal of Pressure Vessel Technology, Vol. 119, pp. 224-231.

36. Marriott, D. L., 1988, "Evaluation of Deformation or Load Control of Stresses under Inelastic Conditions using Elastic Finite Element Stress Analysis", Proceedings of the ASME-PVP Conference, Pittsburgh, Vol. 136.
37. Mendelson, A., 1968, Plasticity: Theory and Application, The Macmillan Company, New York, 1968.
38. Miller, A. G., 1988, "Review of Limit Loads of Structures Containing Defects," International Journal of Pressure Vessels and Piping, Vol. 32, pp. 197-327.
39. Milne, I., Ainsworth, R. A., Dowling, A. R. and Stewart, A. T., 1988, Assessment of the integrity of structure containing defects, International Journal of Pressure Vessels and Piping, Vol. 32, pp. 3-14.
40. Mohamed, A. I., Megahed, M. M., Bayoumi, L. S. and Younan, M. Y. A., 1999, "Applications of Iterative Elastic Techniques for Elastic-Plastic Analysis of Pressure Vessels", Journal of Pressure Vessel Technology, Vol. 121, pp. 24-29.
41. Mura, T and Koya, T., 1992, Variational Methods in Mechanics, Oxford University Press, New York, USA
42. Mura, T. and Lee, S. L., 1963, "Application of Variational Principles to Limit Analysis", Quarterly of Applied Mathematics, Vol. 21, No. 3, pp. 243-248.
43. Mura, T., Rimawi, W. H., and Lee, S. L., 1965, "Extended Theorems of Limit Analysis," Quarterly Journal of Applied Mathematics, Vol. 23, No. 3, pp. 171-179.
44. Mura, T., Lee, S. L. and Rimawi, W. H., 1968, "A Variational Method for Limit Analysis of Anisotropic and Non-Homogeneous Solids", Developments in Theoretical and Applied Mechanics, New Orleans, LA, USA, pp. 541-549.
45. Nadarajah, C., Mackenzie, D. and Boyle, J. T., 1993, "A Method of Estimating Limit Loads by Iterative Elastic Analysis. II - Nozzle Sphere Interactions with Internal Pressure and Radial Load," International Journal of Pressure Vessels and Piping, Vol. 53, pp. 97-119.
46. Pan, L. and Seshadri, R., 2002, "Limit Load Estimation Using Plastic Flow Parameter in Repeated Elastic Finite Element Analyses," Journal of Pressure Vessel Technology, Vol. 124, pp. 433-439.
47. Pan, L. and Seshadri, R., 2003, "Limit Analysis for Anisotropic Solids using Variational Principle and Repeated Elastic Finite Element Analyses", ASME PVP Vol. 442, Vancouver, pp. 149-155.

48. Pan, L., 2003., "Limit Load Estimation for Structures under Mechanical Loads," Ph D Thesis, Faculty of Engineering and Applied Science, Memorial University of Newfoundland.
49. Pastor, T. P. and Hechmer, J., 1997, "ASME Task Group Report on Primary Stress", Journal of Pressure Vessel Technology, Vol. 119, pp. 61-67.
50. Plancq, D. and Berton, M. N., 1998, "Limit Analysis Based on Elastic Compensation Method of Branch Pipe Tee Connection under Internal Pressure and Out-of-plane Moment Loading", International Journal of Pressure Vessels and Piping, Vol. 75, pp. 819-825.
51. Ponter, A. R. S. and Carter, K. F., 1997, "Limit State Solutions, Based upon Linear Elastic Solutions with a Spatially Varying Elastic Modulus," Computer Methods in Applied Mechanics and Engineering, Vol. 140, pp. 237-258.
52. Ponter, A. R. S., Fuschi, P. and Engelhardt, M., 2000, "Limit Analysis for a General Class of Yield Conditions," European Journal of Mechanics-A/Solids, Vol. 19, pp. 401-421.
53. Popov, E. P., 1990, Engineering Mechanics of Solids, Prentice Hall, Englewood Cliffs, New Jersey.
54. Reinhardt, W. D., 1998, "Yield Criteria for the Elastic-Plastic Design of Tubesheets with Triangular Perforation Pattern", ASME PVP Vol. 370, pp. 113-119.
55. Reinhardt, W. D., 1999, "A Fourth-Order Equivalent Solid Model for Tubesheet Plasticity", ASME PVP Vol. 385, pp. 151-157.
56. Reinhardt, W. D. and Mangalaramanan, S. P., 1999, "Efficient Tubesheet Design Using Repeated Elastic Limit Analysis", Proceedings of ASME Pressure Vessels and Piping Conference, PVP-Vol. 385, pp. 141-149.
57. Reinhardt, W. D. and Mangalaramanan, S. P., 2000, "Plastic Limit Analysis of a Tubesheet Using an Elastic Modulus Modification Method", Proceedings of ASME Pressure Vessels and Piping Conference, PVP-Vol. 400, pp. 253-261.
58. Reinhardt, W. D. and Seshadri, R., 2003, "Limit Load Bounds for the malpha Multiplier," Journal of Pressure Vessel Technology, Vol. 125, pp. 1-8.

59. Rice, J. R. and Rosengren, G. F., 1968, "Plain Strain Deformation near a Crack Tip in a Power-law Hardening Material," *Journal of Mechanics and Physics of Solids*, Vol. 16, pp. 1-12.
60. Rimawi, W. H., Mura, T. and Lee, S. L., 1966, "Extended Theorems in Limit Analysis of Anisotropic Solids", *Developments in Theoretical and Applied Mechanics. Volume 3 - Proceedings of the Third Southeastern Conference on Theoretical and Applied Mechanics*, Columbia, SC, USA, pp. 57-71.
61. Save., M. A., and Massonet, C. E., 1972, *Plastic Analysis and Design of Plates, Shells and Disks*, Vol. II, North-Holland Publishing Company, Amsterdam.
62. Seshadri, R., 1990a, "Classification of Stress in Pressure Components using the 'GLOSS' Diagram", *Proceedings of the ASME PVP*, Nashville, Vol. 186, pp. 115-123.
63. Seshadri, R., 1990b, "The Effect of Multiaxiality and Follow-up on Creep Damage", *Journal of Pressure Vessel Technology*, Vol. 112, pp. 378-385.
64. Seshadri, R., 1991a, "The Generalized Local Stress Strain (GLOSS) Analysis - Theory and Applications," *25th Anniversary Volume, ASME Journal of Pressure Vessel Technology*, pp. 219-227.
65. Seshadri, R., 1991b, "Simplified Methods for determining Multiaxial Relaxation and Creep Damage", *ASME PVP*, San Diego, Vol. 210-2, pp. 173-180.
66. Seshadri, R., 1997, "In Search of Redistribution Nodes," *International Journal of Pressure Vessels and Piping*, Vol. 73, pp. 69-76.
67. Seshadri, R., 2000, "Limit Loads Using Extended Variational Concepts in Plasticity", *Journal of Pressure Vessel Technology*, Vol. 122, pp. 379-385.
68. Seshadri, R., 2004, "Integrity Assessment of Pressure Components With Local Hot Spots", To Be Presented At The ASME PVP Conference, San Diego, USA.
69. Seshadri, R., and Fernando, C. P. D., 1992, "Limit Loads of Mechanical Components and Structures using the GLOSS R-Node Method," *Transactions of the ASME: Journal of Pressure Vessel Technology*, Vol. 114, pp. 201-208.
70. Seshadri, R. and Kizhatil, R. K., 1990, "Inelastic Analyses of Pressure Components using the 'GLOSS' Diagram", *Proceedings of the ASME PVP*, Nashville, Vol. 186, pp. 105-113, 1990.

71. Seshadri, R. and Kizhatil, R. K., 1995, "Robust Approximate Methods for Estimating Inelastic Fracture Parameters", *Journal of Pressure Vessel Technology*, Vol. 117, pp. 115-123.
72. Seshadri, R., and Mangalaramanan, S. P., 1997, "Lower Bound Limit Loads using Variational Concepts: The m-alpha method," *International Journal of Pressure Vessels and Piping*, Vol. 71, pp. 93-106.
73. Seshadri, R., and Marriott, D. L., 1992, "On Relating the Reference Stress, Limit Load and the ASME Stress Classification Concepts," *ASME PVP-Vol. 230, Stress Classification, Robust Methods, and Elevated Temperature Design*, pp. 135-149.
74. Seshadri, R. and Wu, S., 2001, "Robust Estimation of Inelastic Fracture Release Rate (J): A Design Approach," *Journal of Pressure Vessel Technology*, Vol. 123, pp. 214-219.
75. Shi, J., Mackenzie, D. and Boyle, J. T., 1993, "A Method of Estimating Limit Loads by Iterative Elastic Analysis. III - Torispherical Heads under Internal Pressure", *International Journal of Pressure Vessels and Piping*, Vol. 53, pp. 121-142.
76. Shih, C. F. and Lee, D., 1978, "Further Developments in Anisotropic Plasticity", *Journal of Engineering Materials and Technology*, Vol. 100, pp. 294-302.
77. Sullivan, R. C., Kizhatil, R. and McClellan, G. H., 1997, "Correction of Equivalent Elastic-plastic Anisotropic Properties of Thick Tubesheets to Preclude Overstiff Response to Monotonic Loading," *PVP-Vol. 354, Orlando/Florida*, pp. 121-126.
78. Vaidyanathan, S., Kizhatil, R. K. and Seshadri, R., 1989, "GLOSS Plot Validation and Application to Elevated Temperature Component Design", *Proceedings of the ASME PVP, Honolulu*, Vol. 161, pp. 25-31.
79. Valliappan, S., Boonluloohr, P. and Lee, I. K., 1976, "Non-linear Analysis for Anisotropic Materials," *International Journal for Numerical Methods in Engineering*, Vol. 10, pp. 597-606.
80. Webster, G. and Ainsworth, R. A., 1994, *High Temperature Component Life Assessment*, Chapman and Hall, London, UK.

APPENDIX: ANSYS APDL MACROS

Macro for Evaluating Limit Loads of Isotropic Components

refnew.txt

```
! Enter number of iterations in EMAP
iter=20

! initial iteration: elastic solution
niter = 0
! Enter the ANSYS input file name
/inp,file_name.txt
finish

/prep7
/nopr
nset,all
eset,all

! Obtain the minimum and maximum number elements and nodes
*get,emin,elem,,num,min !get min element number as emin
*get,emax,elem,,num,max !get max element number as emax
*get,nmin,node,,num,min !get min node number as nmin
*get,nmax,node,,num,max !get max node number as nmax

! Get material properties for the initial iteration
*get,ex,ex,1
*get,nuxy,nuxy,1

! Arrays for iteration results
*dim,itemp,,iter ! for no.of iterations
*dim,shake,,iter ! for iterative stress
*dim,loop,,iter ! for maximum centroidal stress
*dim,lmult,,iter ! for cl. ub results
*dim,lb,,iter ! for cl. lb results
*dim,armon,,iter ! for mo new results
*dim,armop,,iter ! for ponter's lamda results
*dim,armoo,,iter ! for mo old results
*dim,armpn,,iter ! for mp new results
*dim,armpo,,iter ! for mp old results
*dim,armao,,iter ! for ma old results
*dim,arman,,iter ! for ma new results
*dim,armpp,,iter ! for mpn (mp) new results
*dim,revol,,iter ! reference volume for m" results
*dim,ratio_old,,iter ! ratio for m0-old
*dim,ratio_new,,iter ! ratio for m0-new
*dim,ts1,,iter !roots of m0
*dim,ts2,,iter !roots of m0
*dim,d3,,iter !roots of m0
```

```

! Array for Young's Moduli in each element
*dim,arex,,emax,iter+1

! Arrays for Reference Volume m0's
*dim,usor,,emax      !unsorted product
*dim,sor,,emax       !sorted product
*dim,svol,,emax      !corresponding sorted volumes
*dim,rmo,,emax       !reference mo's
*dim,rmon,,emax      !reference new mo's
*dim,rvol,,emax      !reference volume ratios
*dim,volnum,,emax    !order of volumes
*dim,cumvol,,emax    !cumulative volumes
*dim,cumstrs,,emax   !cumulative stresses
*dim,ref_ratio,,emax !reference ratio for m0-old
*dim,norm_strs,,emax !normalized (with yield) stress
*dim,m0_num,,emax    !numerator of m02 for reference volume
*dim,m0_din,,emax    !dinominator of m02 for reference volume

! Reference Parameters for m"
*dim,ref_s1,,emax    ! Term s1bar
*dim,ref_s2,,emax    ! Term s2bar
*dim,term_r,,emax    ! Term R(zeta)
*dim,term_g,,emax    ! Term G(zeta)
*dim,ref_mpp,,emax   ! Reference m"
*dim,cum_s1,,emax    ! Cumulative S1
*dim,cum_s2,,emax    ! Cumulative S2

! Elemental Stress Arrays
*dim,cstrs,,emax     !eqv.stress at elem. centroids
*dim,astrs,,emax     !eqv.stress at elem. centroids for malpha
finish

/post1
etable,censtr,s,eqv   ! centroidal stress
*vget,cstrs(1),elem,,etab,censtr,,0
etable,evoltab,volu   ! table for element volume
*vget,evol(1),elem,,etab,evoltab,,0

*do,count,1,iter,1
    itemp(count) = count
    shake(count) = 100000
    lmult(count) = 100000
*enddo

! Initialize array "arex" with the initial iteration's Young's Moduli
*do,count,emin,emax,1
    arex(count,1) = ex
*enddo

set,last
! Max nodal eqv stress

```

```

nsort,s,eqv,0,1,
*get,elas,sort,,max
nusort

finish
niter=0          !SETTING ITERATION NUMBER TO BE ZERO

/post1
set,last
! Max nodal eqv stress again for
! getting "smax" variable
nsort,s,eqv,0,1,
*get,smax,sort,,max
nusort

! Evaluate limit load multipliers at the initial iteration
/inp,mult_init.txt
finish

! Perform elastic modulus modification for each iteration and solve
*do,niter,1,iter,1
    ! read stresses and calculate new elastic modulus at each element
    ! write new elastic modulus values to arex array
    /inp,mcen.txt
    /solu
    /nopr
    solve
    finish

    /post1
    /nopr
    set,last
    ! Max nodal equivalent stress
    nsort,s,eqv,0,1,
    *get,smax,sort,,max
    nusort

    ! Limit load multiplier evaluations
    /inp,multipliers.txt

    ! Enter the iteration number in which the reference volume is to be calculated
    *if,niter,eq,20,then
        /inp,refr_betastrs_m0.txt
    *endif
    finish
*enddo

! write results out to file
/inp,results.txt
save
/exit,all

```

mult_init.txt

```
tevol=0
m=0
prod1=0
prod2=0
prod3=0
term11=0      !product (term2) for m"
tprod=0 !total product for new form m'
den_in1=0     !din.term of old mo
den_in2=0     !din.term of new mo
den_in3=0     !din.term of p's mo
den_fn1=0     !final din.term of old mo
den_fn2=0     !final din.term of new mo
num_in=0      !num.term of new mo
num_in2=0
num_fn=0      !num.term of new mo

/post1
set,last
etable,nstrs,s,eqv ! centroidal stress
*vget,astrs(1),elem,,etab,nstrs,,,0

!Finding maximum elemental stress
*do,nvol,emin,emax,1
  *if,astrs(nvol),gt,m,then
    m=astrs(nvol)
  *endif
*enddo

loop1=m
shake1=smax
lb1=sm/loop1
!-----
!Estimate old m0, m' and m-alpha multipliers
!Dinominator for old m0
*do,nvol,emin,emx,1
  den_in1=den_in1+((astrs(nvol)**2)*evol(nvol))
  tevol=tevol+evol(nvol)
*enddo
  den_fn1=sqrt(den_in1)

!Estimate old m0
armoo1=sm*sqrt(tevol)/den_fn1

!Estimate old m'
mnum1=2*armoo1*sm*sm
mdin1=(sm*sm)+((armoo1**2)*m*m)
armpo1=mnum1/mdin1

!Estimate old m-alpha
instr=m/sm
a1=(armoo1**4)*(instr**4)+4*(armoo1**2)*(instr**2)-1
```

```

        b1=(-8*(armool**3)*(instr**2))
        c1=4*(armool**3)*instr
        d1=b1**2-4*a1*c1

*if,d1,gt,0,then
    armao1=((-1*b1)+sqrt(b1**2-4*a1*c1))/(2*a1)
*endif
!-----
!Estimate new m0, Ponter's m0, m' and m-alpha multipliers

!Estimate dinominator for new m0
*do,nvol,emin,emax,1
    den_in2=den_in2+(astrs(nvol)**2)*evol(nvol)/ex
    den_in3=den_in3+(astrs(nvol)**2)*evol(nvol)/ex
*enddo
    den_fn2=sqrt(den_in2)

!Estimate numerator for new m0
*do,nvol,emin,emax,1
    num_in=num_in+evol(nvol)/ex
    num_in2=num_in2+(astrs(nvol)*evol(nvol)/ex)
*enddo
    num_fn=sqrt(num_in)
!-----
!Estimate new m0, Ponter's lamda multiplier
armon1=sm*num_fn/den_fn2
armop1=sm*num_in2/den_in3

!Estimate new m' multiplier
mnum2=2*armon1*sm*sm
mdin2=(sm*sm)+((armon1**2)*m*m)
armpn1=mnum2/mdin2

!Estimate new m-alpha multiplier
instr=m/sm
a2=(armon1**4)*(instr**4)+4*(armon1**2)*(instr**2)-1
b2=(-8*(armon1**3)*(instr**2))
c2=4*(armon1**3)*instr
d2=b2**2-4*a2*c2

*if,d2,gt,0,then
    arman1=((-1*b2)+sqrt(b2**2-4*a2*c2))/(2*a2)
*endif
!-----
!-----
!Estimate new m' multiplier

!Estimate dinominator for new m'
*do,nvol,emin,emax,1
    prod1=(armon1*astrs(nvol))**2
    prod2=sm*sm
    prod3=prod3+((prod1-prod2)**2)*evol(nvol)

```

```

*enddo
      tprod=sqrt(prod3)/sqrt(tevol)

mnum3=2*armon1*sm*sm
mdin3=2*sm*sm+tprod
armpp1=mnum3/mdin3

mnum4=2*armon1
mdin4=1+(armon1/armoo1)**2
armsp1=mnum4/mdin4
term11=tprod/(2*sm*sm)
!-----

```

mcen.txt

```

/post1
set,last

! Create an element table for centroidal stresses
etable,censtrs,s,eqv      ! centroidal stress
*vget,cstrs(1),elem,,etab,censtrs,,0

! Calculate elastic modulus modification ratio
! Enter elastic modulus adjustment index
index = 1.0
*do,count,emin,emax,1
      ecsf = (sm/cstrs(count))**index      !evaluate reduction factor
      ecer = arex(count,niter)*ecsf      !calc. new ex
      arex(count,niter+1) = ecer !write ex in array
*enddo
finish

/prep7
/nopr
! modify each element's elastic modulus
*do,count,emin,emax,1
      mp,ex,count,arex(count,niter+1)
      mp,nuxy,count,nuxy
      mat,count
      emod,count
*enddo
finish

```

multipliers.txt

```

! Macro for evaluating lower and upper bound limit load multipliers

tevol=0
prod1=0 !product (term2) for m'
prod2=0 !product (term3) for m'
prod3=0 !product (strain energy) for new form m'
m=0
tprod=0 !total product for new form m'

```

```

den_in1=0      !din.term of old m0
den_in2=0      !din.term of new m0
den_in3=0      !din.term of ponter's m0
den_fn1=0      !final din.term of old m0
den_fn2=0      !final din.term of new m0
den_fn3=0      !final din.term of ponter's lamda
num_in=0       !num.term of new m0
num_fn=0       !num.term of new m0
num_in2=0      !num.term of ponter's lamda

/post1
set,last

etable,nstrs,s,eqv ! centroidal stress
*vget,astrs(1),elem,,etab,nstrs,,0
etable,nstrn,epel,eqv ! centroidal strain
*vget,estrn(1),elem,,etab,nstrn,,0

!Finding maximum elemental stress
*do,nvol,emin,emax,1
  *if,astrs(nvol),gt,m,then
    m=astrs(nvol)
  *endif
*enddo
loop(niter)=m

shake(niter)=smax
lb(niter)=sm/loop(niter)
!-----
!-----
! Estimate old m0, m' and m-alpha multipliers
! Denominator for old m0
*do,nvol,emin,emax,1
  den_in1=den_in1+((astrs(nvol)**2)*evol(nvol))
  tevol=tevol+evol(nvol)
*enddo
  den_fn1=sqrt(den_in1)

! Estimate old m0
armoo(niter)=sm*sqrt(tevol)/den_fn1
ratio_old(niter)=tevol/den_in1

! Estimate old m'
mnum1=2*armoo(niter)*sm*sm
mdin1=(sm*sm)+((armoo(niter)**2)*m*m)
armpo(niter)=mnum1/mdin1

! Estimate old m-alpha
instr=m/sm
a1=(armoo(niter)**4)*(instr**4)+4*(armoo(niter)**2)*(instr**2)-1
b1=(-8*(armoo(niter)**3)*(instr**2))
c1=4*(armoo(niter)**3)*instr
d1=b1**2-4*a1*c1

```

```

*if,d1,gt,0,then
    armao(niter)=[(-1*b1)+sqrt(b1**2-4*a1*c1)]/(2*a1)
*endif
!-----
!-----
! Estimate new m0, m' and m-alpha multipliers

! First estimate dinominator for new m0
*do,nvol,emin,emax,1
    den_in2=den_in2+(astrs(nvol)**2)*evol(nvol)/arex(nvol,niter+1)
*enddo
    den_fn2=sqrt(den_in2)

! Estimate numerator for new m0
*do,nvol,emin,emax,1
    num_in=num_in+evol(nvol)/arex(nvol,niter+1)
*enddo
    num_fn=sqrt(num_in)

! Estimate new m0 multiplier
armon(niter)=sm*num_fn/den_fn2
ratio_new(niter) = num_in/den_in2

! Estimate new m' multiplier
mnum2=2*armon(niter)*sm*sm
mdin2=(sm*sm)+((armon(niter)**2)*m*m)
armpn(niter)=mnum2/mdin2

! Estimate new m-alpha multiplier
instr=m/sm
a2=(armon(niter)**4)*(instr**4)+4*(armon(niter)**2)*(instr**2)-1
b2=(-8*(armon(niter)**3)*(instr**2))
c2=4*(armon(niter)**3)*instr
d2=b2**2-4*a2*c2

*if,d2,gt,0,then
    arman(niter)=[(-1*b2)+sqrt(b2**2-4*a2*c2)]/(2*a2)
*endif
!-----
!-----
! Estimate Ponter's lamda
! Estimate dinominator for lamda
*do,nvol,emin,emax,1
    den_in3=den_in3+(astrs(nvol)**2)*evol(nvol)/arex(nvol,niter+1)
*enddo

! Estimate numerator for lamda
*do,nvol,emin,emax,1
    num_in2=num_in2+(astrs(nvol)*evol(nvol)/arex(nvol,niter+1))
*enddo

! Estimate Ponter's upper bound multiplier

```

```

armop(niter)=sm*num_in2/den_in3
!-----
! Estimate m" multiplier
! Estimate dinominator for new m"
*do,nvol,emin,emax,1
    prod1=(armoo(niter)*astrs(nvol))**2
    prod2=sm*sm
    prod3=prod3+((prod1-prod2)**2)*evol(nvol)
*enddo
    tprod=sqrt(prod3)/sqrt(tevol)

mnum3=2*armoo(niter)*sm*sm
mdin3=2*sm*sm+tprod
armpp(niter)=mnum3/mdin3

term1(niter)=tprod/(2*sm*sm)
term2(niter)=armoo(niter)/(1+term1(niter))
!-----

```

ref_betastrs_m0.txt

```

/post1
set,last

tevol=0
cvol=0
tstrs=0

etable,censtrs,s,eqv      ! centroidal stress
*vget,cstrs(1),elem,,etab,censtrs,,0

!calculate the product before sorting in ascending order
*do,count,emin,emax,1
    usor(count)=cstrs(count)
*enddo

!calculate total volume of the model
total=0
*do,count,emin,emax,1
    tevol=tevol+evol(count)
*enddo

!copy the unsorted product from usor array to sor array
!also copy the usorted volume from evol array to svol array

*do,count,emin,emax,1
    sor(count)=usor(count)
    svol(count)=evol(count)
    volnum(count)=count
*enddo

!perform sorting of sor and svol array in ascending order
*do,count,emin,emax-1,1

```

```

*do,ncou,count+1,emax
  *if,sor(count),lt,sor(ncou),then
    dum1=sor(count)
    dum2=svol(count)
    dum3=volnum(count)
    sor(count)=sor(ncou)
    svol(count)=svol(ncou)
    volnum(count)=volnum(ncou)
    sor(ncou)=dum1
    svol(ncou)=dum2
    volnum(ncou)=dum3
  *endif
*enddo

!Calculate the ratio of appropriate volume to total volume
!corresponding to the sorted product
!to identify at which volume ratio the reference mo volume

*do,count,emin,emax,1
  cvol=cvol+svol(count)
  tstrs=tstrs+(sor(count)**2)*svol(count)
  cumvol(count)=cvol
  cumstrs(count)=tstrs
  rvol(count)=cvol/tevol
*enddo

*vwrite,niter
("At iteration=",f3.0,/)
*vwrite,
("Order of Volumes",/)
*vwrite,volnum(1)
(f8.2)

*vwrite,niter
("At iteration=",f3.0,/)
*vwrite,
("Volume ratios",/)
*vwrite,rvol(1)
(f10.8)

!calculate the reference mo's
*do,count,emin,emax,1
  rmo(count)=sm*(sqrt(cumvol(count)))/sqrt(cumstrs(count))
  ref_ratio(count)=cumvol(count)/cumstrs(count)
*enddo

*vwrite,niter
("At iteration=",f3.0,/)
*vwrite,
("Reference mo's old",/)
*vwrite,rmo(1)
(f12.8)

```

```

*vwrite,niter
("At iteration=",f3.0,/)
*vwrite,
("Reference mo's old ratio",/)
*vwrite,ref_ratio(1)
(f35.30)

!Reference parameters s1, s2 and m"
*do,count,emin,emax,1
  elem_num=volnum(count)
  temp1=temp1+((cstrs(elem_num)**4)*evol(elem_num))
  temp2=temp2+(-2*(cstrs(elem_num)**2)*evol(elem_num))
  cum_s1(count)=temp1
  cum_s2(count)=temp2
*enddo

*do,count,emin,emax,1
  ref_s1(count)=cum_s1(count)/(sm**4*cumvol(count))
  ref_s2(count)=cum_s2(count)/(sm**2*cumvol(count))
  term_r(count)=(ref_s2(count)**2)-(4*ref_s1(count))
  term_g(count)=(((rmo(count)**4)*ref_s1(count))+((rmo(count)**2)*ref_s2(count))+1)
*enddo

*vwrite,niter
("At iteration=",f3.0,/)
*vwrite,
("Reference s1bar",/)
*vwrite,ref_s1(1)
(f25.22)

*vwrite,niter
("At iteration=",f3.0,/)
*vwrite,
("Reference s2bar",/)
*vwrite,ref_s2(1)
(f25.22)

*vwrite,niter
("At iteration=",f3.0,/)
*vwrite,
("Reference Term R(zeta)",/)
*vwrite,term_r(1)
(f25.22)

*vwrite,niter
("At iteration=",f3.0,/)
*vwrite,
("Reference Term G(zeta)",/)
*vwrite,term_g(1)
(f35.30)

```

results.txt

```
*c fopen, file_name, res

*vwrite,
("M-BETA METHOD RESULTS",/)

*vwrite,
("Values before iteration",/)

*vwrite, elas
("Max. nodal eqv. elastic stress =", f16.4, /)

*vwrite, lb1
("Classical Lowerbound =", f16.4, /)

*vwrite,
("Old Mo      m'      ma1", /)
*vwrite, armool, armpo1, armao1
(f12.4, f12.4, f12.4)

*vwrite,
("New Mo      m'      ma1      Ponter's mo", /)
*vwrite, armon1, armpn1, arman1, armop1
(f12.4, f12.4, f12.4, f12.4)

*vwrite,
("new multiplier", /)
*vwrite, armpp1
(f14.5)

*vwrite,
("terms for new mult", /)
*vwrite, term11
(f16.7)

*vwrite,
("Values after iteration", /)

*vwrite,
("Iterative Maximum Stresses", /)
*vwrite, shake(1), loop(1)
(f16.4, f16.4)

*vwrite,
("lowerbound values", /)
*vwrite, lb(1)
(f12.4)

*vwrite, tevol
("Total volume =", f12.4, /)

*vwrite,
```

```
("Old Mo",/)  
*vwrite,armoo(1)  
(f12.4)
```

```
*vwrite,  
("Old m",/)  
*vwrite,armpo(1)  
(f12.4)
```

```
*vwrite,  
("Old ma1",/)  
*vwrite,armao(1)  
(f12.4)
```

```
*vwrite,  
("New Mo",/)  
*vwrite,armon(1)  
(f12.4)
```

```
*vwrite,  
("New m",/)  
*vwrite,armpn(1)  
(f12.4)
```

```
*vwrite,  
("New ma1",/)  
*vwrite,arman(1)  
(f12.4)
```

```
*vwrite,  
("Ponter's Mo",/)  
*vwrite,armop(1)  
(f12.4)
```

```
*vwrite,  
("new multipliers",/)  
*vwrite,armpp(1)  
(f14.5)
```

```
*vwrite,  
("Term term1",/)  
*vwrite,term1(1)  
(f16.7)
```

```
*vwrite,  
("Term term2 based on mo(old)",/)  
*vwrite,term2(1)  
(f16.7)
```

```
*cfclose,file_name,res
```

Input file for Thick Flat Head under Internal Pressure

```
/prep7
p_int=50
r_in=254.0
f_thk=101.6
s_thk=101.6
fil_rad=101.6
cyl_len=406.4
sm=207
ex=207e3
nuxy=0.47

k,1,r_in
k,2,r_in+s_thk
k,3,r_in+s_thk,cyl_len-f_thk-fil_rad
k,4,r_in+s_thk,cyl_len
k,5,r_in-fil_rad,cyl_len
k,6,0,cyl_len
k,7,0,cyl_len-f_thk
k,8,r_in-fil_rad,cyl_len-s_thk
k,9,r_in-fil_rad,cyl_len-f_thk-fil_rad
k,10,r_in,cyl_len-f_thk-fil_rad

larc,10,8,9,fil_rad
ldiv,1
ldiv,1
ldiv,2
l,3,4
l,4,5
ldiv,5
ldiv,6

a,1,2,3,10
a,3,14,12,10
a,14,4,11,12
a,4,15,13,11
a,15,13,8,5
a,5,6,7,8

et,1,182,,,1
mp,ex,1,ex
mp,nuxy,1,nuxy

lesize,11,,,12,1/2
lesize,9,,,12,2
lesize,12,,,14
lesize,10,,,14
lesize,13,,,12,1/2
lesize,14,,,12,1/2
lesize,15,,,12,1/2
```

```
lesize,16,,,12,2
lesize,19,,,12
lesize,17,,,12
lesize,18,,,12,1/2
```

```
eshape,2
esize,10
amesh,all
```

```
sfl,12,pres,p_int
sfl,1,pres,p_int
sfl,3,pres,p_int
sfl,2,pres,p_int
sfl,4,pres,p_int
sfl,19,pres,p_int
```

```
nselect,r,loc,y,0
d,all,uy,0
nall
```

```
/solu
solve
```

Input File for Welded-in Flat Head under Internal Pressure

```
/prep7
p_int=10
r_in=200
f_thk=43
s_thk=21.5
w_rad=18
sm=300
ex=200000
nuxy=0.47
```

```
et,1,42,,,1
mp,ex,1,ex
mp,nuxy,1,nuxy
```

```
k,1
k,2,r_in+2-(w_rad*2)-s_thk
k,3,r_in+2-w_rad
k,4,r_in+s_thk
k,5,r_in+s_thk,f_thk
k,6,r_in+2,f_thk
k,7,r_in+2-(2*w_rad),f_thk
k,8,r_in+2-(w_rad*2)-s_thk,f_thk
k,9,0,f_thk
k,10,r_in+2-w_rad,f_thk-w_rad
k,11,r_in+2-w_rad,f_thk
```

```
larc,7,10,11,w_rad
```

```

ldiv,1
larc,6,10,11,w_rad
ldiv,3

a,1,2,8,9
a,8,2,12,7
a,2,3,10,12
a,3,4,13,10
a,4,5,6,13

k,14,r_in+s_thk,r_in+f_thk
k,15,r_in,r_in+f_thk
k,16,r_in,f_thk
k,17,r_in-8,f_thk
k,18,r_in-8,f_thk+10
l,15,16
larc,6,18,17,10
boptn,keep,yes
lcs1,18,17
ldel,17,18,1
ldel,21,22,1
kdel,16,18,1
k,20,r_in+s_thk,49
a,6,5,20,19
a,19,20,14,15

eshape,2
esize,5
amesh,all

sfl,7,pres,p_int
sfl,10,pres,p_int
sfl,1,pres,p_int
sfl,2,pres,p_int
sfl,4,pres,p_int
sfl,3,pres,p_int
sfl,19,pres,p_int
sfl,20,pres,p_int

/solu
nsel,r,loc,y,r_in+f_thk
d,all,uy,0
nall
solve

```

Limit Analysis of Thick Welded Flat Head Under Internal Pressure

```

/prep7
p_int=50
r_in=254.0
f_thk=101.6
s_thk=101.6

```

fil_rad=101.6
cyl_len=406.4

sm=207
ex=207e3
tb,bkin,1,1
tbdata,1,sm
nuxy=0.3

k,1,r_in
k,2,r_in+s_thk
k,3,r_in+s_thk,cyl_len-f_thk-fil_rad
k,4,r_in+s_thk,cyl_len
k,5,r_in-fil_rad,cyl_len
k,6,0,cyl_len
k,7,0,cyl_len-f_thk
k,8,r_in-fil_rad,cyl_len-s_thk
k,9,r_in-fil_rad,cyl_len-f_thk-fil_rad
k,10,r_in,cyl_len-f_thk-fil_rad

larc,10,8,9,fil_rad
ldiv,1
ldiv,1
ldiv,2
l,3,4
l,4,5
ldiv,5
ldiv,6

a,1,2,3,10
a,3,14,12,10
a,14,4,11,12
a,4,15,13,11
a,15,13,8,5
a,5,6,7,8

et,1,42,,,1
mp,ex,1,ex
mp,nuxy,1,nuxy

lesi,1,,,8
lesi,2,,,8
lesi,3,,,8
lesi,4,,,8
lesize,11,,,12,1/4
lesize,9,,,12,4
lesize,12,,,20
lesize,10,,,20
lesize,13,,,12,1/4
lesize,14,,,12,1/4
lesize,15,,,12,1/4
lesize,16,,,12,4
lesize,19,,,18

```
lesize,17,,,18  
lesize,18,,,12,1/4
```

```
eshape,2  
amesh,all
```

```
nselect,r,loc,y,0  
d,all,uy,0  
nall
```

```
/solu  
p_int=40  
time,p_int  
deltim,p_int  
sfl,12,pres,p_int  
sfl,1,pres,p_int  
sfl,3,pres,p_int  
sfl,2,pres,p_int  
sfl,4,pres,p_int  
sfl,19,pres,p_int  
lswrit  
solve
```

```
p_int=96  
time,p_int  
deltim,2,1,3  
sfl,12,pres,p_int  
sfl,1,pres,p_int  
sfl,3,pres,p_int  
sfl,2,pres,p_int  
sfl,4,pres,p_int  
sfl,19,pres,p_int  
outres,all,all  
autots,on  
pred,on  
lswrit
```

```
p_int=110  
time,p_int  
deltim,0.2,0.1,0.25  
sfl,12,pres,p_int  
sfl,1,pres,p_int  
sfl,3,pres,p_int  
sfl,2,pres,p_int  
sfl,4,pres,p_int  
sfl,19,pres,p_int  
outres,all,all  
autots,on  
pred,on  
lswrit  
solve
```

Limit Analysis of a Welded-in Flat Head under Internal Pressure

```
/prep7
r_in=200
f_thk=43
s_thk=21.5
w_rad=18

sm=300
ex=200000
tb,bkin,1,1
tbdata,1,sm
nuxy=0.3

div1 = 12
div2 = 30
div3 = 8
div4 = 40

et,1,182,,,1
mp,ex,1,ex
mp,nuxy,1,nuxy

k,1
k,2,r_in+2-(w_rad*2)-s_thk
k,3,r_in+2-w_rad
k,4,r_in+s_thk
k,5,r_in+s_thk,f_thk
k,6,r_in+2,f_thk
k,7,r_in+2-(2*w_rad),f_thk
k,8,r_in+2-(w_rad*2)-s_thk,f_thk
k,9,0,f_thk
k,10,r_in+2-w_rad,f_thk-w_rad
k,11,r_in+2-w_rad,f_thk

larc,7,10,11,w_rad
ldiv,1
larc,6,10,11,w_rad
ldiv,3

a,1,2,8,9
a,8,2,12,7
a,2,3,10,12
a,3,4,13,10
a,4,5,6,13

k,14,r_in+s_thk,r_in+f_thk
k,15,r_in,r_in+f_thk
k,16,r_in,f_thk
k,17,r_in-8,f_thk
k,18,r_in-8,f_thk+10
l,15,16
larc,6,18,17,10
```

```

boptn,keep,yes
lcs1,18,17
ldel,17,18,1
ldel,21,22,1
kdel,16,18,1
k,20,r_in+s_thk,49
a,6,5,20,19
a,19,20,14,15

lesi,1,,,div1
lesi,2,,,div1
lesi,3,,,div1
lesi,4,,,div1
lesi,6,,,div1,1/5
lesi,9,,,div1,1/5
lesi,10,,,div1,5
lesi,12,,,div1,1/5
lesi,14,,,div1,1/5
lesi,16,,,div1,1/5
lesi,7,,,div2
lesi,8,,,div1,3
lesi,18,,,div1,1/5
lesi,19,,,div3
lesi,20,,,div4
lesi,22,,,div1,1/5

eshape,2
amesh,all

/solu
nset,s,loc,y,r_in+f_thk
d,all,uy,0
nall

time,1,e-5
lswrit

p_int=8
time,p_int
deltim,p_int
sfl,7,pres,p_int
sfl,10,pres,p_int
sfl,1,pres,p_int
sfl,2,pres,p_int
sfl,4,pres,p_int
sfl,3,pres,p_int
sfl,19,pres,p_int
sfl,20,pres,p_int
lswrit

p_int=26
time,p_int
deltim,1,0.5,2

```

```
sfl,7,pres,p_int
sfl,10,pres,p_int
sfl,1,pres,p_int
sfl,2,pres,p_int
sfl,4,pres,p_int
sfl,3,pres,p_int
sfl,19,pres,p_int
sfl,20,pres,p_int
outres,all,all
autots,on
pred,on
lswrit
solve
```

```
p_int=29
time,p_int
deltim,0.05,0.025,0.1
sfl,7,pres,p_int
sfl,10,pres,p_int
sfl,1,pres,p_int
sfl,2,pres,p_int
sfl,4,pres,p_int
sfl,3,pres,p_int
sfl,19,pres,p_int
sfl,20,pres,p_int
outres,all,all
autots,on
pred,on
lswrit
solve
```

Input file for Plate with a Center Crack

```
/prep7
a=1
l=5
w=5
ex=30e6
sm=25e3
nuxy=0.3
load=20e3
len=1

et,1,plane82,,,2
mp,ex,1,ex
mp,nuxy,1,nuxy

k,1
k,2,w-a
k,3,w-a,l
k,4,-a,l
k,5,-a
```

```

1,1,2
1,2,3
lesize,2,,,4
1,3,4
lesize,3,,,4
1,4,5
lesize,4,,,6,0.2
1,5,1

esize,,5
kscon,1,0.15,1,8
al,1,2,3,4,5
amesh,1

/solu
dl,1,1,symm
dl,4,1,symm
sfl,3,pres,-load
solve

```

Limit Load Analysis of a Plate with a Center Crack

```

/prep7
a=1
ex=30e6
sm=25e3
nuxy=0.3
len=1

tb,bkin,1
tbdata,1,sm
mp,ex,1,ex
mp,nuxy,1,nuxy

k,1
k,2,4
k,3,4,5
k,4,-1,5
k,5,-1

1,1,2
1,2,3
lesize,2,,,4
1,3,4
lesize,3,,,4
1,4,5
lesize,4,,,6,0.2
1,5,1

et,1,plane82,,,2
esize,,5
kscon,1,0.15,1,8

```

```
al,1,2,3,4,5  
amesh,1
```

```
/solu  
load=25000  
dl,1,1,symm  
dl,4,1,symm
```

```
sfl,3,pres,-load  
solcon,on  
nropt,auto  
autots,on  
nsubst,150,200,150  
neqit,50  
outres,all,all  
time,25000  
solve
```

Input File for Compact Tension Specimen

```
/prep7  
a=0.0466  
b=0.003  
w=0.1  
w1=0.125  
h=0.060  
r=0.0125  
e=0.0275  
s=0.003  
d1=0.080  
d2=0.075  
load=20e3/5  
ex=211e09  
sm=488.43e06  
nuxy=0.47
```

```
mp,ex,1,ex  
mp,nuxy,1,nuxy
```

```
k,1,a  
k,2,w  
k,3,w,h  
k,4,,h  
k,5,(w-w1),h  
k,6,(w-w1),s  
k,7,,s  
k,8,(w-d1),s  
k,9,(w-d2)  
k,10,,e  
k,11,,e,e  
circle,10,r,11,4,,8
```

```

l,1,2
*repeat,8,1,1
l,9,1
l,4,12
l,16,7
ksel,s,loc,x,-1e-6,1
lslk,s,1
al,all
ksel,s,loc,x,-1,1e-6
lslk,s,1
al,all
ksel,all
lsl,all

et,1,plane2,,,3
r,1,b
esize,a/4
kscon,1,a/16,1,9
amesh,all
wsort,x
finish

/solution
antype,0

nsl,s,loc,y
nsl,r,loc,x,a,w
d,all,uy,0

nsl,r,loc,x,a
d,all,ux,0
nsl,all

f,515,fy,load
f,516,fy,load
f,8,fy,load
f,9,fy,load
f,6,fy,load
solve

```

Limit Load Analysis of a Compact Tension Specimen

```

/prep7
a=0.046
b=0.003
w=0.1
w1=0.125
h=0.06
r=0.0125
e=0.0275
s=0.003
d1=0.08

```

```

d2=0.075

ex=211e9
sm=488.43e06
nuxy=0.3
load=20000/5

tb,bkin,1
tbdata,1,sm
mp,ex,1,ex
mp,nuxy,1,nuxy

k,1,a
k,2,w
k,3,w,h
k,4,,h
k,5,(w-w1),h
k,6,(w-w1),s
k,7,,s
k,8,(w-d1),s
k,9,(w-d2)
k,10,,e
k,11,,e,e
circle,10,r,11,4,,8
l,1,2
*repeat,8,1,1
l,9,1
l,4,12
l,16,7
ksel,s,loc,x,-1e-6,1
lslk,s,1
al,all
ksel,s,loc,x,-1,1e-6
lslk,s,1
al,all
ksel,all
lsel,all

et,1,plane2,,3
r,1,b
esize,a/4
kscon,1,a/16,1,9
amesh,all
wsort,x
finish

/solu
antype,0
nset,s,loc,y
nset,r,loc,x,a,w
d,all,uy,0

nset,r,loc,x,a

```

```
d,all,ux,0
nset,all

f,515,fy,load
f,516,fy,load
f,8,fy,load
f,9,fy,load
f,6,fy,load

solcon,on
nropt,auto
autots,on
nsubst,75,100,75
neqt,50
outres,all,all
time,20000
solve
```

Input File for a Plate with Multiple Cracks

```
/prep7
ex=210000
sm=480
nuxy=0.3
load=-300

et,1,plane2
mp,ex,1,ex
mp,nuxy,1,nuxy

k,1
k,2,10
k,3,15
k,4,25
k,5,32.5
k,6,40
k,7,50
k,8,0,5
k,9,15,5
k,10,27.5,5
k,11,32.5,5
k,12,50,5
k,13,20,10
k,14,27.5,17.5
k,15,35,25
k,16,27.5,17.5
k,17,0,50
k,18,27.5,50
k,19,50,40
k,20,50,50
k,21,50,100
k,22,0,100
```

```
a,1,2,3,9,8
a,3,4,5,11,10,9
a,5,6,7,12,11
a,8,9,13,14,18,17
a,9,10,16,13
a,10,11,12,19,15,16
a,14,15,19,20,18
a,17,18,20,21,22
```

```
kscon,2,2,1,12
kscon,13,2,1,6
kscon,15,2,1,6
esize,2
lesize,2,,,8
amesh,1,2
```

```
esize,4
lesize,15,,,10
lesize,23,,,15
lesize,16,,,12
lesize,21,,,12
lesize,24,,,12
lesize,25,,,12
```

```
amesh,3
amesh,4,5
amesh,6,7
esize,10
amesh,8
finish
```

```
/solu
nset,s,loc,x,0
d,all,ux,0
nset,all
```

```
nset,s,loc,y,0
nset,r,loc,x,10,50
d,all,uy,0
nset,all
```

```
nset,s,loc,y,100
sf,all,pres,load
nset,all
solve
```

Limit Analysis of a Plate with Multiple Cracks

```
/prep7
ex=210000
sm=480
nuxy=0.3
```

et,1,plane2
tb,bkin,1
tbdata,1,sm
mp,ex,1,ex
mp,nuxy,1,nuxy

k,1
k,2,10
k,3,15
k,4,25
k,5,32.5
k,6,40
k,7,50
k,8,0,5
k,9,15,5
k,10,27.5,5
k,11,32.5,5
k,12,50,5
k,13,20,10
k,14,27.5,17.5
k,15,35,25
k,16,27.5,17.5
k,17,0,50
k,18,27.5,50
k,19,50,40
k,20,50,50
k,21,50,100
k,22,0,100

a,1,2,3,9,8
a,3,4,5,11,10,9
a,5,6,7,12,11
a,8,9,13,14,18,17
a,9,10,16,13
a,10,11,12,19,15,16
a,14,15,19,20,18
a,17,18,20,21,22

kscon,2,2,1,12
kscon,13,2,1,6
kscon,15,2,1,6

esize,2
lesize,2,,,8
amesh,1,2
esize,4
lesize,15,,,10
lesize,23,,,15
lesize,16,,,12
lesize,21,,,12
lesize,24,,,12
lesize,25,,,12

```

amesh,3
amesh,4,5
amesh,6,7
esize,10
amesh,8
finish

/solu
load=-300
nset,s,loc,x,0
d,all,ux,0
nset,all

nset,s,loc,y,0
nset,r,loc,x,10,50
d,all,uy,0
nset,all

nset,s,loc,y,100
sf,all,pres,load
nset,all

solcon,on
nropt,auto
autots,on
nsubst,100,150,100
neqit,50
outres,all,all
time,300
solve

```

Macro for Evaluating Limit Loads of Anisotropic Components

refnew.txt

```

! Enter number of iterations in EMAP
iter=10

! initial iteration: elastic solution
niter = 0
! Enter the ANSYS input file name
/inp,file_name.txt
finish

/prep7
/nopr
nset,all
esel,all

! Obtain the minimum and maximum number elements and nodes
*get,emin,elem,,num,min !get min element number as emin

```

```

*get,emax,elem,,num,max      !get max element number as emax
*get,nmin,node,,num,min !get min node number as nmin
*get,nmax,node,,num,max      !get max node number as nmax

! Get material properties for the initial iteration
! Get Young's and Shear Modulus
*get,ex,ex,1
*get,ey,ey,1
*get,ez,ez,1
*get,gxy,gxy,1
*get,gyz,gyz,1
*get,gxz,gxz,1

! Get Poisson's ratios
*get,nuxy,nuxy,1
*get,nuyz,nuyz,1
*get,nuxz,nuxz,1

! Arrays for iteration results
*dim,loop,,iter      ! for maximum centroidal stress
*dim,lb,,iter        ! for cl. lb results
*dim,armon,,iter ! for mo new results
*dim,armop,,iter ! for ponter's mo results
*dim,armoo,,iter ! for mo old results
*dim,armpn,,iter ! for mp new results
*dim,armpo,,iter ! for mp old results
*dim,armao,,iter ! for ma old results
*dim,arman,,iter ! for ma new results
*dim,armpp,,iter ! for mpn (mp) new results

! Array for Young's Moduli in each element
! matrix for element youngs and shear moduli
*dim,arex,,emax,iter+1
*dim,arey,,emax,iter+1
*dim,arez,,emax,iter+1
*dim,argxy,,emax,iter+1
*dim,argyz,,emax,iter+1
*dim,argxz,,emax,iter+1

! Arrays for Reference Volume m0's
*dim,usor,,emax      !unsorted product
*dim,sor,,emax       !sorted product
*dim,svol,,emax      !corresponding sorted volumes
*dim,rmo,,emax       !reference mo's
*dim,rmon,,emax      !reference new mo's
*dim,rvol,,emax      !reference volume ratios
*dim,volnum,,emax    !order of volumes
*dim,cumvol,,emax    !cumulative volumes
*dim,cumstrs,,emax   !cumulative stresses
*dim,ref_ratio,,emax !reference ratio for m0-old

! Reference Parameters for m"
*dim,ref_s1,,emax    ! Term s1bar

```

```

*dim,ref_s2,,emax      ! Term s2bar
*dim,term_r,,emax     ! Term R(zeta)
*dim,term_g,,emax     ! Term G(zeta)
*dim,ref_mpp,,emax    ! Reference m"
*dim,cum_s1,,emax     ! Cumulative S1
*dim,cum_s2,,emax     ! Cumulative S2

*dim,evol,,emax      !elem volume

! Arrays for normal and shear stresses in x,y,z directions
*dim,sx,,emax
*dim,sy,,emax
*dim,sz,,emax
*dim,sxy,,emax
*dim,syz,,emax
*dim,sxz,,emax
*dim,cstrs,,emax !equivalent stress (Hill's criterion)
finish

/post1
etable,xstrs,s,x
etable,ystrs,s,y
etable,zstrs,s,z
etable,xystrs,s,xy
etable,yzstrs,s,yz
etable,xzstrs,s,xz

*vget,sx(1),elem,,etab,xstrs,,0
*vget,sy(1),elem,,etab,ystrs,,0
*vget,sz(1),elem,,etab,zstrs,,0
*vget,sxy(1),elem,,etab,xystrs,,0
*vget,syz(1),elem,,etab,yzstrs,,0
*vget,sxz(1),elem,,etab,xzstrs,,0

etable,evoltab,volu      ! table for element volume
*vget,evol(1),elem,,etab,evoltab,,0

*do,count,emin,emax,1
  arex(count,1) = ex
  arey(count,1) = ey
  arez(count,1) = ez
  argxy(count,1) = gxy
  argyz(count,1) = gyz
  argxz(count,1) = gxz
*enddo

niter=0      !setting iteration number to be zero

! Evaluate limit load multipliers at the initial iteration
/inp,aniso_init,txt
finish

! Perform elastic modulus modification for each iteration and solve

```

```

*do,niter,1,iter,1
  ! read stresses and calculate new elastic modulus at each element
  ! write new elastic modulus values to arex array
  /inp,aniso_cen,txt

  /solu
  /nopr
  solve
  finish

  /post1
  /nopr
  set,last

  ! Limit load multiplier evaluations
  /inp,aniso_mult,txt

  ! Enter the iteration number in which the reference volume is to be calculated
  *if,niter,eq,20,then
    /inp,refr_betastrs_m0,txt
  *endif
  finish
*enddo

! write results out to file
/inp,results,txt
save
/exit,all

```

aniso_init.txt

```

tevol=0
m=0
prod1=0
prod2=0
prod3=0
term1 l=0      !product (term2) for new form m"
tprod=0 !total product for new form m"
den_in1=0      !din.term of old mo
den_in2=0      !din.term of new mo
den_in3=0      !din.term of p's mo
den_fn1=0      !final din.term of old mo
den_fn2=0      !final din.term of new mo
num_in=0       !num.term of new mo
num_in2=0
num_fn=0       !num.term of new mo

/post1
set,last
!Calculate Effective stress according to Hill's criterion
sm=smx
a12=sm**2*(1/smx**2+1/smy**2-1/smz**2)
a23=sm**2*(-1/smx**2+1/smy**2+1/smz**2)

```

```

a31=sm**2*(1/smx**2-1/smy**2+1/smz**2)
a44=(sm/smxy)**2/3
a55=(sm/smyz)**2/3
a66=(sm/smxz)**2/3

*do,count,emin,emax,1
eff1=0.5*(a12*(sx(count)-sy(count))**2+a23*(sy(count)-sz(count))**2+a31*(sz(count)-sx(count))**2)
eff2=3*(a44*sxy(count)**2+a55*syz(count)**2+a66*sxz(count)**2)
cstrs(count)=(eff1+eff2)**0.5
*enddo

!Finding maximum elemental stress
*do,nvol,emin,emax,1
  *if,cstrs(nvol),gt,m,then
    m=cstrs(nvol)
  *endif
*enddo

loop1=m
lb1=sm/loop1
!-----
!Estimate new m0, Ponter's m0, m' and m-alpha multipliers
!Estimate dinominator for new m0
*do,nvol,emin,emax,1
  den_in2=den_in2+(cstrs(nvol)**2)*evol(nvol)/ex
  den_in3=den_in3+(cstrs(nvol)**2)*evol(nvol)/ex
*enddo
  den_fn2=sqrt(den_in2)

!Estimate numerator for new m0
*do,nvol,emin,emax,1
  num_in=num_in+evol(nvol)/ex
  num_in2=num_in2+(cstrs(nvol)*evol(nvol)/ex)
*enddo
  num_fn=sqrt(num_in)

!Estimate new m0, Ponter's lamda multiplier
armon1=sm*num_fn/den_fn2
armop1=sm*num_in2/den_in3

!Estimate new m' multiplier
mnum2=2*armon1*sm*sm
mdin2=(sm*sm)+((armon1**2)*m*m)
armpn1=mnum2/mdin2

!Estimate new m-alpha multiplier
instr=m/sm
a2=(armon1**4)*(instr**4)+4*(armon1**2)*(instr**2)-1
b2=(-8*(armon1**3)*(instr**2))
c2=4*(armon1**3)*instr
d2=b2**2-4*a2*c2

*if,d2,gt,0,then

```

```

          arman1=(-1*b2)+sqrt(b2**2-4*a2*c2)/(2*a2)
*endif
!-----
!Estimate new m' multiplier
!Estimate dinominator for new m'
*do,nvol,emin,emax,1
      prod1=(armon1*cstrs(nvol))**2
      prod2=sm*sm
      prod3=prod3+((prod1-prod2)**2)*evol(nvol)
*enddo
      tprod=sqrt(prod3)/sqrt(tevol)

mnum3=2*armon1*sm*sm
mdin3=2*sm*sm+tprod
armpp1=mnum3/mdin3

mnum4=2*armon1
mdin4=1+(armon1/armool)**2
armsp1=mnum4/mdin4
term11=tprod/(2*sm*sm)
!-----

```

aniso_cen.txt

```

/post1
set,last
! Element tables for normal and shear stresses in x,y,z directions
etable,xstrs,s,x
etable,ystrs,s,y
etable,zstrs,s,z
etable,xystrs,s,xy
etable,yzstrs,s,yz
etable,xzstrs,s,xz

*vget,sx(1),elem,,etab,xstrs,,0
*vget,sy(1),elem,,etab,ystrs,,0
*vget,sz(1),elem,,etab,zstrs,,0
*vget,sxy(1),elem,,etab,xystrs,,0
*vget,syz(1),elem,,etab,yzstrs,,0
*vget,sxz(1),elem,,etab,xzstrs,,0

!Calculate Effective stress according to Hill's criterion
sm=smx
a12=sm**2*(1/smx**2+1/smy**2-1/smz**2)
a23=sm**2*(-1/smx**2+1/smy**2+1/smz**2)
a31=sm**2*(1/smx**2-1/smy**2+1/smz**2)
a44=(sm/smxy)**2/3
a55=(sm/smyz)**2/3
a66=(sm/smxz)**2/3

*do,count,emin,emax,1
  eff1=0.5*(a12*(sx(count)-sy(count))**2+a23*(sy(count)-sz(count))**2+a31*(sz(count)-sx(count))**2)
  eff2=3*(a44*sxy(count)**2+a55*syz(count)**2+a66*sxz(count)**2)

```

```

cstrs(count)=(eff1+eff2)**0.5
*enddo

! Perform elastic modulus modification
index=1.0
*do,count,emin,emax,1
  rf = (sm/cstrs(count))**index
  arex(count,niter+1) = arex(count,niter)*rf
  arey(count,niter+1) = arey(count,niter)*rf
  arez(count,niter+1) = arez(count,niter)*rf
  argxy(count,niter+1) = argxy(count,niter)*rf
  argyz(count,niter+1) = argyz(count,niter)*rf
  argxz(count,niter+1) = argxz(count,niter)*rf
*enddo
finish

/prep7
/nopr
! modify each elements ex
*do,count,emin,emax,1
  uimp,count,ex,ey,ez,arex(count,niter+1),arey(count,niter+1),arez(count,niter+1)
  uimp,count,nuxy,nuyz,nuxz,nuxy,nuyz,nuxz
  uimp,count,gxy,gyz,gxz,argxy(count,niter+1),argyz(count,niter+1),argxz(count,niter+1)
  mat,count
  emod,count
*enddo
finish

```

aniso_mult.txt

```

tevol=0
prod1=0 !product (term2) for new form m' (added)
prod2=0 !product (term3) for new form m' (added)
prod3=0 !product (strain energy) for new form m' (added)
m=0
tprod=0 !total product for new form m' (added)
den_in1=0      !din.term of old mo
den_in2=0      !din.term of new mo
den_in3=0      !din.term of ponter's mo
den_fn1=0      !final din.term of old mo
den_fn2=0      !final din.term of new mo
den_fn3=0      !final din.term of ponter's mo
num_in=0       !num.term of new mo
num_fn=0       !num.term of new mo
num_in2=0      !num.term of ponter's mo

/post1
set,last
etable,xstrs,s,x
etable,ystrs,s,y
etable,zstrs,s,z
etable,xystrs,s,xy
etable,yzstrs,s,yz
etable,xzstrs,s,xz

```

```

*vget,sx(1),elem,,etab,xstrs,,0
*vget,sy(1),elem,,etab,ystrs,,0
*vget,sz(1),elem,,etab,zstrs,,0
*vget,sxy(1),elem,,etab,xystrs,,0
*vget,syz(1),elem,,etab,yzstrs,,0
*vget,sxz(1),elem,,etab,xzstrs,,0

!Calculate Effective stress according to Hill's criterion
sm=smx
a12=sm**2*(1/smx**2+1/smy**2-1/smz**2)
a23=sm**2*(-1/smx**2+1/smy**2+1/smz**2)
a31=sm**2*(1/smx**2-1/smy**2+1/smz**2)
a44=(sm/smxy)**2/3
a55=(sm/smyz)**2/3
a66=(sm/smxz)**2/3

*do,count,emin,emax,1
  eff1=0.5*(a12*(sx(count)-sy(count))**2+a23*(sy(count)-sz(count))**2+a31*(sz(count)-sx(count))**2)
  eff2=3*(a44*sxy(count)**2+a55*syz(count)**2+a66*sxz(count)**2)
  cstrs(count)=(eff1+eff2)**0.5
*enddo

!Finding maximum elemental stress

*do,nvol,emin,emax,1
  *if,cstrs(nvol),gt,m,then
    m=cstrs(nvol)
  *endif
*enddo

loop(niter)=m
lb(niter)=sm/loop(niter)
!-----
! Estimate new m0, m' and m-alpha multipliers
! First estimate dinominator for new m0
*do,nvol,emin,emax,1
  den_in2=den_in2+(cstrs(nvol)**2)*evol(nvol)/arex(nvol,niter+1)
*enddo
  den_fn2=sqrt(den_in2)

! Estimate numerator for new m0
*do,nvol,emin,emax,1
  num_in=num_in+evol(nvol)/arex(nvol,niter+1)
*enddo
  num_fn=sqrt(num_in)

! Estimate new m0 multiplier
armon(niter)=sm*num_fn/den_fn2
ratio_new(niter) = num_in/den_in2

! Estimate new m' multiplier
mnum2=2*armon(niter)*sm*sm

```

```

mdin2=(sm*sm)+((armon(niter)**2)*m*m)
armpn(niter)=mnum2/mdin2

! Estimate new m-alpha multiplier
instr=m/sm
a2=(armon(niter)**4)*(instr**4)+4*(armon(niter)**2)*(instr**2)-1
b2=(-8*(armon(niter)**3)*(instr**2))
c2=4*(armon(niter)**3)*instr
d2=b2**2-4*a2*c2

*if,d2,gt,0,then
  arman(niter)=((-1*b2)+sqrt(b2**2-4*a2*c2))/(2*a2)
*endif
!-----
! Estimate Ponter's lamda
! Estimate dinominator for lamda
*do,nvol,emin,emax,1
  den_in3=den_in3+(astrs(nvol)**2)*evol(nvol)/arex(nvol,niter+1)
*enddo

! Estimate numerator for lamda
*do,nvol,emin,emax,1
  num_in2=num_in2+(cstrs(nvol)*evol(nvol)/arex(nvol,niter+1))
*enddo

! Estimate Ponter's upper bound multiplier
armop(niter)=sm*num_in2/den_in3
!-----
! Estimate m" multiplier
! Estimate dinominator for new m"
*do,nvol,emin,emax,1
  prod1=(armoo(niter)*cstrs(nvol))**2
  prod2=sm*sm
  prod3=prod3+((prod1-prod2)**2)*evol(nvol)
*enddo
  tprod=sqrt(prod3)/sqrt(tevol)

mnum3=2*armoo(niter)*sm*sm
mdin3=2*sm*sm+tprod
armpp(niter)=mnum3/mdin3

term1(niter)=tprod/(2*sm*sm)
term2(niter)=armoo(niter)/(1+term1(niter))
!-----

```

Equivalent Stress for Fourth-order Criterion

```

p=0.5153796
q=14.39346
r=5.24605
t=10.31122
y1=0.2553
y2=y1

```

y3=3

st1=0.5*(sx(count)+sz(count))
st2=0.5*(sx(count)-sz(count))
st3=sxz(count)

eff11=p*st1**4+q*(st2**2+st3**2)**2+r*(st1**2*(st2**2+st3**2))
eff12=t*st1*st2*(st2**2-3*st3**2)
eff1=(eff11+eff12)**0.5
eff21=y1*sy(count)**2-y2*(sy(count)*(sx(count)+sz(count)))
eff22=y3*(sxy(count)**2+syz(count)**2)
eff2=eff21+eff22
cstrs(count)=(eff1+eff2)**0.5

Input file for Orthotropic cylinder under Internal Pressure

/prep7
ri=30
ro=40
div=30
hi=(ro-ri)/div
prsr=250

xx=579.2
yy=472.3
zz=630.9
rr=262.9
ss=262.9
tt=262.9

ymx=xx**2
ymy=yy**2
ymz=zz**2
smxy=rr**2
smyz=ss**2
smxz=tt**2

pxy=0.47*yy**2*(1/xx**2+1/yy**2-1/zz**2)
pyz=0.47*zz**2*(-1/xx**2+1/yy**2+1/zz**2)
pxz=0.47*zz**2*(1/xx**2-1/yy**2+1/zz**2)

et,1,42
keyopt,1,3,1

uimp,1,ex,ey,ez,ymx,ymy,ymz
uimp,1,nuxy,nuyz,nuxz,pxy,pyz,pxz
uimp,1,gxy,gyz,gxz,smxy,smyz,smxz

k,1,ri,0
k,2,ro,0
k,3,ro,hi
k,4,ri,hi

```
l,1,2,div,1  
l,2,3,1  
l,3,4,div,1  
l,4,1,1
```

```
a,1,2,3,4  
amesh,1
```

```
/solu  
d,all,uy,0
```

```
nselect,s,loc,x,ri  
sf,all,pres,prsr  
nselect,all  
solve  
finish
```

Limit Analysis of Orthotropic Cylinder

```
/prep7  
ri=30  
ro=40  
div=30  
hi=(ro-ri)/div  
prsr=250
```

```
xx=579.2  
yy=472.3  
zz=630.9  
rr=262.9  
ss=262.9  
tt=262.9
```

```
ymx=100993  
ymy=95793.6  
ymz=100593  
smxy=36147.6
```

```
pxy=0.3610  
pyz=0.345  
pxz=0.3406
```

```
et,1,42  
keyopt,1,3,1
```

```
uimp,1,ex,ey,ez,ymx,ymy,ymz  
uimp,1,nuxy,nuyz,nuxz,pxy,pyz,pxz  
uimp,1,gxy,gyz,gxz,smxy,smyz,smxz  
tb,aniso,1  
tbmodif,1,1,xx  
tbmodif,1,2,yy  
tbmodif,1,3,zz  
tbmodif,3,1,xx
```

```
tbmodif,3,2,yy
tbmodif,3,3,zz
tbmodif,5,1,rr
tbmodif,5,2,ss
tbmodif,5,3,tt
```

```
k,1,ri,0
k,2,ro,0
k,3,ro,hi
k,4,ri,hi
l,1,2,div,1
l,2,3,1
l,3,4,div,1
l,4,1,1
a,1,2,3,4
amesh,1
```

```
/solu
time,1
autots,1
kbc,0
nsubst,100,500,20
neqit,40
outres,all,all
```

```
d,all,uy,0
nselect,s,loc,x,ri
sf,all,pres,prsr
nselect,all
solve
finish
```

Input file for Bridgman Notch Specimen

```
/prep7
load=500
d1=26.416
d2=21.082
r=6.858
h=30
```

```
smx=579.2
smy=472.3
smz=579.2
smxy=262.9
smyz=262.9
smxz=366.6
```

```
mod_ex=smx**2
mod_ey=smy**2
mod_ez=smz**2
mod_gxy=smxy**2
```

```

mod_gyz=smyz**2
mod_gxz=smxz**2

nuxy=0.47*smy**2*(1/smx**2+1/smy**2-1/smz**2)
nuyz=0.47*smz**2*(-1/smx**2+1/smy**2+1/smz**2)
nuxz=0.47*smz**2*(1/smx**2-1/smy**2+1/smz**2)

et,1,plane182
keyopt,1,3,1

uimp,1,ex,ey,ez,mod_ex,mod_ey,mod_ez
uimp,1,nuxy,nuyz,nuxz,nuxy,nuyz,nuxz
uimp,1,gxy,gyz,gxz,mod_gxy,mod_gyz,mod_gxz

blc4,0,0,d1/2,h
cyl4,d2/2+r,0,r
asba,1,2

k,10,0,h/2,,
k,11,d1/2+1,h/2,,
kbet,7,9,0,rati,0.5,
l,10,11
l,2,10
asbl,3,1
asbl,2,2
lesize,4,,,20,10,
lesize,12,,,20,0.1,
lesize,9,,,20,0,1,
lesize,1,,,12,1,
lesize,3,,,12,1,
lesize,5,,,12,1,
lesize,6,,,12,1,
lesize,7,,,12,1,
lesize,8,,,12,1,
lesize,10,,,12,1,
asel,all
amesh,all
csys,0
nset,s,loc,y,0
d,all,uy,0
nall

nset,s,loc,x,0
d,all,ux,0
nall

/solu
nset,s,loc,y,h
sf,all,pres,-load
nset,all
solve

```

Input file for Equivalent Solid Model of a Tubesheet for Hill's Yield Criterion

```
/prep7
phri=77.5      ! Primary head inside radius
phro=phri+7    ! Primary head outside radius
ro=72.0644     ! outermost tube center radius
ri=16.8592     ! innermost tube center radius
ttp=1.0        ! Tube pitch
ttd=0.758      ! Tubehole diameter
h=ttp-ttd      ! nominal width of ligament between tubes
cr=1/16        ! corrosion allowance
trs=ro+0.25*(ttp-h) ! Tubesheet R*
trsi=ri-0.25*(ttp-h) ! Tubesheet Ri*
tsro=167*0.5   ! Tubesheet outer diameter
tthk=3+25/32-cr ! thickshell thickness at tubesheet
ssri=tsro-tthk ! Secondary shell inside radius
tst=21.5-cr    ! Tubesheet thickness
phh=50.44      ! Primary head height
dcen=11.125    ! distance from bottom of TS to Prim head center
phct=phh+dcen  ! Primary head centre
dhp=phct-phh
dhs=-phct+phh+tst

div1 = 16
div2 = 2
div3 = 4
div4 = 3
div5 = 16

pri_pres=2.5e3
sec_pres=250

smx=9.2704e3
smy=12.853e3
smz=9.2704e3
smxy=6.287e3
smyz=6.287e3
smxz=5.5909e3
sm=smx

mod_ex=smx**2
mod_ey=smy**2
mod_ez=smz**2
mod_gxy=smxy**2
mod_gyz=smyz**2
mod_gxz=smxz**2

nuxy=0.49*smy**2*(1/smx**2+1/smy**2-1/smz**2)
nuyz=0.49*smz**2*(-1/smx**2+1/smy**2+1/smz**2)
nuxz=0.49*smz**2*(1/smx**2-1/smy**2+1/smz**2)

et,1,solid186
uimp,1,ex,ey,ez,mod_ex,mod_ey,mod_ez
```

uimp,1,nuxy,nuyz,nuxz,nuxy,nuyz,nuxz
uimp,1,gxy,gyz,gxz,mod_gxy,mod_gyz,mod_gxz

k,1
k,2,trs,-dhp !could be tbs OD (this is final)
k,3,trs,dhs !could be tbs OD (this is final)
k,4,trsi,-dhp !tbs IR
k,5,trsi,dhs
k,6,0,-dhp+(phro-phri)*0.5 !related to tbs
k,7,tsro,-dhp+(phro-phri)*0.5 !related to tbs
k,8,0,dhs-(tsro-ssri) !related to tbs
k,9,tsro,dhs-(tsro-ssri) !related to tbs

a,2,3,5,4
l,6,7
l,8,9
lcsl,5,1
lcsl,9,3
lcsl,5,6
lcsl,8,13
ldel,9,11,2
ldel,6,10,4

k,,,-trs
k,,trs
l,1,15
lcsl,6,14
ldel,8
larc,15,14,1,trs

a,4,2,10,11
a,11,10,15,16
a,16,15,13,12
a,12,13,3,5

lesize,4,,div1
lesize,12,,div1
lesize,16,,div1
lesize,2,,div1
lesize,11,,div1
lesize,1,,div2
lesize,5,,div2
lesize,3,,div2
lesize,7,,div2
lesize,8,,div3
lesize,9,,div3
lesize,10,,div4
lesize,13,,div4
lesize,6,,div5

adel,1
type,1
vdrag,2,3,4,5,,6

```

vmesh,all

asel,s,,6
asel,a,,,10
asel,a,,,14
asel,a,,,18

nsla,s,1
d,all,ux,0
d,all,uz,0
d,all,uy,0
nall
nselect,s,loc,x,0
d,all,ux,0
nall

nselect,s,loc,z,0
d,all,uz,0
nall

sfa,19,,pres,sec_pres
sfa,1,,pres,pri_pres
allsel

/solu
solve

```

Input file for Tubesheet with Fourth Order Yield Criterion

```

/prep7
phri=77.5      ! Primary head inside radius
phro=phri+7    ! Primary head outside radius
ro=72.0644    ! outermost tube center radius
ri=16.8592    ! innermost tube center radius
ttp=1.0       ! Tube pitch
ttd=0.758     ! Tubehole diameter
h=ttp-ttd     ! nominal width of ligament between tubes
cr=1/16       ! corrosion allowance
trs=ro+0.25*(ttp-h) ! Tubesheet R*
trsi=ri-0.25*(ttp-h) ! Tubesheet Ri*
tsro=167*0.5  ! Tubesheet outer diameter
tthk=3+25/32-cr ! thickshell thickness at tubesheet
ssri=tsro-tthk ! Secondary shell inside radius
tst=21.5-cr   ! Tubesheet thickness
phh=50.44    ! Primary head height
dcen=11.125  ! distance from bottom of TS to Prim head center
phct=phh+dcen ! Primary head centre
dhp=phct-phh
dhs=-phct+phh+tst
pri_pres=2.5e3
sec_pres=250

```

```

smx=9.271e3
smy=12.853e3
smz=12.296e3
smxy=6.287e3
smyz=6.287e3
smxz=5.5909e3
sm=0.242*45e3

nuxy=0
nuyz=0
nuxz=(smy**2-smxz**2)/(smy**2+smxz**2)

mod_ex=smy**2
mod_ey=smxz**2
mod_ez=smy**2
mod_gxy=(smy**2*smxy**2)/(2*smxz**2*(1+nuxz))
mod_gyz=(smy**2*smxy**2)/(2*smxz**2*(1+nuxz))
mod_gxz=smy**2/(2*(1+nuxz))

et,1,solid185
uimp,1,ex,ey,ez,mod_ex,mod_ey,mod_ez
uimp,1,nuxy,nuyz,nuxz,nuxy,nuyz,nuxz
uimp,1,gxy,gyz,gxz,mod_gxy,mod_gyz,mod_gxz

k,1
k,2,trs,-dhp      !could be tbs OD (this is final)
k,3,trs,dhs       !could be tbs OD (this is final)
k,4,trsi,-dhp     !tbs IR
k,5,trsi,dhs
k,6,0,-dhp+(phro-phri)*0.5      !related to tbs
k,7,tsro,-dhp+(phro-phri)*0.5   !related to tbs
k,8,0,dhs-(tsro-ssri)           !related to tbs
k,9,tsro,dhs-(tsro-ssri)        !related to tbs

a,2,3,5,4
l,6,7
l,8,9
lcsl,5,1
lcsl,9,3
lcsl,5,6
lcsl,8,13
ldel,9,11,2
ldel,6,10,4
k,,,-trs
k,,trs
l,1,15
lcsl,6,14
ldel,8
larc,15,14,1,trs

a,4,2,10,11
a,11,10,15,16
a,16,15,13,12

```

```
a,12,13,3,5  
lesize,4,,,16  
lesize,12,,,16  
lesize,16,,,16  
lesize,2,,,16  
lesize,11,,,16
```

```
lesize,1,,,2  
lesize,5,,,2  
lesize,3,,,2  
lesize,7,,,2  
lesize,8,,,4  
lesize,9,,,4  
lesize,10,,,3  
lesize,13,,,3  
lesize,6,,,16
```

```
adel,1  
type,1  
vdrag,2,3,4,5,,,6  
vmesh,all
```

```
asel,s,,,6  
asel,a,,,10  
asel,a,,,14  
asel,a,,,18
```

```
nsla,s,1  
d,all,ux,0  
d,all,uz,0  
d,all,uy,0  
nall
```

```
nsl,s,loc,x,0  
d,all,ux,0  
nall
```

```
nsl,s,loc,z,0  
d,all,uz,0  
nall
```

```
sfa,19,,pres,sec_pres  
sfa,1,,pres,pri_pres  
allsel
```

```
/solu  
solve
```

